PROVISIONAL EXTRACELLULAR MATRIX CITRULLINATION AS A STIMULUS FOR PATHOLOGICAL FIBROBLAST ACTIVATION

A Dissertation
Presented to
The Academic Faculty

By

Victoria Lauren Stefanelli

In Partial Fulfillment
of the Requirements for the Degree
Doctor of Philosophy in the
Wallace H. Coulter Department of Biomedical Engineering

Georgia Institute of Technology and Emory University
May of 2018

PROVISIONAL EXTRACELLULAR MATRIX CITRULLINATION AS A STIMULUS FOR PATHOLOGICAL FIBROBLAST ACTIVATION

Approved by:

Dr. Thomas Barker, Advisor
School of Biomedical Engineering
University of Virginia

Dr. Melissa Kemp
School of Biomedical Engineering
Georgia Institute of Technology

Dr. Johnna Temenoff
School of Biomedical Engineering
Georgia Institute of Technology

Dr. Eric White
Medical School
University of Michigan

Dr. Matthew Torres
School of Biological Sciences
Georgia Institute of Technology

Date Approved: March 29th, 2018

ACKNOWLEDGEMENTS

The completion of this work was truly a group effort. I would like to start by thanking all those who provided technical and scientific assistance, especially including the following post-doctoral and graduate student mentors: Ashley Brown, Alison Douglas, Dwight Chambers, John Nicosia, Vincent Yeh, Ping Hu, and Leandro Moretti. For literally working alongside to assist in various animal and benchtop experiments, even when it was outside the scope of their own responsibilities, I would like to acknowledge Vincent Yeh, Dwight Chambers, Mary Harp, Dan Abebayehu, and Riley Hannan. I'm also very grateful to my two awesome undergraduate students Kelly Pesson and Tommy Ng for being so diligent in their work and making my life much easier in the process. And, of course, this work would not have been shaped into its current form without the invaluable scientific feedback of my committee members including Dr. Tom Barker, Dr. Johnna Temenoff, Dr. Eric White, Dr. Matthew Torres, and Dr. Melissa Kemp.

Certainly, "any road followed precisely to its end leads precisely nowhere" (Dean Herbert). The goal of my graduate studies was to prepare myself for the next stage of my scientific career, and so I am also grateful to everyone who assisted in my career exploration and development these past few years. To this end I would like to give a special thanks to my mentor Tom Barker who contributed greatly to my growth as an independent researcher by allowing me to pursue a project outside the scope of our lab's existing research and to truly make it my own. Further, he granted me permission to take three months off for an industrial internship as well as to attend conferences strictly for

the goal of professional development. I also need to thank my boss at Amgen, Dr. Abraham Gurerro for his instrumental professional guidance, as well as everyone at Amgen who took the time to offer both life and scientific advice. Finally, I want to thank Sally Gerrish, the Emory BEST program, and the Georgia Tech Career Development Center for sponsoring excellent guest speakers and workshops that provided insights into every aspect of scientific careers and career preparation that I could have possibly wanted.

Finally, I need to acknowledge that the journey that has become my thesis work has not been without its struggles. In fact, I have never failed so many times at so many things as during my time as a graduate student. Of course, if "success is going from failure to failure without a loss of enthusiasm" (Winston Churchill) I have many to thank for helping to maintain my sanity and at least a modicum of enthusiasm for my work throughout graduate school. Special mentions are necessary to Dwight Chambers, Jessica Joyce, Erin Hannen Edwards, Betsy Campbell, Cheryl Lau Emeterio, Travis Meyer, Claire Segar Olingy, Thien Tran, Amy Su, and Daniel Brown. And last but not least, I need to thank my family, in particular my parents and my brother who offered me endless love and support throughout this journey. Despite their own busy lives, they somehow always found the time for phone calls and offered nothing but empathy, even in face of my tendency to ramble on about research woes for which I'm sure they had little real interest. After all, "no young person on earth is so excellent in all respects as to need no uncritical love" (Kurt Vonnegut).

TABLE OF CONTENTS

LIST OF TABLES

LIST OF FIGURES

LIST OF SYMBOLS AND ABBREVIATIONS

ACPA	Anti-Citrullinated Peptide Antibody
AFM	Atomic Force Microscopy
CAF	Cancer Associated Fibroblast
CHO	Chinese Hamster Ovary Cell
Cit-Fibrin	Citrullinated Fibrin
Cit Fib	Citrullinated Fibrinogen
Cit Fn	Citrullinated Fibronectin
ECM	Extra-Cellular Matrix
FA	Focal Adhesion
FAF	Fibrosis Associated Fibroblast
FLS	Fibroblast-like Synoviocyte
GSK	Glycogen Synthase Kinase
HFF	Human Foreskin Fibroblast
IF	Immunofluorescence
IHC	Immunohistochemistry
ILD	Interstitial Lung Disease
IL	Interleukin
IPF	Idiopathic Pulmonary Fibrosis
MMP	Matrix Metallo-Proteinase
MS	Mass Spectrometry
OA	Osteoarthritis
PAD	Peptidyl Arginine Deiminase

pECM	Provisional Extra-Cellular Matrix
pFAK	Phospho-Focal Adhesion Kinase
PTM	Post-Translational Modification
RA	Rheumatoid Arthritis

SUMMARY

Activated fibroblasts have been implicated as drivers of disease progression in a variety of conditions including rheumatoid arthritis (RA), fibrotic diseases, and cancer. Cell characteristics such as invasiveness, hyperproliferation, apoptotic resistance, excessive contraction, extracellular matrix (ECM) secretion and remodeling, and enhanced inflammatory cytokine secretion are some of the main factors underlying disease exacerbating capabilities in these cells. Attempts to prevent, cure, or otherwise modulate the pathophysiology of these diseases to date has in part been hindered by a lack of understanding as to how fibroblasts become activated and are able to maintain their activated states, in some cases, even in the absence of immune or inflammatory stimuli.

The central hypothesis of this work is that an inflammation-mediated provisional extracellular matrix (pECM) modification called citrullination may be responsible in whole or in part for activated fibroblast phenotypes. Citrullination is a post-translational protein modification that is known to occur extensively and at very early stages within inflamed RA, fibrotic, and cancer tissues. To explore whether co-localization of activated fibroblasts with citrullinated pECM is merely a phenomenon or is sufficient to drive activated phenotypes, this research aimed to understand how citrullination of pECM alters cellular interactions and signaling at the molecular scale as well as to explore whether exposure to citrullinated pECM is a sufficient stimulus to bring about changes in a variety of fibroblast behaviors.

To investigate the influence of citrullinated pECM at a molecular level, mass spectrometry (MS) analysis was performed on citrullinated fibronectin (Cit Fn); integrin

interactions were studied via bio-layer interferometry (BLI), co-immunoprecipitation (Co-IP), and immunocytochemistry (ICC) assays; and finally, downstream signaling and protein products were explored via both Co-IP and ICC assays. MS identified 24 unique citrullination sites, five of which reside in the cell-binding domain of fibronectin (Fn), and result in a preference for α5β1 integrins over αvβ3 integrins on Cit Fn compared to Fn. The consequence of this α5β1 to αvβ3 integrin switch is initiation of mechanotransduction signaling including elevated levels of phospho-focal adhesion kinase (pFAK), phospho-Src (pSRC), phospho-integrin-linked kinase (pILK), vinculin, F-actin, and glycogen synthase kinase (GSK), all of which are integral components of focal adhesions and signaling networks critical in cytoskeletal remodeling and cell motility.

To investigate the ability of Cit-pECM to modulate fibroblast behavior, adhesion, proliferation, metabolic, apoptotic, gel contraction, and migration assays were performed in addition to atomic force microscopy (AFM) to probe cell stiffness and α-actinin and confocal video analysis to probe focal adhesion (FA) turnover. Cit Fn was chosen as the representative pECM protein for these studies due to its prevalence within inflammatory environments as well as known dominance in fibroblast preferential binding among pECM proteins. Fibroblasts were determined to possess decreased adhesion and spreading, increased stiffness, increased FA turnover, and enhanced migration on Cit Fn compared to Fn. No differences in proliferation or metabolism were observed. Apoptotic resistance to oxidative stress was shown to be enhanced in the presence citrullinated fibrin but not on Cit Fn compared to Fn.

Altogether, the findings from these studies indicate that while citrullination of pECM cannot bring about every phenotype associated with fibroblast activation, it is

sufficient to change several different fibroblast behaviors relevant to disease progression, especially that of enhanced migration which can contribute to cell invasiveness. Further, the fundamental nature of the α5β1 to αvβ3 integrin switch implies that citrullination has the potential to impact the interaction of many different cells with their ECM leading to potentially diverse phenotypes. Taken together, these results indicate that citrullination within the pECM is has significant consequences on cell function, and it may therefore constitute a viable therapeutic target in helping to prevent or ameliorate inflammation-mediated disease.

CHAPTER 1. INTRODUCTION AND SPECIFIC AIMS

Activated fibroblasts are a prominent feature in a variety of conditions, including rheumatoid arthritis (RA), fibrotic diseases, and cancer, and to varying degrees they have been shown to both drive and exacerbate the pathophysiology of these conditions. Some of the principal features associated with activated fibroblasts, compared to their senescent counterparts, are enhanced invasiveness, apoptotic resistance, extracellular matrix (ECM) remodeling, increased contractile ability, and excessive cytokine and protease secretion. Our current understanding of both how fibroblasts initially become activated and how they are able to maintain those activated phenotypes is incomplete, however, and filling this knowledge gap will provide essential information to develop newer and more effective therapeutics for these diseases.

The purpose of this current work was to explore one promising potential fibroblast activating factor: citrullination. Citrullination is an enzyme-mediated post-translational modification that occurs extensively in chronic inflammatory environments. Importantly, it is a very early event in disease development, occurring up to about ten years prior to disease onset in the case of RA. While many proteins are capable of being citrullinated, those associated with and upregulated in chronic inflammatory conditions—and therefore become more permanent structures of the cell microenvironment—are of particular interest here. Therefore, the central question of this research is as follows:

How does citrullination of the provisional extra-cellular matrix (pECM) influence fibroblast function?

This question was addressed through two specific aims:

Aim #1: Understand how citrullination of the pECM protein fibronectin (Fn) alters fibroblast integrin engagement and downstream signaling.

The *hypothesis* was that integrin engagement would be detrimentally impacted in an RGD-mediated manner, and that this would result in an alteration in outside-in signaling impacting such molecules as focal adhesion kinase (FAK), integrin linked kinase (ILK), and Rac and Rho. Experiments for Aim # 1 began with a MS analysis of Cit Fn to identify specific sites of modification. Bio-Layer Interferometry (BLI), adhesion assays using cells possessing only one type of integrin, as well as direct immunocytochemical (ICC) staining and immunoprecipitation (IP) assays were implemented to explore functional changes to integrin binding of Cit Fn. ICC and force-inducible IP assays were utilized in the exploration of downstream signaling resulting from alterations in integrin binding.

Aim 2: Investigate how Cit Fn as a stand-alone stimulus influences healthy fibroblast phenotypes.

The *hypothesis* was that changes in several of the phenotypes associated with fibroblast activation, including that of migration, apoptotic resistance, contraction, and proliferation would become altered as a result of exposure to Cit Fn. A variety of adhesion, Bromodeoxyuridine (BrDU), 3-(4,5-Dimethylthiazol-2-yl)-2,5-diphenyltetrazolium bromide (MTT), caspase 3/7, and wound healing assays were utilized to investigate cell spreading, proliferation, metabolism, apoptotic resistance, and migration, respectively. Additionally, atomic force microscopy (AFM) was employed to evaluate cell stiffness, gel

contraction assays were used to analyze cell contractility, and both α-actinin staining and confocal videos were used to determine differences in focal adhesion (FA) turnover.

Significance:

Cancer is one of the greatest causes of death worldwide, RA affects about one percent of the world population, and about 50 thousand new cases of pulmonary fibrosis are diagnosed each year. Altogether, the World Health Organization (WHO) estimates that 40% of all deaths can be attributed to a fibrotic response—either idiopathic or resulting from an underlying primary pathology—so together, these diseases and other chronic inflammatory conditions have a wide reach of harmful impact. To varying degrees for each, there currently exists a substantial unmet clinical need for therapeutic interventions that can cure or ameliorate disease symptoms in a wider range of patients. For instance, 40% of RA patients currently fail to completely respond to available treatments, and in the case of idiopathic pulmonary fibrosis, even the leading pharmaceutical interventions succeed only in slowing down disease progression. Activated fibroblasts are known to play a substantial role in driving disease progression in all of these conditions, yet few interventions, depending on the disease type, currently target their capabilities specifically, due in large part to a lack of understanding of their mechanisms of activation. Therefore, possessing a comprehensive understanding of activated fibroblasts and the factors that contribute to their activation is essential for developing therapeutics with maximal benefit for patients currently suffering from a panoply of inflammatory conditions.

CHAPTER 2. BACKGROUND INFORMATION

2.1 Citrullination in Human Health and Disease

2.1.1 What is Citrullination?

Citrullination is a post-translational protein modification that results in an arginine residue being converted to a citrulline residue through the primary ketimine group being replaced by a ketone group[1]. The immediate consequence is a slight mass increase of 0.984 daltons, the loss of a positive charge, and the alteration of the iso-electric point from 11.41 to 5.91 for every modification site [2]. At the molecular level, this modification can negate the ability of the former arginine to participate in ionic interactions with negatively-charged substrates and co-factors[3]. It can also influence the hydrogen bond forming ability of the protein [2, 3]. Through these mechanisms and others, citrullination may also result in an alteration of protein secondary or tertiary structure [4]. As a result of any of these changes, independently or combined, the overall function of citrullinated proteins and their ability to interact with other biomolecules and/or cells may be fundamentally altered.

2.1.2 Anti-Citrullinated Peptide Antibodies

While the phenomenon of citrullination was first identified in 1948 [5] it didn't become an object of serious scientific inquiry until its occurrence became associated with rheumatoid arthritis (RA), and even this realization took about three decades. It started when a mysterious new class of "anti-filaggrin" antibodies was discovered in the 1960's [6] that turned out to be a better diagnostic indicator for the development of RA than even

Rheumatoid Factor (RF), the gold standard at the time. RF is a self-antibody, first identified in the 1940's that is detected at an elevated frequency in the sera of 70-90% of RA patients. It is what allowed RA to be defined as one of the first autoimmune diseases [7, 8]. RF, however, is not a sufficiently RA-specific indicator since it is also found in several other chronic diseases as well as in a high percentage of healthy persons, especially the elderly, and it is currently thought to be a general consequence of immune activation [7, 9]. These "anti-filaggrin" antibodies on the other hand were found to be present in 60-76% of RA patients, but in less than 2% healthy individuals or patients with other diseases [2, 10, 11], and importantly, they were also present in patients with RF-negative RA [5]. A landmark 1998 paper eventually identified citrulline as the essential component being recognized by these "anti-keratin" antibodies, and this class of antibodies, re-labeled anti-citrullinated peptide antibodies (ACPAs) have been a standard component of RA diagnostics ever since [7].

Enhancing the diagnostic potential of ACPAs is the fact that they can be detected more than 10 years before the onset of RA, prior to occurrence of synovitis, a hallmark of the disease [7, 12]. Blood samples taken at these early stages indicate that ACPAs initially react to only a single citrullinated epitope [13], though with time, ACPA reactivity expands to a wider array of proteins, often cross-reacting with multiple different types of citrullinated proteins [2]. The overall specificity and sensitivity of ACPA and RA is 95% and 75%, respectively [14]. A second-generation citrullination diagnostic test, called the CCP2 test has since been developed, and this has a specificity and sensitivity of 98% and 80%, respectively [2, 15]. The CCP2 was developed by selecting a large panel of randomly-generated citrulline-containing peptides and testing these against both RA and control serum

obtained from numerous persons. The combination of sequences with the greatest sensitivity and specificity were eventually adopted for clinical use [9], and this is now the gold-standard in RA diagnostics [14]. It should be noted though, that since the CCP2 test does not correspond to citrullinated proteins generated *in vivo* for a particular patient, the test is not of much use for investigating disease etiology and pathogenesis [9].

ACPAs may even play a direct role in RA disease onset and progression. To start, the overall presence and titer level of ACPAs correlate to RA activity and severity, as determined through presence of other clinical RA indicators like presence of rheumatoid nodules, radiological destruction scores, and bone erosion [16]. ACPA-positive RA is also associated with denser lymphocyte infiltrations in the synovium, and more generally, a higher rate of joint destruction and erosion [2, 17]. ACPAs binding to citrullinated vimentin on the surface of osteoclasts has even been shown to activate these cells in a manner to promote bone resorption [7]. Nevertheless, the ACPAs themselves do not cause RA, as determined in a study whereby ACPAs administered to mice did not elicit an arthritic response. In a collagen-induced arthritis (CIA) mouse model, however, administration of ACPA resulted in a more severe course of arthritis [9, 18].

2.1.3 HOW does Citrullination Occur: An Introduction to Peptidyl Arginine Deiminase Enzymes and their Function

A class of intracellular enzymes called peptidyl arginine deiminases (PADs) represent the only way citrulline can be introduced into a protein [19]. There exist five PAD isoforms, all encoded by a single gene cluster on chromosome 1p35-36 [9], and with a single-species inter-isozyme conservation rate at about 50 percent [5]. The conservation of

each isotype among mammals is 70-95% [15]. The primary difference among PAD isotypes is their respective tissue expression locations. PAD1 is primarily expressed in the epidermis and uterus [2, 20]. PAD2 is the most widely expressed, being found in muscle cells, brain tissue, mammary glands, and haematopoeitic cells [20]. Its expression is, in part, regulated by hormones, with estrogen-changes correlating to expression levels in the pituitary glands and uteri in fetal rats [15]. PAD3 is mostly localized to hair follicles and the upper epidermal layer [2, 9]. PAD4 is predominantly expressed in immune cells as well as in the spleen, secretory glands, and several cancer cell lines [5, 21, 22]. It is the only PAD possessing a nuclear localization signal [23, 24]. PAD4 was formerly called PAD5 since it was the human homolog of rodent PAD4 and owing to its different reaction kinetics, believed to be a novel PAD [15]. Subsequent sequencing and expression data has since indicated that PAD4 and 5 are identical. Finally, PAD6 is expressed in eggs, ovaries, testes, the small intestine, spleen, lung, liver, skeletal muscle cells, and early embryos [2]. Nevertheless, it is missing a conserved cysteine residue found at the active centers of all the other PAD isotypes [20], and it is therefore believed to be a pseudoenzyme [24].

The citrullination reaction requires a supraphysiological concentration of calcium divalent ions in order to occur. PADs 1,3, and 4 bind directly to five calcium ions, and PAD2 binds to six calcium ions, all at distinct sites. The residues involved in these calcium interactions are conserved across the PAD family, and while the calcium may not be directly involved in catalysis, it can induce a series of protein conformational changes that are necessary for the formation of a functional catalytic site [24]. Binding of calcium to allow this bioactive conformation increases PAD activity 10,000-fold [21]. The calcium concentration required to achieve maximal PAD activation is about 100-times higher than

cytosolic calcium levels [19], with half-maximal activity occurring at 40-60uM [15]. This requisite calcium concentration may be achieved through any event that causes the mobilization of free intracellular calcium, including cellular differentiation, chemokine receptor ligation, apoptosis, and necrosis [9].

The apoptosis and necrosis of various immune cells, especially macrophages, is thought to be the primary source of calcium during citrullination reactions and helps explain why this post-translational modification (PTM) is predominantly associated with and localized to sites of inflammation [19, 25]. While all PADs are normally found intracellularly [26], the high-incidence of cell apoptosis and necrosis during inflammation also explains how such a wide array of extracellular proteins can come to be citrullinated. In fact, within synovial joints of arthritic rats it has been noted that extracellular proteins appear to be the predominant site of citrullination staining, though the local cells do stain positively as well [6]. To date, a pathway for cellular secretion of PAD has yet to be discovered. It should also be noted that autoantibodies developed to PAD enzymes themselves possess the ability to further activate PAD enzymes to augment citrullination [7].

2.1.4 WHERE Does Citrullination Occur

In theory, any accessible arginine moiety is susceptible to citrullination. Accessibility, of course, may be influenced by both the structure of protein substrates, steric hindrance of nearby accessory proteins, as well as pre-existing PTMs. In fact, methylation and deimination are generally thought to be mutually antagonistic PTMs [24]. PADs do also contain, however, several residues that are capable of specifically recognizing the

sequence of a peptide backbone and preferentially catalyzing citrullination at some locations over others. Both arginines located nearby to proline as well as those located within alpha helices are rarely citrullinated. NRRC, a sequence frequently found in beta turns, is the most likely sequence to be citrullinated [19, 24]. Assohou et. al. set out to explore the substrate specificity of PADs 2 and 4, investigating 320 and 178 citrullination sites, respectively, for the two enzymes [27]. PAD4 was found to be the more specific of the two enzymes, which means it tends to modify fewer sites compared to PAD2. For both PAD 2 and 4, a glycine or tyrosine located in the +1 or +3 position, respectively, relative to arginine resulted in a high likelihood of citrullination [27].

The particular class of proteins that can be citrullinated seems to be only limited by the location and accessibility of PAD enzymes. At least 53 distinct citrullinated proteins have been identified within the sera and synovial fluid of RA patients [2]. Currently, the only known method for elimination of citrullination marks is proteolysis of the affected protein. Even citrullinated histones can undergo proteolysis as a part of chromatin remodeling. Nevertheless, the dynamic presence of citrullination modifications on histones—at a rate faster than would be expected from histone proteolysis—seems to imply that there may also exist a class of enzymes capable of reversing citrullination, though as of yet, no such enzyme has been discovered [24, 28].

2.1.4.1 Citrullination of Fibrin(ogen)

Fibrin(ogen) is one of the most common targets for protein citrullination, with 75% of ACPA-positive patients possessing antibodies specific for citrullinated fibrinogen (Cit Fib)[29] . Fifty four out of its 81 arginines, or 66%, are susceptible to modification by

PADs 2 and 4, the type most commonly associated with RA and lung disease [30]. Among the modification sites are both RGD motifs, both thrombin cleavage sites, three locations involved in αvβ3 binding, and multiple sites within both the heparin and fibronectin binding domains. The majority of these sites (32) are found in the alpha chain, the cumulative effect of which is sufficient to produce an electrophoretic shift in just this chain when run on a denaturing gel [31]. The 17 or five modification sites in the beta or gamma chains, respectively, are insufficient to elicit a similar band shift. Further, since plasmin—the major protease responsible for fibrin clot degradation—cleaves its targets at basic amino acids like lysine and arginine, it is likely that citrullination of fibrin impairs normal degradation processes [19, 32]. Meanwhile, citrullination at thrombin cleavage sites has been shown to prevent the formation of fibrin knobs A and B; therefore fully citrullinated fibrinogen cannot be converted into fibrin [31].

The functional consequences of this modification are several. Citrullinated fibrin(ogen) is capable of binding to toll-like receptor-4 (TLR4) in a way that enhances macrophage stimulation beyond that capable with its unmodified counterpart [9, 33]. The result of this enhanced stimulation is an increased production of TNF-α, IL-1, IL-8, and Il-13 in macrophages [19, 33].

2.1.4.2 Citrullination of Fibronectin

While not as much is known about specific citrullination sites within fibronectin (Fn), thus far, nine distinct regions of Fn containing ten distinct citrullinated residues have been identified via mass spectrometry across two separate studies [25, 34]. These include the amino acids located at positions 234, 241, 1035, 1036, 1131, 1162, 1542, 2325, and

2356, none of which correspond to the RGD or PHSRN synergy sites. It should be noted however, that one MS study only analyzed Fn samples from two different RA patients, with coverage of only 53 or 28% respectively. This study identified the double-citrullination at residues 1035/36 as the most commonly targeted among Fn residues, being recognized by ACPA in 50% of established RA patients as well as in 45% of ACPA-positive early RA patients [25].

Not only is citrullination of Fn specific to inflammatory diseases, but its mere presence within the synovial fluid is specific to RA, as extracellular Fn accumulation does not occur in osteoarthritis patients [3]. In fact, the amount of Fn deposited on the surface of articular cartilage and found within synovial fluid is positively correlated to joint destruction in RA patients [3, 4].

More importantly, the citrullination of Fn is known to alter its interaction with bio-molecules and cells in a variety of ways. Cit Fn has demonstrated an enhanced affinity for vascular endothelial growth factor (VEGF) as well as a decreased affinity for both αv and β1 integrins, though it should be noted that in the case of β1 affinity, the tests were conducted as solid-phase binding experiments rather than with cells [35]. The study showing decreased αv affinity attributed it to citrullination at R234 in the DGR sequence that exists and can bind αv after it's been converted from NGR in an age-related chemical modification (see location in Figure 1) [34, 36]. The overall adhesion and spreading of fibroblasts, from both heathy and RA patients, on Cit Fn is reduced compared to that on unmodified Fn by about as much as 60% at early timepoints; this decrease of cell adhesion on Cit Fn appears to persist through to about 70 minutes following initial cell contact[4]. While as of yet, no direct link to RGD modifications have been found, it has been noted that

phosphorylation of FAK and paxillin within fibroblasts on Cit Fn is decreased compared to those on unmodified Fn [1, 4].

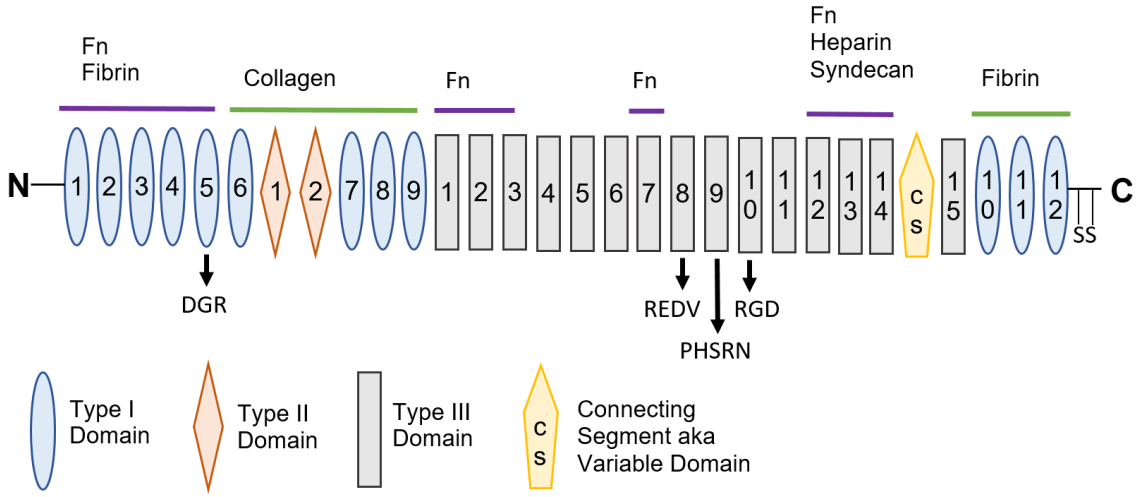

Figure 1: Fibronectin Functional Domains
This diagram depicts the various functional domains of the fibronectin (Fn) molecule with Type I domains shown as blue ovals, Type II Domains as orange diamonds, Type III Domains as grey rectangles, and the type III connecting segment as a yellow pentagon. On the underside of the Fn molecule are black arrows indicating the location of amino acid motifs relevant to integrin binding. Above the Fn molecule are colored lines indicating regions responsible for interactions with other ECM molecules.

Through altered β1 and αv attachment, citrullinated influences several characteristics of synovial fibroblasts. To start, Cit Fn promotes the secretion of proinflammatory cytokines, including TNF-α (in RA fibroblasts) , and IL-1 (in both RA and OA fibroblasts). [3]. No differences in IL-17 secretion were observed upon Cit Fn stimulation. Furthermore, Cit Fn possesses a protective effect with regards to apoptosis. For these experiments, RA or OA synovial fibroblasts were incubated with 2ug/mL Fn in solution, which served as a pro-apoptotic stimulus. Incubation with Cit Fn, in lieu of Fn, reduced cell apoptosis levels to those seen in fibroblasts incubated with the negative controls of BSA or citrullinated BSA, though it should be noted that differences between Fn and Cit Fn were only observed with activated RA cells and not those of OA patients. Apoptosis in

these cells was detected via Annexin V and Terminal deoxynucleotidyl transferase (TdT) dUTP Nick-End Labeling (TUNEL), in addition to changes in survivin, caspase-3, Bcl2, and cyclin-B1 transcriptional expression levels [3]. Similar apoptotic protective effects were observed with Cit Fn and a leukemia HL-60 cell line using both plasma and cellular Fn [35].

2.1.4.3 Citrullination of Collagen

Collagen II is one of the major targets of autoimmunity in both RA and lung disease [11, 29]. The GFOGER sequence can be modified by citrullination (Cit-GFOGER), and there also exist several additional sites that represent likely targets for citrullination [37]. These include both the repeating G-X-R-G-hydrophobic residue motif of collagen II (CII), and the RGD sites in collagen-integrin bridging molecules (COLINBRIs) [1, 11]. The ultimate result of this modification is a reduction of both cell adhesion and spreading on both Cit-CII and Cit-GFOGER in comparison to their unmodified counterparts. These results held true for a variety of cell types including osteosarcoma cells, synovial fibroblasts, and mesenchymal stem cells (MSCs), where reduction in adhesion was 20%, 50%, and 40% respectively. MSCs became completely detached from citrullinated surfaces within 48 hours, implying that citrullination of CII compromises the survival of this cell type [34, 37].

The underlying integrins responsible for this Cit-CII sensitivity were investigated through an exploration of CHO cells transfected with α1β1, α2β1, α10β1, or α11β1 binding to Cit-CII or Cit GFOGER. It was found that α10β1 and α11β1 integrins are very sensitive to collagen citrullination, since the PTM disrupts a crucial electrostatic sandwich that would normally be formed between GFOGER and either α10 or α11. On the other hand, α2β1

integrins are only minimally sensitive to collagen citrullination while α1β1 integrin binding is not affected by CII citrullination [37].

Somewhat surprisingly, α2β1 binding to citrullinated collagen IX (CIX), primarily associated with cartilage, was also detrimentally affected. This finding is important because while α2β1 binding to CIX is known to be arginine-dependent, CIX does not contain any GFOGER motifs. This therefore implies that citrullination sites outside of GFOGER, across the various collagen types, may also likely have impacts on cell function [37].

2.1.5 The Role of Citrullination in Disease

The influence of citrullination in human health and disease can most clearly be seen through its ability to elicit an immune response, as detected, in part, through the production of ACPAs. It has since been determined that this immune reactivity originates largely from the structure of MHC class II molecules carried on the surface of antigen-presenting cells. These MHC II molecules possess a highly conserved region responsible for antigen binding, and one of the pockets, termed P4, within this conserved region is positively charged and therefore prefers to interact with either polar or uncharged amino acids [5, 38]. Therefore, when proteins become citrullinated, and the positive charge of arginine is removed, they become much more readily able to interact with these P4 pockets, thus activating antigen-presenting cells and eliciting an immune response [38].

Substantiating this mechanism of immune activation are the several animal studies that have demonstrated the ability of citrullinated proteins to elicit immune responses in rodents. Lundberg et. al. investigated the immunogenicity of citrullination in one of the most common immune-compromised rodent arthritis models, “collagen-induced arthritis” or CIA

[6, 39]. In this study, while administration of both collagen II (cII) and citrullinated collagen II (Cit-cII) were sufficient to generate immune responses in rats, the Cit-cII was associated with an earlier onset and overall higher incidence of arthritis symptoms than its native counterpart. In the case of rat serum albumin (RSA), neither the native or citrullinated counterparts were sufficient to induce clinical arthritis, but citrullinated RSA did result in an antibody response [6]. These differential impacts of Cit-cII and Cit –RSA imply that the development of autoimmune responses to citrullinated proteins versus that of RA joint damage likely occur through separate mechanisms. That is, the presence of citrulline alone seems sufficient to activate autoimmunity, but protein-specific citrullination underlies other changes in cell responses.

There is also substantial evidence directly linking Cit Fib with immunogenicity. Hida et. al. demonstrated that immunization of healthy Balb/c mice with Cit Fib plus one of two different adjuvants was sufficient to generate an antibody response even though this was not accompanied with any clinical symptoms of arthritis or inflammation [40]. Hill et. al. immunized both an immune-compromised mouse line, along with wild type B6 mice with citrullinated or unmodified fibrinogen. In the immune-compromised mice, 35% of those immunized with Cit Fib developed progressive arthritis, versus 0% of mice given unmodified fibrinogen. While none of the B6 mice developed clinical arthritis, those immunized with Cit Fib did demonstrate some antibody reactivity along with T cell proliferation and increased IFN-γ production [38]. Yet another study demonstrated the ability of monoclonal IgM or IgG antibodies reactive with Cit Fib to exacerbate arthritis symptoms in a CIA model [11]. It should also be noted that fibrinogen-deficient mice are incapable of developing arthritis in the CIA model [33].

Citrullination has been associated with and is thought to play at least a contributory role in the development and exacerbation of a variety of diseases. Some of the more prominent of these diseases include multiple sclerosis [16, 32], lupus [24, 41], psoriasis [15], and most importantly, rheumatoid arthritis (RA)[35], interstitial lung disease (ILD)[13], and cancer [22]. The latter three of these diseases are of interest in part because evidence, in the form of serum ACPA titers and histological staining, is the most robust, but also because they share certain fundamental characteristics. Namely, each RA, lung disease, and cancer, is associated with excessively aberrant ECM deposition co-incident with abnormal fibroblast behaviors including hyperplasia and invasiveness; importantly, these abnormal cell behaviors are considered drivers of disease progression. Therefore, understanding the basic link between citrullinated provisional ECM and fibroblast function may produce important insights for each of these diseases.

2.1.5.1 Citrullination in Rheumatoid Arthritis

Rheumatoid arthritis is the single disease with the clearest connection to citrullination, with 76% of RA patients possessing ACPA in their sera compared to about 2-5% of non-RA patients[7]. ACPA titre level has also been shown to positively correlate with both RA activity and severity, including such factors as bone erosion, density of lymphocyte infiltrations, and the rate of joint destruction, [2, 16, 17]. ACPAs can be detected up to ten years before development of clinical RA symptoms, thus implying that the modification may possess a causative role in disease progression. Importantly, protein citrullination can also occur independent of an ACPA presence, since citrullinated fibrin has been found in synovial tissue of CIA mice whose serum did not contain ACPA [16]. Within an inflamed RA joint, extracellular protein deposits constitute the primary source of positive

citrullination staining, although cells and cartilage within this milieu do stain positively as well [6].

The enhanced immunogenicity to citrullinated proteins in RA patients may be explained by various immune mutations commonly found in these patient populations. The MHC class II HLA-DRB1 allele or shared epitope is the primary and best understood risk factor for RA [9, 42, 43] accounting for approximately one third of its heritability [17]. Expression of this allele can influence T-cell selection, antigen presentation, and peptide affinity, all of which can influence the development and progression of an autoimmune response [43]. The *PTPN22* gene, related to T and B cell receptor signaling and which has been shown to allow autoantigen-specific T cells to avoid clonal deletion, has also been linked to RA [5, 9, 17].

There also exist more direct links to citrullination and risk for RA development. Polymorphisms of the *PADI4* gene, which encodes the PAD4 enzyme, is associated with RA development in Korean, Japanese, and other Asian cohorts. This link is more controversial among Caucasian populations [9]. Also, P. gingivalis, the bacteria that causes periodontal disease (PD), are capable of producing and secreting their own distinct type of PAD enzyme, PPAD, that can effectively citrullinate mammalian proteins [9]. PPADs are unique in that they can deiminate free arginines as well as C-terminal arginines, unlike mammalian PADs. Further, at sufficiently high pH PPAD can remain active even without calcium [42]. PD is therefore considered a risk factor for RA and may constitute the event that breaks immune-tolerance for these patients [1, 44]. Importantly, ACPA titres are higher in RA patients with PD compared to their non-PD counterparts [42].

2.1.5.2 Citrullination in Lung Disease and Fibrosis

There exists such an extensive amount of overlap between citrullination in RA and lung disease that it can be difficult to separate the two; in fact, some scholars are of the opinion that they should not be separated at all, having defined a sub-class of interstitial lung disease (ILD) termed "RA-ILD" [45, 46]. These connections stem from the fact that 10-30% of RA patients also present with clinical ILD [47], and an additional 30% of RA patients have sub-clinical indications of ILD, such as bronchial wall thickening (specific to respiratory bronchiolitis ILD), that can be visualized on a CT scan. Monitoring of these sub-clinical cases shows that 34-57% will demonstrate radiographic disease progression over the following two years [48]. Pulmonary complications ultimately account for mortality in 10-20 percent of RA patients [47]. To look at this connection from the converse perspective, about 15% of ILD cases are also associated with connective tissue disease [49].

Further, there is direct evidence for citrullination occurring in the lungs. Lung samples from both RA-ILD and idiopathic pulmonary fibrosis (IPF) patients have been shown to stain positively for citrulline in 44 or 46% of cases, respectively [47, 50]; this is compared to positive staining in only 20% of healthy controls [50]. Further, both PAD2 and PAD4 protein and mRNA expression is upregulated in the lungs of IPF and RA-ILD patients above that seen in controls [51, 52]. While not all patients with positive citrulline lung staining necessarily develop an ACPA response, RA patients with clinically diagnosed ILD possessed an ACPA titer 46-273% higher than RA patients without ILD, and notably, high ACPA titer correlates with more severe ILD [45, 48]. Of course, as has already been mentioned, ACPA titer level is also positively correlated to a more severe course of RA [2, 17].

Smoking has independently been cited as the greatest environmental risk factor for both RA and ILD [17, 42, 53]. With the thousands of toxic compounds found in cigarette smoke, many of which can directly activate immune cells, cause tissue damage, and spur inflammation, this link with ILD may not seem surprising [9], but assuredly, the evidence for its deleterious effects in RA are just as strong. Available data demonstrates that smoking contributes a 21-fold increased risk for developing RA in ACPA-positive HLA-positive patients compared to HLA-negative patients [17, 46], and that overall, its contribution to developing an ACPA response is larger than that of genetics alone. This increased risk of ACPA-positive RA persists even in cases where smoking was discontinued up to 19 years before disease onset [13]. Finally, the Arthritis and Rheumatism Council's Twin study analyzed 13 pairs of monozygotic twins, all discordant for RA and smoking. Strikingly, in 12 out of these 13 cases, the RA patient was also identified as the smoker [9, 54].

Importantly, enhancement of citrullination has been cited as one of multitudinous effects of smoking. A study by Makrygiannakis showed that cigarette smoke has the ability to directly increase the expression of PAD2 in bronchoalveolar cells [55]. Notably, this also translated into positive citrulline staining in lung biopsies of 56% or 17% of smokers using two different antibodies, compared to 7% or 0% in non-smokers using those same respective antibodies. It's also been shown that PAD4 mRNA expression is higher in smokers [51], PAD2 expression is higher in the bronchial mucosa of smokers, and PAD4 protein concentrations are higher in the serum of lung cancer patients who smoke compared to those who do not [10].

Of course, smoking may also simply be a means for introducing inflammation into the lungs, which in turn, leads to citrullination. Bronchiectasis, a structural lung abnormality

associated with lung infections, is a significant risk factor of ACPA-positive RA, regardless of a patient's smoking status [56]. Further, a study by Lugli et. al. attempted to isolate the link between smoking and citrullination by studying the lungs of 40 human lung cancer patients who either had a concurrent diagnosis of chronic obstructive pulmonary disease (COPD) , or no COPD [12]. It's important to note that COPD is associated with pulmonary inflammation, capable of persisting even after a patient has long-since stopped smoking. This study found that in addition to PAD2 and PAD4, citrullinated proteins were found in lung samples from all 40 patients, though the overall amount of citrullination was significantly increased in patients presenting with COPD. The difference in citrullination was minimal between smokers and non-smokers, though the amount of PAD2 was larger in the lungs of smokers. Further, while across all patients signs of citrullination were found in multiple different organs, a comparative and substantially larger amount was consistently found in the lungs, indicating that this organ may possess an innate proclivity towards citrullination.

Taken together, a leading model for this evidence posits that citrullination, an inflammation-mediated modification, occurs first in the lungs, becomes exacerbated by an immune response, and then independently or concurrently builds in the lungs and/or the joint space. Factors like smoking serve to enhance inflammation, and certain genetic susceptibilities can worsen the immune response. Substantiating this theory is the fact that in the case of RA, when serum ACPAs are first detected, often up to 10 years in advance of symptoms, direct evidence of citrullination of synovial proteins typically cannot be found, implying that immune reactions must start in some location other than the joint [7, 13]. Further, blood samples taken in the earliest stages of ACPA presence (well before RA onset)

produce ACPAs that tend to only react against a single specific epitope [13]. Yet there ultimately ends up being a substantial overlap in citrullinated targets in both the lungs and joints of RA patients, indicating that there might be a common initiating site for this immune-intolerance [57]. Essentially, the lungs may represent a primary site of extra-articular RA manifestation, and through the chronic inflammation and immune responses associated with RA and ILD, they serve to create a mutually destructive disease course.

2.1.5.3 Citrullination in Cancer

As complex and as multi-faceted a disease like cancer is, one cannot argue that citrullination is the single root cause; nevertheless, there is substantial evidence to suggest that it acts as a crucial contributory factor in both its cause and exacerbation. As in all other instances of citrullination, the route for introduction in cancer would seem to be through chronic inflammation that allows for subsequent PAD enzyme activation. Cancer is associated with extreme amounts of fibrin generation, as observed in patient plasma, which is an indirect indicator of inflammation [58]. Further, there is a direct link between high levels of inflammation-associated proteins three years after cancer treatment and risk of both cancer returning and mortality [22].

The immunohistological evidence for presence of PAD4 in cancerous tissues is staggering. PAD4 is overexpressed in the majority of cancers to varying degrees [20], and while it is normally an intracellular enzyme, it can be detected in the plasma of patients with malignant tumors in abundance [28]. Interestingly, the strongest PAD4 staining is found in highly invasive tumors, including all adenocarcinomas, as well as cancers of the lung, breast, bone, colon, bladder, ovaries, and more [19, 22, 58, 59]. Meanwhile, there is no

PAD4 found in benign or non-tumorous tissues [23], and minimal to no PAD4 staining in hyperplastic conditions such as cervical polyps, teratomas, neurofibromas, and others [22]. While tumor ECM can stain positively for citrullination, the most intense staining is typically found within the cytoplasm or nuclei of the tumor cells as well as the monocytes and macrophages surrounding the tumors [10, 22]. Further, compared to healthy tissue, many more fibroblast-like cells within the tumor stroma region of adenocarcinomas show elevated expression of PAD4 [58]. This distribution of PAD4–predominantly intracellularly—may distinguish the role citrullination plays in a disease like cancer compared to RA and ILD, both of which are associated with significantly more extracellular staining.

The mechanisms through which PAD4 is thought to play a role in cancer progression are several. It has been shown to act as a co-factor for epithelial growth factor (EGF) activity as well as to activate transforming growth factor (TGF-β) signaling through citrullination of glycogen synthase kinase (GSK3β) [22, 60]. Of course, its primary means is that of a transcriptional regulator. PAD4 is known to have control over the genes *ING4*, *p300*, *HDAC2*, and *OKL38*/*BDGI*, as well genes regulated by the estrogen and thyroid receptors [59, 61, 62]. It is also known to decrease tumor suppression miRNAs like microRNA-16, which plays a key role in cell cycle regulation and proliferation [61]. Most strikingly, PAD4 is able to repress expression of p53 and all its associated genes, including p21, and pro-apoptosis genes like *BAX*, *AIP1*, and *NOXA* [62].

PAD4 citrullination of cytokeratin and antithrombin can also have deleterious consequences. In the case of cytokeratin, citrullination confers a resistance to degradation through caspases. Cytokeratin cleavage plays a role in membrane blebbing, cytoplasmic

shrinkage, cytoskeletal disassembly, and nuclear fragmentation in apoptotic cells, and thus by inhibiting these functions, PAD4 can interfere with normal cell death mechanisms [58]. Further, malignant cancers are associated with elevated serum levels of citrullinated antithrombin; modification of this enzyme renders it incapable of inhibiting thrombin [59]. Importantly, thrombin stimulates cell proliferation and inflammation. Thrombin also enhances formation of fibrin from fibrinogen, induces expression of β3 integrins, and increases the transcription of VEGF, all of which can promote angiogenesis [58, 59].

Finally, the proven effectiveness of PAD inhibitors in a variety of cancer cell lines and in animal cancer models gives incontrovertible credence behind PAD4's considerable role in cancer progression. One particular PAD inhibitor, Cl-amidine, has been demonstrated to possess dose-dependent cytotoxic effects in human promyelocytic leukemia HL-60 cells, breast cancer MCF-7 cells, osteosarcoma U2OS cells, and colon adenocarcinoma HT-29 cells, at concentrations as low as 500nM [59, 62]. Cl-amidine also possesses the ability to differentiate colon cancer HT-29 and leukemic HL-60 cells towards less cancerous phenotypes with expression of p21 [59]. Further, Cl-amidine was able to significantly reduce tumor multiplicity in a mouse model of colitis-associated colorectal cancer [61]. Importantly, Cl-amidine, has not shown cytotoxic effects towards non-cancerous cells like NIH-3T3s or HL-60 granulocytes [59]. Depletion of PAD4 through siRNA had similarly cytotoxic effects in U2OS cells, implying that inhibition of PAD4 is indeed the mechanism of Cl-amidine's effectiveness [62].

Cancer is a family of diseases that arise through a variety of often-combinatorial genetic mutations and which can impact a variety of different tissues and organs. Citrullination, while important, is just one component of the disease. While the results of

the various Cl-amidine cancer studies are certainly promising, it is also important to note that while dose-dependent, the *in vitro* cytotoxic effects of Cl-amidine are limited. Essentially, at higher doses, the effectiveness of this treatment starts to exhibit marginal changes in cell death, and ultimately it stops short of eliciting complete cell death [59]. Therefore, any future PAD inhibitory strategies for cancer would also need to focus on additional cancer targets.

2.1.6 Citrullination Inhibition Efforts

Due to the preponderance of evidence correlating citrullination presence with disease, and in some cases directly linking the two, a variety of efforts have been under way to develop a therapeutic strategy for inhibiting PAD function and therefore minimizing or eliminating citrullination *in vivo.* The earliest of these attempts focused on an existing chemotherapeutic agent, paclitaxel, that normally targets tubulin but at higher doses is also capable of inhibiting PAD [44]. Its efficacy for ameliorating RA was first acknowledged during its use to treat cancer in two different human patients [63], and it has since demonstrated an ability to both regress existing arthritis or altogether prevent its onset when administered prophylactically in both CIA rat and mouse arthritis models [44, 64]. It has also shown promising results in a phase I clinical trial, although its performance in a phase II trial was less conclusive [64]. Of course, paclitaxel is also known to inhibit cell proliferation and migration due to its interference of the microtubule cytoskeleton, and thus its anti-RA efficacy is likely a result of more than PAD inhibition alone. There also exist serious concerns about its toxicity profile, including severe gastrointestinal symptoms, among others [63].

There exist several therapeutics in development that more specifically target the PAD enzymes or their substrates with potentially fewer off-target side-effects. One of these is Component 18, which preferentially targets the non-calcium-binding form of PAD4 in a reversible manner. In targeting the inactive form of PAD4, component 18 functions predominantly intracellularly, and it arguably inhibits citrullination at its source [24]. 4SC Discovery in Germany is in an early stage of its PAD inhibitor program. Also, ModiQuest in the Netherlands is developing monoclonal antibodies against specific PAD-modified substrates, such as citrullinated histones. Their hope is that by maximizing the specificity of their antibody, it will ultimately be a safer therapy, especially considering that the full range of citrullination's physiological role is still not understood [65].

Both GlaxoSmithKline (GSK) and Bristol Myers Squibb have been involved with another class of PAD inhibitor called GSK484 in some sources. This compound non-covalently binds to a channel in PAD4 that that induces a large conformation change within the enzyme's active site [21, 65]. GSK484's action is reversible, it possesses negligible off-target activity, and pre-treatment of either human or mouse stimulated neutrophils at a concentration of 10uM was able to significantly reduce citrullination of histone H3 as well as NET formation [21]. It appeared that development of GSK484 was suddenly halted after about 10 years, possibly because PAD2 is also known to play a significant role in RA, and they realized that targeting PAD4 alone was insufficient. GSK484 was licensed to Padlock in 2015 and shortly thereafter acquired by Bristol Myers Squibb for further development [65].

Finally, there is Cl-amidine, a pan-PAD inhibitor that has been the subject of the largest number of animal trials to date, among PAD-specific inhibitors. It covalently binds

to PAD such that a conserved cysteine residue within the active site is modified, resulting in irreversible inactivation [61]. Though it is effective against all PAD isozymes at low micromolar potencies, Cl-amidine's efficiency varies such that it is most efficient at inhibiting PAD1 and then PAD4, PAD3, and PAD2 [20, 26]. Importantly, it preferably targets the calcium-bound form of PAD, and Cl-amidine itself requires calcium for proper functioning, facts which together should limit its activity to active sites of inflammation [24, 44].

Cl-amidine has been successfully used in a variety of pre-clinical models. In one mouse model of collagen-induced arthritis (CIA), it inhibited the clinical disease activity scores up to 55% without influencing T-cell, B-cell, or monocyte populations [26, 44]. Reportedly, work by Venables et. al. as demonstrated the ability of a Cl-amidine derived drug to completely halt the progression of RA in mice, though this work has not yet been published [65]. Cl-amidine has also shown efficacy in reducing the severity of disease in a mouse model of ulcerative colitis, though it is possible that its mechanism of action may have been different here, since ACPAs are not produced in this disease [66]. In a further departure from classic citrullination-associated diseases, Cl-amidine has also shown efficacy in diminishing arterial thrombosis and overall atherosclerosis burden in a mouse model [67]. Finally, Cl-amidine has shown efficacy against a variety of cancer cell lines as well as in pre-clinical cancer models, including two separate studies that investigated breast and colorectal cancer [24, 61].

It has been well-established that Cl-amidine's bio-availability profile is suboptimal, thus limiting its maximal therapeutic potential [20, 24, 41]; thus several optimization efforts have been under way. Cl-amidine's limited bio-availability—defined as short circulation

time and limited permeability through cell membranes—is tied to the facts that it is polar and highly water soluble [20, 24]. YW3-56 was designed circumvent these limitations by possessing increased hydrophobicity. YW3-56 was also given changes to its amino acid backbone that improves its PAD4 inhibition ability about 5-fold. Its cytotoxic effects against U2OS cancer cells and mouse sarcoma cells was improved by about 60 and 50-fold respectively compared to unmodified Cl-amidine. Further, it demonstrated an ability to reduce the tumor size in a mouse S-180 xenograft model to 51.5% or 27.1% of untreated controls when administered alone, or in combination with vorinostat, an FDA-approved treatment for this cancer, respectively. No adverse effects were observed with regards to the whole body or vital organ weight of nude mice after three months of YW3-56 treatment, implying that side-effects of this therapy are low, if at all existent [20].

BB-Cl-amidine is another more hydrophobic alternative developed by the same group that originally developed Cl-amidine. It is equipotent against PAD4 but 10 times more potent towards PAD2 [68]. Its cellular potency against U2OS osteosarcoma cells is 20-fold higher than Cl-amidine. Further, its half-life is 1.75 hours compared to just the 15 of minutes of Cl-amidine in mice. BB-Cl-amidine's use in a MRL/lpr mouse model of lupus demonstrated an ability to reduce disease severity by reducing splenomegaly, down-regulating several IFNγ-responsive genes, reducing renal inflammation, decreasing the urine albumin/creatinine ratio, and improving muzzle alopecia. These same improvements were also observed with Cl-amidine treatment, thought to a lesser extent [41]. Further, BB-Cl-amidine has been successfully used to almost completely reverse joint inflammation, both histologically and clinically in a pre-clinical RA mouse model at 10mg/kg [68]. This compares to the more moderate 50% improvement previously observed in a prophylactic

RA mouse model using 50mg/kg of Cl-amidine [26]. Importantly, no adverse effects, such as weight loss, have yet to be observed with BB-Cl-amidine administration [68].

2.1.7 The Physiological Function of PAD Enzymes and Citrullination

Owing to the therapeutic efficacy of PAD inhibitors thus far in a variety of pre-clinical disease models, an important question moving forward will be the possible deleterious side-effects of PAD inhibition in both a site-specific and off-target manner. Citrullination was first discovered in the context of antibody production in RA; before that, nothing was known of its normal physiological role, and to date, existing research efforts have fallen short of completely uncovering the full role citrullination plays in regulating various physiological functions. Nevertheless, citrullination has been shown to be involved in innate immunity, skin protection, gene regulation, and brain plasticity, among other areas, and thus additional research will be needed before the safety implications of PAD inhibition can be fully understood.

Citrullination's role in innate immunity stems from the ability of PAD enzymes to hypercitrullinate histones, resulting in a phenomenon called Neutrophil Extracellular Traps or NETosis [1]. Removal of the positive charge on histone tails decreases their ability to cling to negatively-charged DNA, thus allowing it to become unraveled. When this occurs to an extreme extent within neutrophils, the unraveled chromatin can be expelled outside of the cell forming a complex web-like structure with utility in physically entangling pathogens, especially bacteria [24]. Therefore, some fear inhibition of PADs may have negative impacts on immunity, although so far PAD4 rodent knockouts have not shown any increased risk of developing infections [65]. Importantly, increased amounts of aberrant

NETosis have also been observed in the pathogenesis of various autominnune diseases, including RA, lupus, and Alzheimer's disease, and thus it is possible that NETosis is involved in more than just innate immunity [24].

The ability of PADs to modify histones also allows them to more generally influence gene regulation through chromatin decondensation [24]. All four arginines on the tail of histone H3 are susceptible to citrullination, as shown through *in vitro* experiments, and importantly, this prevents recognition by methyltransferase. PADs can go so far as to reverse existing single histone methylation [28]. While citrullination has been documented to influence a variety of gene clusters, those of note include genes related to estrogen receptors, cellular differentiation, inflammatory cytokines, and p53 [19, 24, 65]. It is also thought that citrullination may be related to apoptosis and terminal differentiation, since de-condensation of nucleosomes renders DNA more susceptible to degradation, a phenomenon common to both of these processes [15].

Citrullination is also thought to play a role in areas as disparate as brain plasticity and skin structuring. While almost all myelin basic protein (MBP) is citrullinated in children under two, this number generally decreases with age to about 18% in healthy adults, and generally, the degree of citrullination is thought to be correlated with brain plasticity [19]. Further, citrullination up to about 45% is thought to contribute to de-myelination and the development of multiple sclerosis [16, 19, 23]. With regards to skin structure, citrullination of both keratin and filaggrin can alter both cleavage and cross-linking sites, along with protein shape, so that the overall 3D bundling structure of these proteins is altered [9, 23].

2.2 Activated Fibroblasts

Fibroblasts are spindle-shaped interstitial cells constituting the most abundant cell type within connective tissues. In homeostatic conditions they are considered to be a static population whose main function is the secretion, degradation, and general maintenance of healthy ECM [69, 70]. In the instance of wound repair they are known to become temporarily activated, a state generally associated with enhancements of proliferation, secretory profile, migration, and contraction, after which they return to a senescent state [71]. A relatively heterogeneous cell type both within and between tissue types, it is difficult to identify a universal fibroblast-specific marker, though staining for fibroblast specific protein 1 (FSP1), mesenchymal markers like collagen I and vimentin, or more generally the lack of expression of markers associated with other cell lineages has been met with some measure of success. Fibroblasts have also been identified by virtue of their hardiness and ability to be relatively easily isolated in culture via several passages on tissue culture plastic [69, 70].

The aberrant activation and/or maintenance of an activated phenotype in fibroblasts in diseases such as Rheumatoid Arthritis (RA), fibrosis, and cancer is well documented, and in each case it is thought to exacerbate or drive disease progression [72-74]. Understanding the underlying causes of aberrant fibroblast activation is therefore essential to our ability to treat and possibly prevent each of these conditions. While there is much overlap in the phenotype of activated fibroblasts across diseases, it would be erroneous to claim that they are all the same, and thus a detailed explanation of the specific roles activated fibroblasts play in RA, fibrosis, and cancer, the three main disease types with which they are commonly associated, is provided below.

2.2.1 Rheumatoid Arthritis Background

Rheumatoid arthritis (RA) affects 0.5 to 1 percent of the adult population worldwide, and it is traditionally considered to be an autoimmune condition [75, 76], therefore distinguishing itself as the most frequent human autoimmune condition [16]. Symptomatically, it is primarily associated with inflammation and pain in the small joints of the hands and feet, but larger joint inflammation is common [75]. Radiographic and histologic analysis of RA joints shows that joint destruction in the form of cartilage degeneration, and deformation and destruction of joint tendons, ligaments, bone, and cartilage underlie these symptoms [43, 77-79]. In fact, within one year of an RA diagnosis, 80% of patients are predicted to have experienced some amount of joint bone loss [43].

Unsurprisingly, as a chronic autoimmune condition, the inflammation associated with RA is not limited to joints. Cardiovascular disease constitutes the leading cause of death in RA patients owing largely to an increased rate of atherosclerotic artery disease that ultimately leads to myocardial infarction and cerebrovascular events [43, 49]. Pulmonary complications account for 10-20% of RA mortalities making it the second leading cause of death in RA patients [48, 49]. Up to 30% of RA patients are diagnosed with interstitial lung disease (ILD) [47, 48]. Furthermore subclinical airway abnormalities can be detected via CT scans in 66% of early-stage RA patients [80] leading many to believe that the lungs constitute an extra-articular site of RA development. RA has also been linked to chronic fatigue, skin ulcerations, skeletal disorders, lymphoma, and more [43, 49].

There certainly exists a strong genetic component to RA, half of which can be attributed to mutations in the *PTPN22* and *HLA-DRB1* genes [17], and both of which

substantiate the autoimmune basis of RA. *PTPN22* encodes protein tyrosine phosphatases that regulate both T and B cell receptor signaling [5, 9]. Importantly, this gain-of-function mutation allows autoantigen-specific T cells to escape clonal deletion therefore predisposing individuals to autoimmunity [5]. The *HLA-DRB1* gene controls major histocompatibility complex (MHC) expression and is possibly the greatest genetic risk factor for RA [42, 43] accounting for about one third of RA's heritability [17]. Mutations of this gene are associated with altered thymic T cell repertoire selection, decreased activation of regulatory T cells, and increased activation of self-reactive T cells [9]. Notably, this mutation enhances the preference for binding and presenting citrullinated peptides to the immune system [5].

Of course, genetic linkages do not tell the complete story. The concordance rate of RA among monozygotic twins is only 15% [9, 43], suggesting a strong influence of environmental and other factors. Possibly the largest known environmental factor is that of lung irritants including that of silica exposure, textile dust, and smoking [42, 43]. Smoke exposure increases the risk of ACPA-positive RA even upon discontinuation 10-19 years before disease onset [13]. In fact, a twin study of monozygotic twins discordant for RA and smoking found that in 12 of the 13 sibling pairs studied, the sibling that developed RA was also the smoker [54].

2.2.2 Activated Fibroblasts in Rheumatoid Arthritis

While autoimmunity and inflammation are certainly prominent and deleterious components of RA, environmental and other factors are also very important and help to explain why there still exists an unmet clinical need for RA therapies that are fully effective

for all patients. Almost all existing approved RA therapies can be classified as either steroidal or immunosuppressant drugs. Tumor necrosis factor-alpha (TNF-α)-inhibitors, a leading choice, are ineffective in a full one third of patients, and the benefits of TNF blockers generally fail to last following termination of drug administration [77, 79]. Other therapeutic targets include janus kinase (JAK), Fas Ligand, interleukin-6 (IL)-6, IL-1, and b-lymphocyte antigen (CD-20) [16, 75, 81-83]. Unfortunately, 40% of RA patients do not respond fully to any individual or combination of these existing therapies with many experiencing periods of disease remission followed by flare-ups and disease progression [81]. Sustained remission is rarely accomplished, and patients usually require lifelong pharmaceutical intervention [83]. Furthermore, the benefits felt from existing treatments tend to diminish over time [43] , owing likely to a build-up of therapeutic tolerance, but also of failing to target the instigating or driving factors of the disease.

In particular, activated fibroblasts are largely considered to be the primary drivers of RA disease. Within joints, so called fibroblast-like synoviocytes (FLS) are normally organized into a thin 1-3 cell-thick layer within the inner synovium, and they serve to produce molecules constituting the ECM and lubricant fluid essential for joint health [75, 76]. Upon activation, however, these cells become hyperproliferative, and along with resident macrophages produce a thickened intimal layer ranging from 10-20 cells thick [75]. Contributing to this thickened intima is FLS development of apoptotic resistance. In particular, activated FLS have been shown to be resistant to FasL-induced apoptosis [84] along with displaying increased expression of the anti-apoptotic proteins Bcl-xl, Mcl-1, and Bcl-2 [78, 79, 84] (see supplement Table 5 for abbreviations). This enhanced survivability even in the presence of chronic inflammatory stimuli—which has been shown to produce

abundant DNA breaks in FLS detectable via TUNEL—likely contributes to the many gene mutations that have been observed, most notably in the *p53*, *p21*, and *PTEN* tumor suppressor genes, which among other mutations leads to several pathologic phenotypes[75, 79].

Possibly the most striking pathology of activated FLS is their invasiveness, specifically into cartilage and bone tissues where they wouldn't normally be found, but also from one joint to another. Activated FLS have displayed both anchorage-independent growth [78] as well as a lack of contact inhibition [79] both of which may contribute to their ability to metastasize. Additionally, activated FLS possess an enhanced ability to adhere to collagen type IV, fibronectin, laminin, and tenascin compared to normal FLS [85], which is likely connected with their known upregulation of a variety of adhesion molecules [86, 87] including that of αv, α5, α6, β1, and β4 integrin subunits [85, 87] as well as I-CAM and V-CAM, the latter of which is constitutively expressed in active FLS [75]. Blocking studies have shown that β1-blocking partly or completely eliminates the ability of activated FLS to attach to a variety of ECM proteins and further, that the impact of this blocking was enhanced on RA FLS compared to normal FLS [85].

Exacerbating the enhanced migration tendency and adhesion molecule expression in activated FLS is the fact that inflamed joints are well-known to harbor excessive quantities of fibroblast-adhesive proteins—most notably those of the provisional ECM. A fibrin-rich pannus along articular surfaces of RA joints is one of the most conspicuous and consistent features of both human and experimental animal models of RA [29, 77], and it is thought to contribute to both leukocyte and fibroblast invasion into cartilage, a theory supported by the

fact that fibrinogen-deficient mice show diminished pathological and clinical RA development [33].

There also exist aberrantly high levels of fibronectin (Fn) within RA joints. Synovial fluid samples contain a 4-fold increase of Fn in RA patients compared to normal patients [88]. Histological staining shows prominent quantities of Fn on the cartilage surface as well as throughout connective tissue of RA patients compared to both osteoarthritis (OA) and heathy patients [74, 89]. Intensifying these differences is the fact that activated FLS are capable of producing and secreting excessive amounts of Fn, which can be demonstrated by *in vitro* culture of primary RA-FLS compared to OA-FLS [90]. Furthermore, concentrations of Fn detected within RA synovial fluid and joint tissues tends to far exceed the amount found within plasma indicating local synthesis [89]. The heavy presence of Fn containing extra alternate splice domains A and B (EDA and EDB) within RA joints confirms that the protein is being locally produced, since only about 1-2% of plasma Fn would be expected to possess these alternate splicing patterns [90]. Finally, it's important to note that a substantial portion of this Fn within RA joints is known to be citrullinated, which has been confirmed both from the presence of Cit-Fn specific ACPAs as well as co-localization of Fn and peptidyl-citrulline histological staining [35].

Not only do activated FLS migrate into cartilage and bone, but they also possess the ability to produce and secrete enzymes that degrade these tissues. This includes an assortment of matrix-metalloproteinases (MMPs) including MMP-1, 3, 8, 9, 13, 14, 15, and 16 [43, 74], all of which contribute to breakdown of collagen of types II, IX, and X along with Fn, aggrecan, and any other leucine rich proteins like fibromodulin [78, 79]. Activated FLS are also known to secrete cathepsins B, L, and K along with

a disintegrin and metalloproteinase with a thrombospondin type (ADAMTS) 4 and 5, all of which further exacerbate soft tissue destruction. Once activated FLS arrive at bone they are able to directly activate osteoclasts to enhance bone erosion and destruction through a combination of myostatin expression and production of nuclear factor-kB (RANKL) [78, 79].

Finally, activated FLS possess the ability to activate and recruit immune cells through secretion of a mixture of growth factors and inflammatory cytokines. CXCL1 and vascular endothelial growth factor (VEGF), the latter of which is constitutively expressed by activated RA FLS in culture, contribute to angiogenesis [74, 79]. Activated FLS are also known to produce IL-6, 8, 7, 15, 16 18, 33, and 32, along with TGF-β, MCP-1, and TNF-α [17, 74, 75, 79, 81, 87] (See Table 3 in supplement for abbreviations). Activated FLS are considered the primary producers of Il-6 within RA joints [75], and co-culture of active FLS with monocyte –derived macrophages regulates almost one third of TNF-induced genes [74]. Activated FLS are also known to directly activate immune cells through direct binding of V-CAM-I and ICAM-I [76] as well presentation of auto-antigens via MHC II receptors [74]. It's also important to note that through a combination of enhanced expression of toll-like receptors 1 through 10 [17, 74] as well as constant exposure to a variety of cytokines within the inflammatory milieu, FLS can be stimulated to produce even more excessive quantities of both inflammatory cytokines as well as MMPs in a destructive feed-forward loop [74, 81].

The fact that cytokines produced by both activated FLS and a variety of immune cells are capable of reciprocally activating each other may lead some to question which activity comes first and which is the primary driver of disease. This query currently has no

definitive answer, but several pieces of evidence showing the destructive natures of active-FLS even in the absence of inflammation and immune activation point towards them being the drivers of RA disease. First, in an MRL-lpr/lpr mouse model of RA, the FLS were shown to become activated and invade joint structures prior to any inflammatory cells reaching the synovium [79, 91]. Second, when cadherin-11, a cell-cell adhesion molecule expressed only by FLS in synovial linings, was knocked out in a mouse model of RA, inflammation was reduced by 50%, and cartilage erosion was prevented [76]. Third, and possibly most convincing is a study be LeFevre et. al. whereby activated human RA FLS were implanted along with healthy cartilage into just a single joint each of SCID immune-compromised mice. The researchers found that not only were the RA-FLS able to invade into and degrade the cartilage where they were implanted, but they were also able to migrate to the contralateral joints and invade and degrade the cartilage there as well [86].

2.2.3 Activated Fibroblasts in Fibrosis

Fibrotic activated fibroblasts (FAFs), or myofibroblasts as they are often called, are widely considered to be the drivers of fibrotic disease, especially in the case of lung fibrosis [92]. Similar to activated RA FLS, they display such characteristics as enhanced migration, increased cytokine and growth factor secretion, improved integrin surface expression, excessive proliferation, and apoptotic resistance [71, 93-97]. Also like RA FLS, FAFs are capable of retaining these activated phenotypes even after being separated from their diseased environment [98]. Unlike with RA FLS, however, these altered phenotypes tend to have a more localized impact on a single organ or tissue. For example, in the case of idiopathic lung fibrosis (IPF) the enhanced fibroblast migration results only in translocation from the interstitial compartment of the lungs into the air spaces [95].

Another distinguishing feature of myofibroblasts is their relationship with the inflammatory environment. Fibrosis is commonly thought of as a disease of chronic wound healing in which inflammation plays the most prominent role in early stages and less so later on, and possibly because of this, treatment of IPF with immunosuppressive therapies has had only limited benefits [93, 99]. Activation or myofibroblast differentiation is a normal component of wound healing whereby the enhanced migratory capacity allows typically stationary fibroblasts to migrate into the wound environment and to secrete copious amounts of ECM proteins, in particular Fn, to provide a tissue scaffold for subsequent migration of epithelial and immune cells essential for the normal repair processes [97]. In later stages of this wound healing response, the ability to contract with enhanced force is imperative for bringing the edges of the wound together to minimize the surface area of denuded tissue [94]. The final contributions of myofibroblasts in normal wound repair is secretion of MMPs and other proteinases to restructure the ECM so that it matches that of normal tissue, and finally, to enter into an apoptotic pathway or become senescent since the number of fibroblasts required for maintenance of healthy tissue function are much lower than that required for active wound healing [53, 97].

Myofibroblasts become pathologic then when they fail to cease their wound healing functions and instead continue proliferating, secreting large amounts of ECM molecules, and contracting the environment around them. So while FAFs also secrete MMPs and actively restructure their environment similar to RA FLS, rather than degrading the tissue around them, FAFs are more infamously known for causing an excessive build-up of matrix proteins to the point where the bulk modulus of the tissue increases resulting in stiffer tissue that is impaired in function. In alignment with this phenomenon, the key symptoms of IPF

are progressive breathlessness, a decrease in Forced Vital Capacity (FVC), and ultimately respiratory failure [71, 97]. This being said, fibrotic tissues tend to be quite heterogeneous with regards to stiffness whereby there exist regions of dense fibroblast presence and ECM deposition—termed fibroblastic foci—intermixed with soft and seemingly healthy tissue [100, 101]. Generally, a greater overall number and area of fibroblastic foci correlates to a more severe progression of IPF [71].

Myofibroblasts have the ability to enhance the stiffness of their environments through a variety of mechanisms, the first of which is aberrant mechanotransduction. An abnormally high proportion of fibroblasts in IPF lungs are known to be negative for the thy-1 receptor (thy1-/-) resulting in the misinterpretation of soft surfaces as being stiff [102]. All cell types, and in particular fibroblasts, are known for engaging in substrate stiffness matching, [103], and so aberrant interpretation of an environment as being stiff can actually lead a fibroblast to transform its environment into a stiff one. This task is primarily accomplished through a combination of enhanced protein secretion and contraction. Such fibroblasts can mostly be identified via expression of alpha-smooth muscle actin (α-SMA), a protein important in the production of strong traction and contraction forces that is not normally expressed by senescent fibroblasts [96, 104]. Along with enhanced α-SMA, myofibroblast also express unusually high amounts of myosin heavy chain, vinculin, Rho and ROCK kinases, and F-actin, all of which are important to cell contraction and mechanotransduction [96, 105]. The end result is tissue, which in the case of bleomycin-induced fibrosis, generates twice the contractile force of normal lung [106].

Of course, a key driver of tissue stiffening is myofibroblast secretion of excessive quantities of matrix proteins. Myofibroblasts are the primary source of ECM proteins

deposited during lung fibrosis [72]. Their deposition of collagen, primarily types I and III, but also types IV, V, and VI [107, 108] occurs to such an extent that the majority of IPF patients show positive collagen staining within dense fibroblast clusters throughout the lung, whereas in normal adults the constitutive rate of collagen synthesis is low enough that fibroblasts would normally remain unstained [106]. Myofibroblasts also deposit large quantities of glycoproteins and proteoglycans including Fn, laminin, and tenascin [107]. Importantly, the majority of the Fn secreted by myofibroblasts contains the EDA splice segment, which is known to promote both further myofibroblast differentiation and also cell migration [92, 96].

2.2.4 Activated Fibroblasts in Cancer

According to the World Health Organization, cancer is quickly becoming the largest single cause of mortality in the world, surpassing even heart and vascular disease [109]. Traditionally, cancer treatments have focused on specifically targeting cancer cells, and they largely ignored the tumor stroma, defined roughly as the basement membrane, ECM, capillaries, immune cells, and fibroblasts that surround cancer cells [98]. Research in the past few decades, however, has elucidated the supreme benefit of tumor stroma towards tumorigenesis, malignancy, and even therapeutic resistance, thus shifting the perceived importance of this tissue compartment and the cells therein [110, 111]. Key characteristics of tumor stroma include an abnormally high presence of fibroblasts, enhanced blood vessel density, and increased concentrations of primarily collagen type I and fibrin compared to normal stroma [98].

When the tumor stroma is sufficiently modified by its surrounding cells, it becomes desmoplastic, or similar to stroma that may be seen in fibrotic tissues [98]. Indeed, desmoplasmic tumor stroma have been described by many in the field as wounds that never heal [111]. Desmoplasia can be found in association with both primary tumors and in metastatic sites, and they are generally correlated with poor prognosis [73, 112]. Similar to fibrotic tissues, tumor desmoplasia are on average stiffer than healthy tissues due to an increased deposition of ECM constituents, primarily fibrin, Fn, and collgens types I and III [98]. Unlike fibrotic tissues, however, desmoplasia tend to display an increase in degraded type IV collagen, and further, whereas organ fibrosis is associated with a reduction in microvascular presence, desmoplasia actually tend to be better vascularized than normal tissues [98, 112].

Not only is the presence of fibroblasts enhanced within tumor stroma, but a majority of these—over 80 percent in the case of breast cancer—become activated [111]. Cancer activated fibroblasts (CAFs) are found in almost all solid tumors though they are particularly abundant in the stroma of prostate, breast, and pancreatic tumors [73, 112]. Importantly, the current cancer literature identifies CAFs as key mediators in tumor proliferation, invasion, and metastasis [73, 98]. Similar to FAFs, CAFs can mostly be identified via α-sma staining, and similar to both FAFs and RA FLS, CAFs share several altered phenotypes including enhanced proliferation, migration, cytokine secretion, growth factor secretion, integrin expression, protease secretion, and apoptotic resistance [98, 113-115].

The primary difference between CAFs and both RA FLS and FAFs is that whereas the latter two are considered primary effectors of disease—i.e. they are each independently capable of driving their respective diseases, if not causing them—CAFs mainly serve to

facilitate the deleterious capabilities of their associated cancer cells. This influence can be quite drastic, as in a study of melanoma cell metastasis it was shown that the only cells able to metastasize were the ones influenced by fibroblasts [116]. Further, CAFs have been documented potentiate the malignancy of epithelial cells that were otherwise phenotypically and morphologically normal as well as to facilitate the progression of tumors of immortalized but non-tumorigenic cells [110]. These impacts are possible even in the absence of a functional immune system, as CAFs from human breast carcinoma injected into imuno-deficient mice along with the cancer cell line MCF-7 resulted in more quickly growing carcinoma than in the case where CAFs were co-injected with normal fibroblasts [117].

CAFs mediate these impacts primarily by secreting an impressive quantity and variety of cytokines, chemokines, and growth factors. While this is also a feature of FAFs and RA FLS, the secretion profile of CAFs is both more diverse and has an emphasis on signaling that promotes angiogenesis. Angiogenic growth factors secreted by CAFs include EGF, FGF-2, IGF-1, bFGF, PDGF, and VEGF [111] (see Table 4 in supplement for abbreviation definitions). VEGF in particular is a key stimulator of de novo blood vessel growth, and PDGF is important for the stabilization of these vessels. Angiogenic chemokines secreted by CAFs include GDF-15, TGFβ-2, CCL-5, CXL-12, CCL-11, CSF-1, CSF-2, SDF-1 and IFNγ. SDF-1, in particular, plays an integral role in recruiting endothelial progenitor cells [111, 112]. It's also important to note that the secretion of cytokines, like Il-6, and growth factors, like TGF-β, by cancer cells and CAFs alike has a reciprocal effect on cell activation [110, 111].

Finally, CAFs mediate their effects by secreting and modifying the ECM that makes up the tumor stroma. CAFs secrete enhanced quantities of collagens I, III, IV, and V, laminins, Fn, and fibrinogen in addition to a variety of enzymes that allow for enhanced cross-linking and bundling of these proteins [98, 109]. Aligned collagen fibers are characteristic of tumor stroma, and these have been shown to promote tumorigenesis, early dissemination, and metastasis of breast cancer cells [110]. Concurrently, CAFs secrete a panoply of proteases, including MMPs 1,2,3,7, 9, 12, 13, and 14, all of which contribute to the breakdown of tissue boundaries that ultimately promotes tumor expansion, invasion, and metastasis as well as angiogenesis [109, 112]. Additionally, they can contribute to cleaving—and thereby activating—growth factors and pro-inflammatory cytokines and receptors as well as releasing bound growth factors from matrix molecules. Protease cleavage can also incapacitate cell adhesion molecules which can influence cell motility and epithelial to mesenchymal transition (EMT) [109, 111, 112]. Finally, CAFs utilize force-mediated matrix remodeling dependent on α3 and α5 integrins and rho-signaling to generate tracks in this dense ECM through which cancer cells can potentially follow [73, 109].

2.3 Integrin-Mediated Mechanotransduction

In beginning to understand how citrullination of the provisional matrix may influence fibroblast phenotype, one first needs to understand how fibroblasts interact with their physical environment. Fibroblasts form physical attachments to the ECM predominantly using varying combinations of integrin proteins that extend across the cell membrane to physically link the ECM to the actomyosin cytoskeleton. Through these attachments, fibroblasts are able to both exert forces on their environment as well as to sense the rigidity of their surroundings, a process termed mechanotransduction [118]. Rigidity

sensing alone can influence a multitude of cell phenotypes including proliferation, migration, and differentiation [118-120].

There exists copious evidence that fibroblasts are able to sense and respond to changes in substrate stiffness. The first is a phenomenon called stiffness matching whereby fibroblasts possess the ability to adjust their own shear moduli so that they are matched or just below that of the surfaces on which they are plated. Fibroblasts exhibit stiffness matching as a linear function on substrates ranging from 0.5 to 4kPa, achieving a maximal shear modulus of around 10kPa [103]. Cell stiffness also strongly correlates with cell spread area, and starting at around 2-3kpa, fibroblasts begin to produce stress fibers which increase in number and become thicker as they get reinforced and bundled on progressively stiff surfaces [103, 120, 121].

As fibroblasts are exposed to increasingly stiff substrates, they also exhibit changes in their focal adhesions (FAs). FAs are the macromolecular complexes consisting of integrins and downstream adaptor and signaling molecules that allow cells to biochemically respond to ECM interactions [118]. As fibroblasts are exposed to increasingly stiff substrates, their FAs increase in both size and number with a variety of integrin subtypes becomes upregulated [103, 121]. Contributing to the increase in FA size is the phenomenon of integrin clustering whereby multiple integrins are recruited to a single attachment site to help reinforce the strength of attachment up to about 6-fold [121, 122]. In particular, both α5 and β1 integrin subunits demonstrate enhanced cell surface expression in the presence of stiff environments [119].

2.3.1 Mechanotransduction Signalling

Downstream of integrin adhesion and clustering, a plethora of adhesome complex proteins—at least 180 in total—can become engaged in scaffolding and/or signal transduction [120]. A mechanosensory review by Horton et. al.[118] describes four main axes of mechanotransduction signaling as follows: the Kindlin-ILK-Pinch axis, the FAK-Paxillin axis, the Talin-Vinculin axis, and the α-actinin-VASP axis. As downstream signaling is an inordinately complex process with substantial overlap among pathways, a summary of the main signaling events as described by Horton et. al., Windmaier et. al., Harburger et. al., Mitra et. al. and Wu et. al is provided in Figures 1 and Figures 2 below which divides the signaling into three main pathways [118, 123-126]. Several key players are represented in these pathways, though it should be acknowledged that many intermediate and terminal steps as well as alternate signaling pathways were omitted for the sake of simplicity.

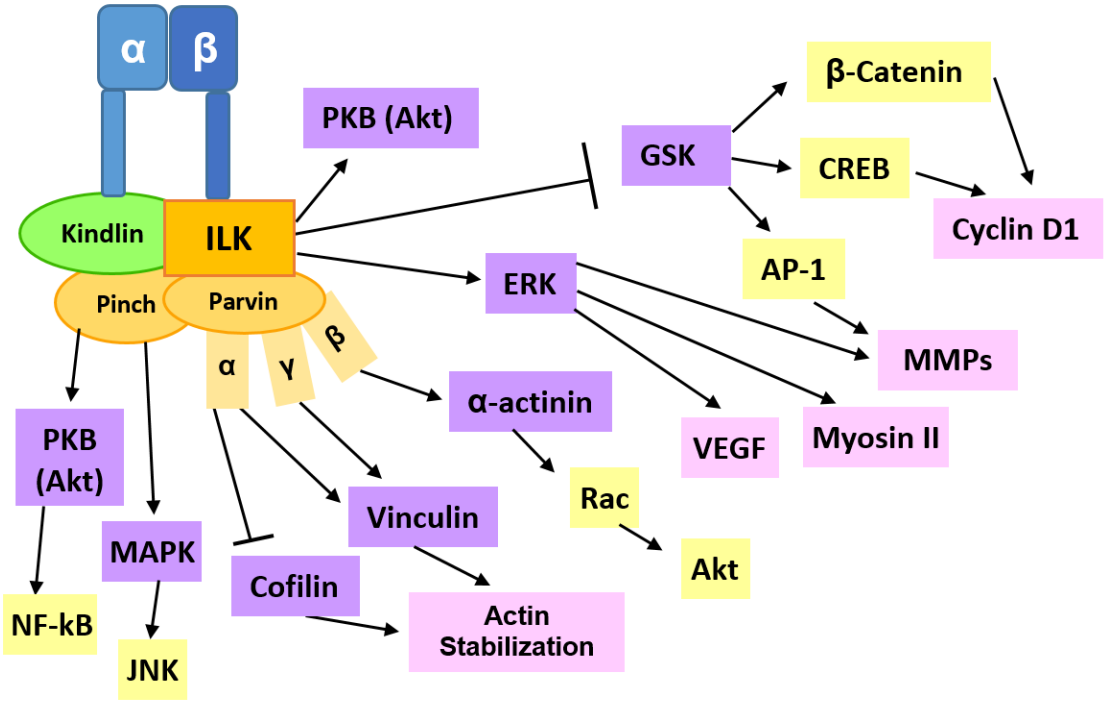

Figure 2: The ILK-Kindlin Mechanotransduction Axis The above diagram depicts the particular axis of signaling that can transpire from integrin engagement (depicted in blue). Arrows indicate an activating step whereas inverted "T" shapes indicate inhibitory steps. Proteins representing the terminal step of a pathway are shown in pink. Shapes placed in direct contact with each other (without an arrow in between) are representative of proteins that are bound to one another as opposed to engaging in a transient interaction.

Many of the proteins depicted in figures 2 and 3 are directly involved in actin-stabilization. One of these is α-actinin, which is recruited in all three of the pathways depicted, binds directly to F-actin, and is required for reinforcement of adhesion sites in fibroblasts; its presence generally correlates with stable FAs [118, 124]. Vinculin also appears in all three pathways, both as a downstream effector and as an entity that binds directly to scaffolding proteins attached to integrin tails. Its recruitment to talin, in particular, is very sensitive to local stress application, responding to just a few pico-newtons of force [120, 127].

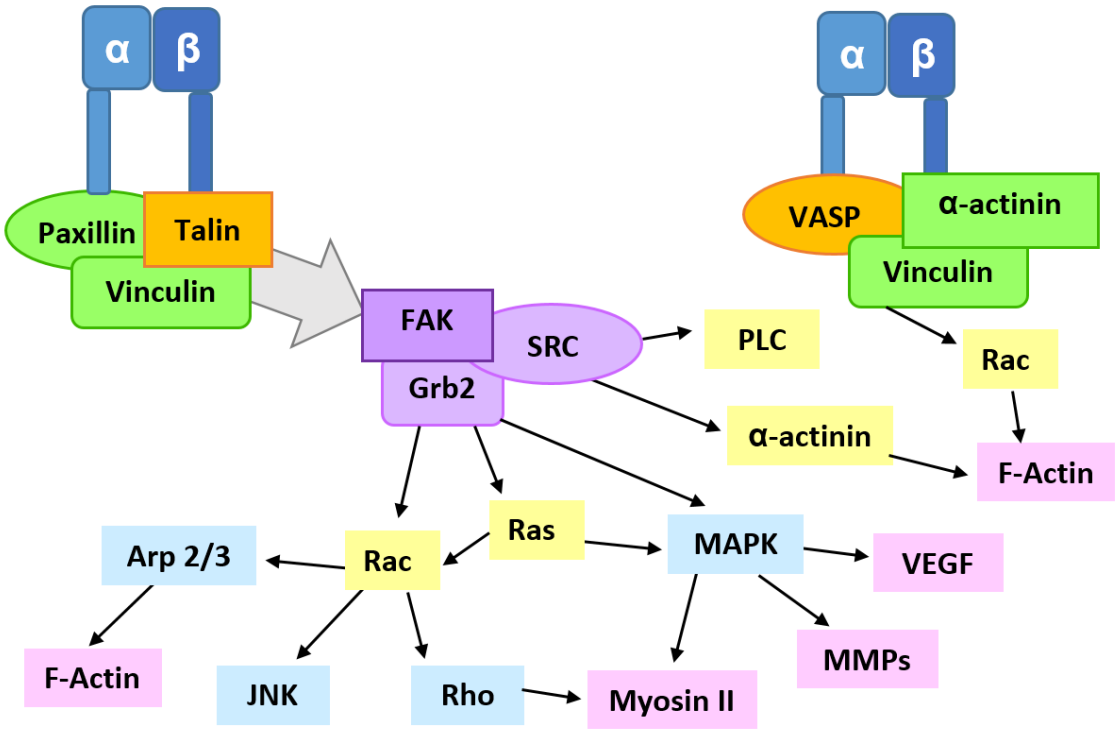

Figure 3: The Paxillin-Talin and VASP-Actinin Machanotransduction Axes
The above diagram depicts two different axes of signaling that can transpire from integrin engagement (depicted in blue). Arrows indicate an activating interaction. Proteins representing the terminal step of a pathway are shown in pink. Shapes placed in direct contact with each other (without an arrow in between) are representative of proteins that are bound to one another as opposed to engaging in a transient interactions. Each color change represents a molecule that is further downstream of a signaling cascade.

Also of prime interest is focal adhesion kinase, or FAK. FAK can only be activated in direct association with the integrin β1 [128]. It's clearly an effector of a variety of downstream pathways, though it is generally known as a mediator of FA turnover and cell migration. FAs can still form in the absence of FAK, but their disassembly is dependent on FAK phosphorylation, as demonstrated in FAK-null fibroblasts that displayed excessive formation of focal contacts [124, 129]. Inhibition of FAK in fibroblasts stimulated with PDGF resulted in a significant reduction of migration in a dose dependent manner of FAK

inhibitor. Such effects play an important role in the pathology of fibrotic and other diseases, as highlighted by the ability of a FAK inhibitor to protect against lung fibrosis in mice [128].

Table 1: Signaling Proteins

Protein Abbreviation	Full Name	Type
Akt or PKB	Protein Kinase B	kinase
AP-1	Activator Protein-1	transcription factor
Arp2/3	Actin-Related Protein2/3 Complex	scaffold proteins
CREB	cAMP response element-binding protein	transcription factor
ERK	Extracellular Signal-regulated Kinases	kinase
FAK	Focal Adhesion Kinase	kinase
Grb2	Growth Factor Receptor-Bound Protein 2	adaptor protein
GSK	Glycogen Synthase Kinase	kinase
ILK	Integrin Linked Kinase	kinase
JNK	c-Jun N-terminal Kinases	kinase
MAPK	Mitogen-Activated Protein Kinase	kinase
MMP	Matrix Metalloproteinase	protease
NF-kB	Nuclear Factor kappa-light chain	transcription factor
Pinch	Particularly Interesting Cys-His-rich protein	adaptor protein
PLC	Phospholipase C	enzyme
Rac	Ras-related C3 botulinum toxin substrate	G protein
Rho	Ras-homologous	G protein
Src	Proto-oncogene tyrosine kinase Src	kinase
VASP	Vasodilator-simulated phosphoprotein	adaptor protein
VEGF	Vascular Endothelial Growth Factor	growth factor

Another key effector protein is Integrin Linked Kinase (ILK), which carries out its many functions in a variety of different fashions. ILK is directly recruited to β1 and β3 cytoplasmic domains, though it has a strong preference for β1 [125, 130]. Through one set of pathways, it acts as a scaffolding protein with various combinations and types of Pinch and Parvin molecules which then enact an assortment of downstream signaling [125, 131] that can impact cell phenotypes such as survival, proliferation, and migration [123]. ILK also possesses direct catalytic function and can activate both ERK (aka MAPK) and PKB

(aka Akt), as well as inhibit glycogen synthase kinase (GSK3-β)-related signaling. Akt has been linked to cell survival and proliferation, and unsurprisingly, ILK is therefore known to be overexpressed in many forms of cancer [125]. Inhibited GSK actually results in the activation of β-catenin signaling as part of the canonical Wnt signaling pathway that targets several tumor suppressor genes [132-134] and is known to impact a myriad of cell functions including proliferation, migration, apoptotic resistance, differentiation, MMP secretion, and more [134-136]. Predictably, inhibition of GSK was shown to exacerbate skin fibrosis in a skin scleroderma model [137].

CHAPTER 3. THE INFLUENCE OF CITRULLINATED FIBRONECTIN ON INTEGRIN BINDING AND DOWNSTREAM SIGNALING

3.1 Abstract

Citrullinated fibronectin (Cit Fn) is abundantly present within tissues of a variety of chronic inflammatory diseases, and there is currently a dearth of understanding with regards to how Cit Fn interacts with fibroblasts, a cell type of particular interest in the progression of many of these diseases. To begin elucidating these interactions, mass spectrometry (MS) was performed on Cit Fn and identified 24 unique citrullination sites, five of which reside in the Fn cell-binding domain. Interferometry was used to probe the precise nature of α5β1 and αvβ3 integrins with Cit Fn demonstrating minimal change in the former and a decrease in the latter. A variety of fibroblast immunocytochemistry and force-inducible co-immunoprecipitation assays were employed to evaluate integrin-mediated signaling changes and identified not only an αvβ3 to α5β1 integrin shift, but an increase of β1-linked mechanotransduction including enhancement of focal adhesion kinase (FAK), integrin linked kinase (ILK), glycogen synthase kinase (GSK), F-actin, and other proteins. Altogether, findings indicate that exposure of fibroblasts to Cit Fn is sufficient to elicit prominent changes in mechanotransduction signaling that would be expected to have fundamental impacts on cell phenotype.

3.2 Introduction

Citrullination is an inflammation-mediated post-translational modification (PTM), and therefore, in determining how it is likely to impact fibroblast interactions with the ECM, it is logical to focus on the proteins most likely to be present in an inflammatory environment, or the so-called provisional matrix. The two most obvious candidates are therefore fibrin, a blood coagulation protein, and fibronectin (Fn), a plasma protein also present in inflammatory environments that is not only capable of attaching directly to fibrin, but is also considered to be one of the main binding partners of fibroblasts [138]. Fibrin interacts with fibroblasts primarily through its RGD site which binds to αv integrins, although attachment strength is not particularly strong [139]. Therefore fibroblast interactions with the provisional ECM are expected to be dominated by Fn, and thus this protein has been the focus of this research.

Fibronectin is a large glycoprotein dimer consisting of two identical 250kDa subunits each containing several different binding sites for other matrix proteins, growth factors, and integrins, and all of which are conformation sensitive. Fn's structure can be further subdivided into three distinct types of modules termed type I, II, and III, where type III repeats in particular can be induced to unfold and reveal new biochemical signatures upon mechanical stretching [140, 141]. Several sites throughout Fn have been documented to interact directly with integrins. Fragments of Fn type I repeats 1-9 and type II repeats 1-2, located within the N-terminal region of Fn have each demonstrated an ability to bind α5β1 integrins [138]. The REDV motif within the 8^{th} type III repeat can bind α9β1 integrins on fibroblasts [142, 143]. The type III repeat connecting segment acts as a binding site for fibroblast α4β1 integrins [97]. Finally, fragments representing the age-related chemical

modification of the NGR sequence to DGR in the type I 5th repeat are capable of binding to αv integrins [36].

The main region for integrin interactions within Fn, however, is the aptly named cell-binding domain which constitutes the 9th through the 10th type III repeats. An RGD sequence resides within the 10th type III repeat presented in a looped structure that extends about 10 angstroms away from the surface of the protein [144]. This represents the most important recognition site for about half of all known integrins, though with regards to fibroblasts it is capable of binding to integrins αvβ3, αvβ5, αvβ8, α8β1, αvβ1, and α5β1 [143, 145]. The integrins α5β1 and αvβ3 are probably the best studied and most frequent to engage this binding site.

Within the cell-binding domain of Fn there also exists a PHSRN or "synergy site" situated within the 9th type III repeat about 35 angstroms away from and spatially on the same side of Fn as the RGD loop[142, 144, 146]. While PHSRN does not possess any intrinsic integrin binding capacity, in combination with RGD, it has the ability to enhance α5β1 integrin binding by about 100 fold [146]. Importantly from the perspective of citrullination—which again modifies arginine—mutagenesis studies have shown that the R of PHSRN is the most important residue for proper PHSRN engagement with α5β1 [142]. Importantly from the perspective of stiffened pathologic matrices, conformation of the cell binding domain is of supreme importance, as stretching of the 9th and 10th type III repeats so that the separation of the RGD and PHSRN sites increases from 3.6 to a mere 4.3 nanometers apart results in a reduction of α5β1 affinity from 12nM to only about 2.5uM, thus causing a shift in fibroblast integrin preference towards αvβ3-dominant binding [141].

Fibroblast adhesion to Fn is therefore anything but a simple matter. A variety of integrin types compete for the same attachment sites, and the particular combination of integrins used for attachment even within the same fibroblast can change over time as a result of altered Fn conformation [141]. Further, the particular combination of integrin types engaged in Fn adhesion is not a trivial matter; the particular ratio of αvβ3 to α5β1 is known to have impacts on a variety of signaling pathways with significant pathologic consequences in diseases including cancer, RA and fibrosis. For example, deletion of αv integrin has shown protective benefits in mouse models of lung fibrosis [72], and high levels of α5β1 in tumors is correlated with poor cancer prognosis [87].

Differences resulting from preference for αvβ3 vs α5β1 can even be observed at the cellular level. The capability of αvβ3 integrins to respond to variations in low stiffness is greater than α5β1 integrins and is advantageous for allowing αvβ3-dominant cells to more effectively reorient their cytoskeleton in the direction of strain in response to high strain rates [147]. The rate of attachment for αvβ3 integrins is faster than that of α5β1 integrins, and thus αvβ3 integrins tend to dominate especially at early attachment timepoints [120, 148]. Adhesion strength, however, is predominantly mediated through α5β1 integrins [122, 147], to such a greater extent that attachment to Fn-coated beats using α5β1 alone was found to be greater than when cells were capable of only using αvβ3 integrins or a combination of αvβ3 and α5β1 integrins [148]. With regards to fibroblast migration, α5β1 integrins also appear to dominate [149], as β1 blocking was effectively shown to reduce fibroblast migration by 85% compared to only a 15% reduction due to αv blocking in a wound healing assay [128].

Clearly, the particular integrins used to engage with the ECM makes a significant difference in the context of molecular signaling, cell function, and disease progression. Understanding how Cit Fn, abundantly present in a variety of chronic inflammatory diseases, impacts integrin attachment and downstream signaling is therefore imperative for understanding the pathologies of these diseases and potentially in developing new therapeutic interventions to help prevent or ameliorate their damage. In the current study we began elucidating fibroblast-Cit-Fn interactions by identifying specific sites of citrullination within the Fn molecule with particular interest given to the arginines present in both the RGD and PHSRN sites, known to differentially impact αvβ3 and α5β1 attachment. Integrin affinity for Cit Fn was also directly evaluated via interferometry as well as through cell binding assays. Finally, to ascertain the full influence of Cit Fn on fibroblast binding and signaling, a combination of immunocytochemistry and force-induced co-immunoprecipitation studies were carried out to analyze individual integrin subunits as well as downstream signaling molecules of interest.

3.3 Materials and Methods

3.3.1 Protein Citrullination

Unless otherwise mentioned, all proteins were citrullinated as follows, in a PAD reaction buffer containing final concentrations of 100mM Tris-HCl, 5mM $CaCl_2$, 0.3mg/mL protein and at pH 7.4. Proteins were incubated with 10U/mL PAD4 (Cayman Chemical) and 5.6ug/mL PAD2 (SignalChem) at room temperature overnight with shaking at 200 rpm after which reactions were quenched with 20mM EDTA. In all cases, non-citrullined

proteins used for experimental comparisons were subjected to identical buffers and incubation conditions with the exception of PAD enzyme presence.

3.3.2 Coating Coverslips with Protein

Unless mentioned otherwise, 10mm diameter coverslips were first cleaned in 2M HCl at 60^{o}C for 4 hours, washed with water, and then coated overnight with 20ug/mL Fn or Cit Fn in PBS at 4^{o}C. All coverslips were blocked with 1% heat-denatured bovine serum albumin (hd-BSA) for 1 hour at room temperature prior to plating cells. Negative control coverslips were either coated with 1% hd-BSA or poly-L-lysine (PLL) in lieu of adhesive proteins. PLL-coated coverslips were washed 3X in water prior to being blocked with 1% hd-BSA.

3.3.3 Cell Culture

Unless otherwise specified, all experiments utilized Human Foreskin Fibroblasts (HFFs) from ATCC at or below passage twelve. Cells were cultured in 4.5g/L glucose DMEM +pyruvate, + L-Glutamate, supplemented with 15% FBS and 1% pen/strep. All experiments were performed in the above media without serum, designated serum-free media, or SFM, unless otherwise specified. Quenching of trypsin reactions prior to plating in SFM was carried out with soybean trypsin inhibitor (Sigma). For some longer-duration experiments, SFM was supplemented with a small amount of FBS from which fibronectin (Fn) had previously been depleted via overnight incubation with gelatin-sepharose beads with confirmation via SDS-PAGE. Knockdown of β1 integrin was carried out using β1 shRNA plasmids (sc-72028-SH) and β1 lentiviral particles sc-72028-V, or control shRNA lentiviral particles (sc-108080) from Santa Cruz.

3.3.4 COLDER Assay for Citrullination Verification

A colorimetric assay for in situ detection of citrulline was performed according to the methods of Knipp. et. al [150]. Briefly, 10uM or 5uM of soluble Fib along with fibrin clots (75uL 0.5mg/mL fibrinogen, 1unit/mL thrombin) were compared to standard curves of purified L-Citrulline. A range of PAD enzyme concentrations (PAD4 = 1-14 units per mg protein or PAD2= 0.56- 15.68ug/mg protein) was utilized for overnight citrullination of proteins. Final citrulline content in wells was determined via colorimetric measurements at 540nm.

3.3.5 Dot Blot Citrullination Verification

To verify citrullination of soluble proteins, a dot blot on nitrocellulose membranes was performed using protein masses ranging from 0.2ug to 0.025ug in serial dilutions. Membranes were blocked in 5% BSA in tris-based buffer (TBS) and stained with anti-peptidyl citrulline (Millipore MABN328) at 1:4000 followed with anti-mouse 800CW infrared secondary (Li-Cor)

3.3.6 In-Gel Protein Digestion for Mass Spectrometry

In-gel protein digestion was conducted as previously described[151], with modifications. Briefly, selected protein bands were excised from the Coomassie-stained gel, diced into small pieces, and then destained with HPLC-grade water (Avantor) and 1:1 acetonitrile (ACN)/ammonium bicarbonate (ABC) (Sigma-Aldrich). The de-stained gel pieces were then dehydrated with multiple ACN washes until rock hard, followed by air drying for ~10 minutes. The gel pieces were rehydrated for 30 minutes with 50mM

dithiothreitol (Sigma-Aldrich) to reduce disulfide bonds, followed by replacement with 100mM iodoacetic acid (Sigma-Aldrich) and 45 minutes shaking at 750 rpm in the dark to alkylate the reduced thiols. After reduction/alkylation, the gel pieces were once again washed and dehydrated as before, and then chilled on ice for 10 minutes. In-gel digestion was achieved by rehydrating the gel pieces with either trypsin (40µg/mL, Promega Cat # V511A), gluC (40µg/mL, Calbiochem Cat # 324713), chymotrypsin (50µg/mL, Promega Cat # V1062) or a mixture of trypsin and gluC. In each case, 50µL of the sequencing grade enzyme solution was added to the gel pieces and incubated on ice for 30 minutes. Excess enzyme solution was then removed and replaced with 100µL 50mM ABC and the pieces were incubated overnight at 37°C with shaking at 750 rpm. Resultant proteolytic peptides were extracted by two rounds of dehydration using 100µL ACN and collection of the resulting extract into low-retention microfuge tubes, which were frozen solid at -80°C and then sublimated by centri-vapping. The dried peptides were reconstituted by sonication in 5% ACN/0.1% formic acid and stored at -80°C prior to analysis.

3.3.7 Mass Spectrometry

LC-MS analysis of peptides produced by in-gel digestion was carried out with an UltiMate™ 3000 RSLCnano System UPLC system (Dionex) with Acclaim PepMap RSLC column (75µm x 25cm nanoViper C18 2µm, 100Å) coupled to a Q-Exactive Plus Orbitrap mass spectrometer (Thermo Scientific) run in data-dependent acquisition mode (top-8). Resultant RAW files were analyzed using Proteome Discoverer 2.1 with embedded SEQUEST search algorithm operating with an allowable 1% false-discovery rate, wherein the human fibronectin (P02751) isoforms 1-17 were used as targets for spectral matching. Mass deviations for precursor ions and fragment ions were set to 10 ppm and 0.6 Da

respectively. Besides citrullination (R), other modifications such as deamidation (N, Q), oxidation (M), phosphorylation (S, T, Y), acetylation (protein N-terminus), and caramidomethylation (C) were included in the analysis. Additionally, the citrullinated sites were checked manually.

3.3.8 Interferometry

Binding affinity between recombinant human αvβ3 (3050-AV-050) or α5β1 (3230-A5-050) integrins purchased from R&D Systems and either Fn or Cit Fn was determined via Bio-Layer Interferometry(BLI) on a Pall forteBIO Octet RED96 interferometer. Integrins (ligands) were immobilized to amine-reactive ARG2 sensors using standard EDC/sulfo-NHS chemistry. Fn or Cit Fn was diluted in freshly prepared analyte buffers containing 1mM $MnCl_2$ (for integrin activation), 150NaCl, 25mM tris-HCl, and 1mg/mL BSA (for blocking) at pH 7.4. For αvβ3 interactions, a 2X analyte buffer containing 0.02% tween 20 was utilized to assist in molecular dissociation. Integrin-ligand interactions were measured across five concentrations of Fn/Cit Fn diluted in analyte buffer with serial dilutions starting at 80nM or 320nM for α5β1 or αvβ3 integrin interactions, respectively. Experiments were performed under constant plate shaking at 1000rpm. Results were analyzed using forteBIO analysis software using a global fit model for 1:1 binding interactions. Data processing included subtraction of signal from a reference probe and alignment of the y-axes at the start of the association phase. Each integrin-protein interaction was measured via three separate interferometry runs.

3.3.9 CHO Cell Adhesion Assays

To independently measure the physiological interaction of α5β1 or αvβ3 integrins with Fn/Cit Fn, two different types of Chinese Hamster Ovary (CHO) cells were utilized. CHO-K1 cells endogenously express hamster α5β1, and will henceforth be designated CHO- α5β1. CHO-B2, a clone of CHO-k1 cells chosen for low surface expression of α5 integrin, were transfected with human αvβ3 integrin—henceforth designated CHO- αvβ3. Coverslips were coated overnight with 20ug/mL Fn/Cit Fn, Fib/Cit Fib, or 1% hd-BSA. All coverslips were subsequently blocked with 1% hd-BSA for 1 hour.

To evaluate integrin attachment, separately, CHO- α5β1 and CHO- αvβ3 cells were plated on Fn- or Cit for 1 hour at a density of 5000cells/cm^2. As a negative control, CHO-αvβ3 cells were also plated on coverslips coated with hd-BSA, or Fib/Cit Fib, the latter of which is only able to engage αvβ3 integrins. Cells were subsequently washed with PBS++ (supplemented with 2mM Ca^{2+} and 1mM mg^{2+} for maintenance of integrin activation), fixed with 4% paraformaldehyde, and stained with fluorescent phalloidin and hoescht. Fluorescent microscopy was utilized to determine the number of cells remaining attached post-washing.

3.3.10 Focal Adhesion Complex Staining

For immunocytochemical (ICC) analysis of integrin subunits and downstream signaling molecules, HFFs were plated on Fn/Cit Fn or PLL-coverslips at 5000 cells/cm^2 for 30 minutes at which point they were washed 1X with PBS++ (2mM $CaCl_2$, 1mM $MgCl_2$), fixed with 4% paraformaldehyde, permeablized with 0.2% triton-X, blocked with normal goat serum and incubated with primary antibody sets, as appropriate, overnight at 4^oC. The following primary antibodies were used: anti-β1 (9EG7) at 1:500, anti- αvβ3

(LM609)at 1:200, anti- α5 (AB1928) at 1:500, anti-alpha V (272-17E6, abcam16821) rabbit anti-paxillin (Y113, ab32084, abcam) at 1:400, mouse anti-paxillin (thermofischer SH11)at 1:300, anti-GSK (Cell Signaling mAb #9832) at 1:250, anti-phospho-s9 GSK-beta (Abcam, ab107166) at 1:400, anti-MLC at 1:200, anti-phosphor-MLC (Thermo)at 1:300, anti-ILK (ER 1592, Abcam 76468)at 1:800, anti-phospho-ILK (Millipore Ser 246, Ab1076) at 1:500, anti-vinculin (SPM22), anti-pFAK (BD pY397, cat#611722) at 1:600, anti-p-c-src (sc9AC) at 1:100.

Imaging was conducted via PerkinElmer spinning disk confocal microscope using a 63X objective. Only isolated cells (those lacking contact with any other cells) were included in analysis. Where applicable, paxillin fluorescent signal was utilized to both identify the focal plan of imaging for cell adhesion as well as focal adhesion location. For staining of total F-actin content as well as total p-ILK and p-GSK content, confocal z-stacks of 10-slices each spanning the entire cell thickness were acquired. Cell area, or volume, as appropriate, was determined from phalloidin staining (1:40). Nuclear volume was determined from hoesct signal. Image analysis, thresholding, and quantitation was performed using Volocity quantitation software.

3.3.11 Rac and Rho GLISAs

HFFs were plated at 10K cells/cm^2 in 100mm petri dishes pre-coated with Fn or Cit Fn and allowed to attach for 30 minutes before being collected, lysed, and analyzed using the Rac1 (BK128-S) or Rho (BK124-S) colorimetric GLISA assays from Cytoskeleton, Inc. Protein loading was normalized to total protein content determined according to 660nm

protein quantification assay. A total of two plates of cells were prepared per substrate, with duplicate wells analyzed per sample. Each GLISA was performed twice.

3.3.12 Magnetic Bead Force-Inducible Co-Immunoprecipitation

Invitrogen M-280 Tosylactivated Dynabeads were covalently bound to Fn or Cit Fn and subsequently blocked in hd-BSA using manufacturer recommended protocols. HFFs were plated at a density of 2.5 x 10^6 cells per 10cm petri dish for six hours after which a cell scraper was used to remove cells along dish periphery (which would have been outside the subsequent applied magnetic field), and remaining cells were serum-starved 24 hours in Opti-MEM media. Protein-coated beads were allowed to incubate with cells for 1 hour (Figure 4) after which a magnetic force was applied, or not, from a distance of 20mm for the +force and no force conditions, respectively. Unbound beads were washed away with cold PBS solution, after which the remaining beads were collected via cell scraping and addition of lysis buffer. Protein loading for SDS PAGE and subsequent western blotting was normalized using Pierce 660nm Protein Assay Reagent. The following antibodies were utilized for western blot analysis: anti-αv H075 integrin from sant cruz (sc-10719), anti- α5 anti-a5 (AB1928), anti p-ILK ser246 (AB1076), and anti-paxillin Y113 (ab32084) from abcam, anti-p-src D49G4, anti-src 32G6, and anti-ILK (#3862) from cell signaling, anti-pFAK 44-624G from thermo fischer, and anti-FAK pY397 from BD Biosciences. Appropriate mouse or rabbit horse radish peroxidase (HRP)-conjugated antibodies were utilized for secondary staining. Chemiluminescent western blot signals were read and interpreted using a GE Amersham Imager 600.

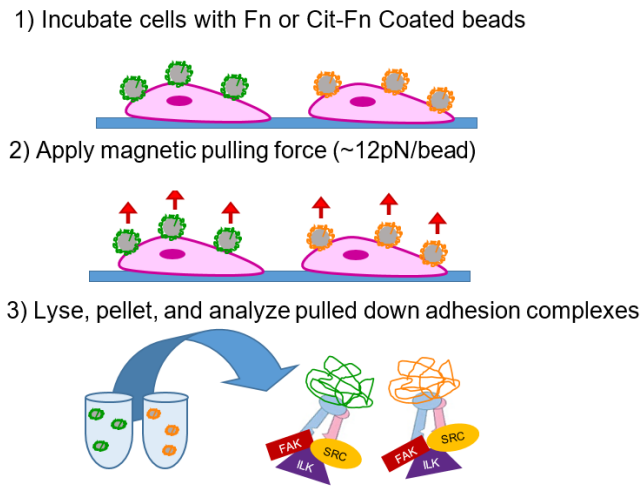

Figure 4: Force-Inducible Magnetic Bead Co-Immunoprecipitation Protocol

3.3.13 Statistical Analysis

All statistical analysis was performed using GraphPad Prism software with 2-tailed t-tests or one-way ANOVAs and Tukey post-hoc analysis, as appropriate for the experimental set-up. Alpha was set at 0.05 for all analyses. In the case of larger data-sets, such as with fluorescent signal analysis of cell components in microscopy images, outliers were removed using the ROUT method with a Q of 1% prior to further statistical analyses. The Shapiro-Wilk test was utilized to test for normality of data distribution, and in cases where null hypothesis was rejected, the Mann-Whitney test was applied to ascertain statistical significance.

3.4 Results

3.4.1 Protein Citrullination can be Confirmed as a Dose-Dependent Function of PAD Concentration

Dot blots using anti-peptidyl citrulline antibody shows preferential staining for Cit Fn over Fn in a dose-dependent manner of modified proteins (Figure 5C). A similar trend of staining was observed for citrullinated FnIII 9-10 Fragments (Cit- 9*10) over unmodified 9*10, as well as for Cit Fib over Fib. The anti-peptidyl citrulline antibody also non-specifically stained unmodified proteins, but adequate distinctions in antibody staining could be attained by dot blotting sufficiently low concentrations of protein. Modification of Cit Fib could be observed via lack of clottability (i.e. conversion of Cit Fib into a Cit-Fibrin clot) as previously observed [31], as well as via a band shift in electrophoresis (Figure 5A). As Fn is a larger protein than fibrinogen with fewer citrullination sites, a similar band shift could not be visualized with Cit Fn, even after proteolytic protein digestion. The COLDER assay, as previously reported [152], produced relatively variable results with low signal that was very sensitive to protein type and buffer contents. Therefore, reproducible signal could only be attained using Cit-Fibrin and Cit Fib. Titration of PAD enzymes utilizing the COLDER assay revealed that maximal PAD modification is attained using a dose of 10units/mL PAD4 and 5.6ug/mL PAD2 (Figure 5B). Total levels of citrulline plateau at greater PAD concentrations.

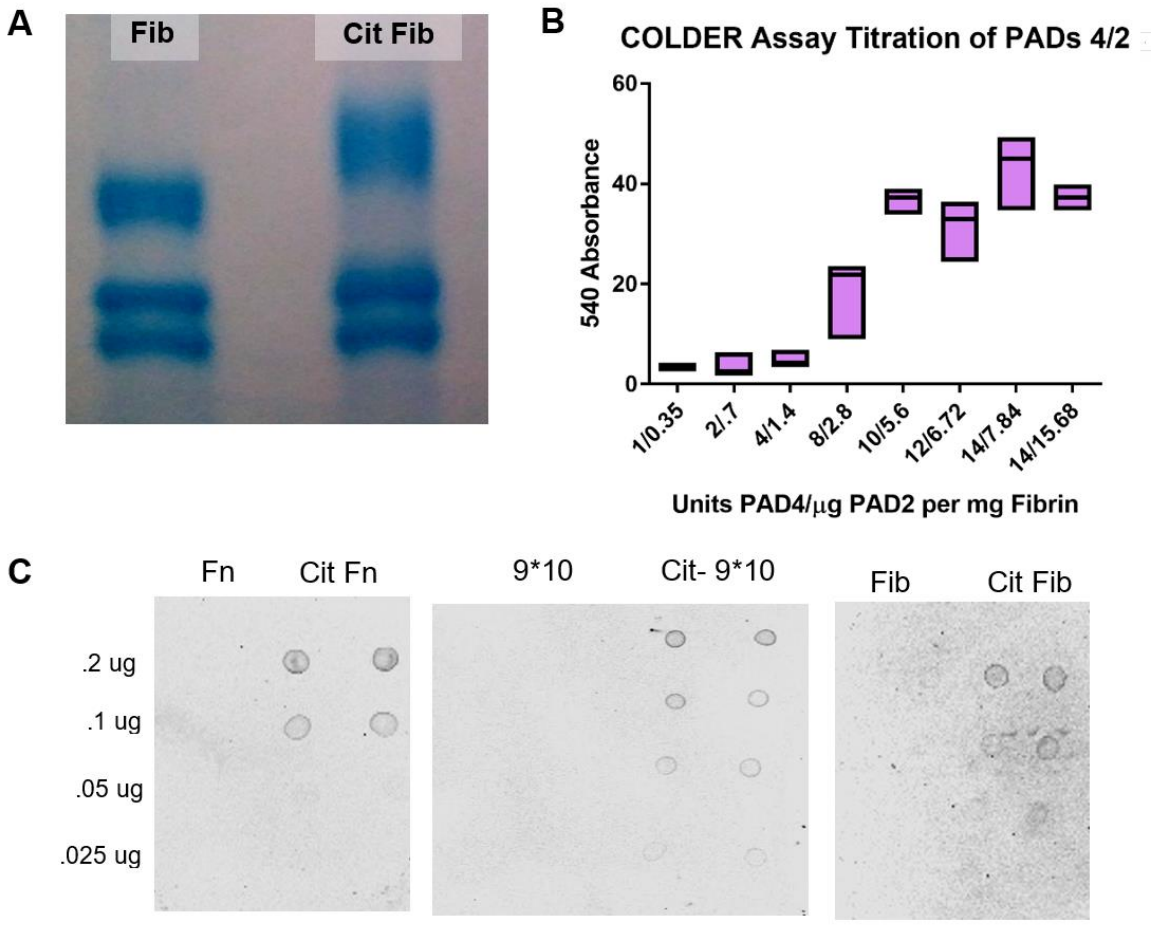

Figure 5: Citrullination is Verified via SDS PAGE, COLDER Assay, and Dot Blot
(A) Coomasie-stained SDS PAGE gel shows retardation of the fibrinogen alpha chain as a consequence of citrullination. (B) Absorbance readings from three wells per condition are plotted for a COLDER assay where fibrin clots were incubated with various concentrations of PADs 2 and 4. (C) Dot blot results for Cit Fn, Cit-9*10, and Cit Fib are shown with four different concentrations of each protein, listed on left.

3.4.2 Mass Spectrometry Identifies 24 Unique Sites of Fn Citrullination

Mass spectrometry analysis of Cit Fn modified by PAD 2 alone, PAD4 alone, or PADs 2 and 4 together identified a total of 24 unique citrullination sites (Figure 6), with an aggregate protein coverage of 80 percent.

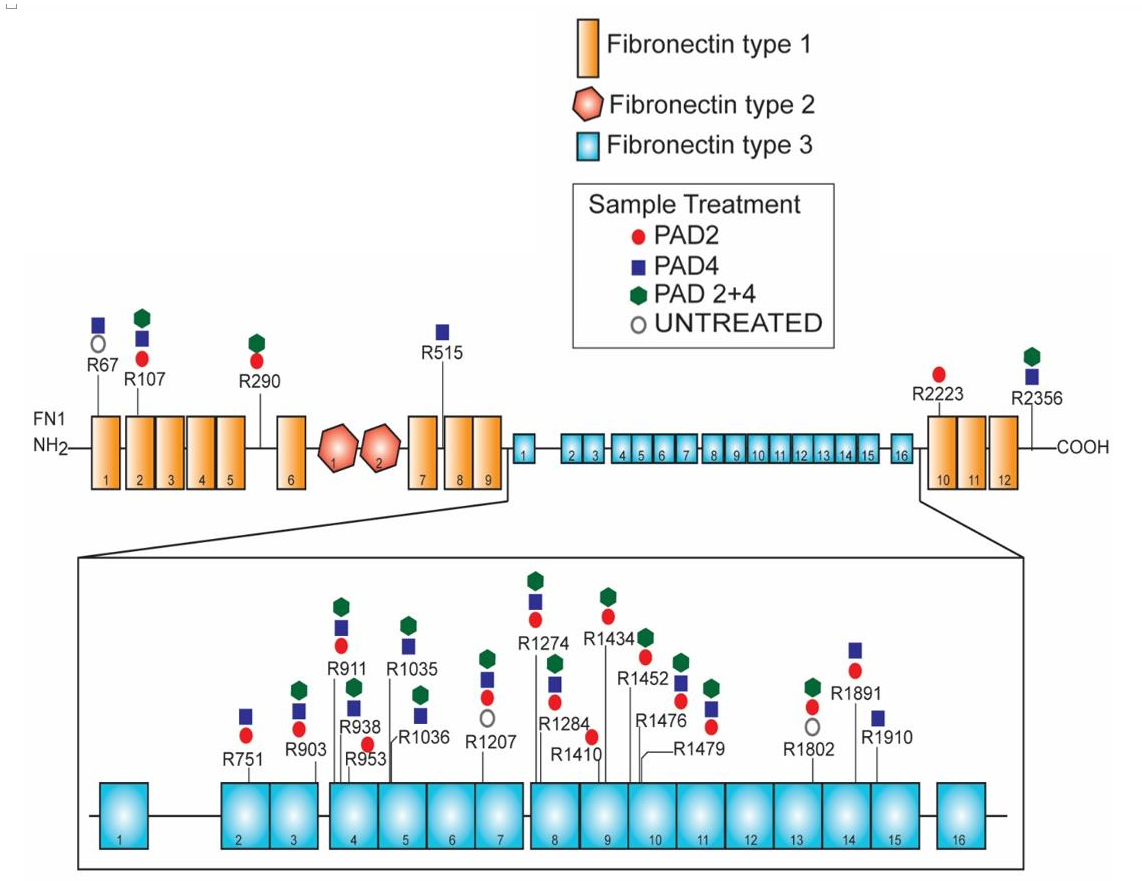

Figure 6: Analysis of PAD Isotype-Specific Fibronectin Citrullination Sites
The above diagram symbolically depicts the full Fn molecule and the accurate layout of type I, II, and III domain repeats. Confirmed citrullination sites are overlaid on the Fn diagram, and with each site, the specific arginine residue as well as the PAD isotypes capable of bringing about the modification are specified.

The majority of these, or 18 out of the total 24, were found to reside within type III Fn repeats, and of these, five were found to reside specifically within the cell binding domain. The RGD motif was not modified by any combination of PAD treatments, although R1410 within the PHSRN synergy site was found to be modified. There does appear to be some enzyme specificity with regards to Fn citrullination, as only 10, or less than one half of all modified sites, were determined to be targets of both enzymes. Of the remaining sites, seven

were determined to be modified by only PAD4 and another 7 were found to be modified by PAD2 only; among this latter group of PAD2-specific modifications was the PHSRN synergy site. A majority of citrullination sites identified reside within regions of known function relating to fibrin binding, heparin binding, collagen binding, or cell attachment (Figure 7).

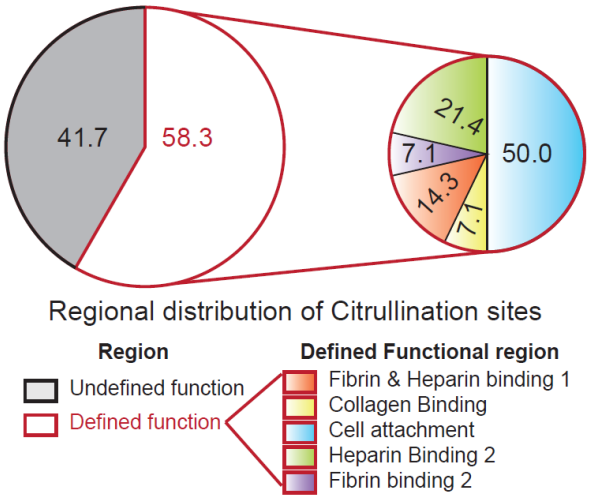

Figure 7: Attribution of Possible Biological Function for Identified Fn Citrullination Sites
The pie chart above shows which percentages of identified Fn citrullination sites lie within regions of known biological function, and further breaks defines those functions and how many citrullination sites can possibly be attributed to each.

3.4.3 Citrullination of Fn Decreases αvβ3 Adhesion and Has Minor Impacts on α5β1 Attachment

Bio-Layer Interferometry (BLI) with α5β1integrins (Figures 9, 10, and 11) resulted in very strong affinity in association with both citrullinated and unmodified fibronectin, although citrullination appears to produce a slight improvement in attachment. The average K_D over three runs was 0.741nM and 0.3016nM for Fn and Cit Fn, respectively (Figure 8B), where K_D is defined as k_{off}/k_{on}, and a lower molarity represents a generally improved

tendency for association vs disassociation. These values are very close to that of the R&D Systems' (the vendor for these integrins) predicted K_D value of 0.5nM for α5β1and full-length human Fn. The r^2 for all global curve fits for both α5β1 and αvβ3 analyses was > 0.9. k_{off} rates for both proteins were very low such that it is difficult to visually detect a decrease in BLI signal during the dissociation phase, and thus the k_{on} rates appear to be more informative. The average k_{on} rates were 1.24866 x 10^5 and 1.776 x 10^5 $M^{-1}s^{-1}$ for Fn and Cit Fn, respectively (Figure 8A), where the higher number here for Cit Fn indicates an improved ability to associate with immobilized α5β1 integrins.

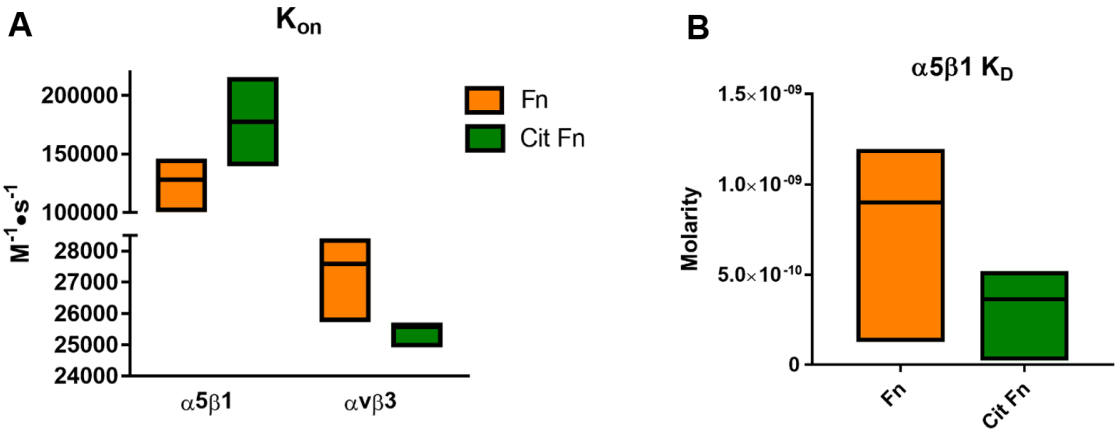

Figure 8: Bio-Layer Interferometry Average K_{on} and K_D values
Graphs above represent the average k_{on} (A) and K_D (B) values for three separate BLI runs for each combination of integrin and protein. K_D is defined as k_{off}/k_{on} .

BLI with αvβ3 produced almost no dissociation (supplement, Figures 33, 34), such that predicted K_D values were in the pM range, which is definitely not accurate for this integrin interaction with Fn; expected K_D values should if anything be higher than those obtained for α5β1 integrins. This result is most likely due to experimental parameters rather than representative of actual K_D values. Nevertheless, association curves did appear

approximately as expected (i.e. properly shaped and with a dose-dependent separation in signal) with average K_{on} values of 2.724 x10^4 and 2.540 x10^4 for Fn and Cit Fn respectively being predictably lower, by about 10-fold, than those produced by α5β1-Fn interactions(Figure 8A). Of note, the K_{on} values for Cit Fn are lower than those for Fn (p =0.0908).

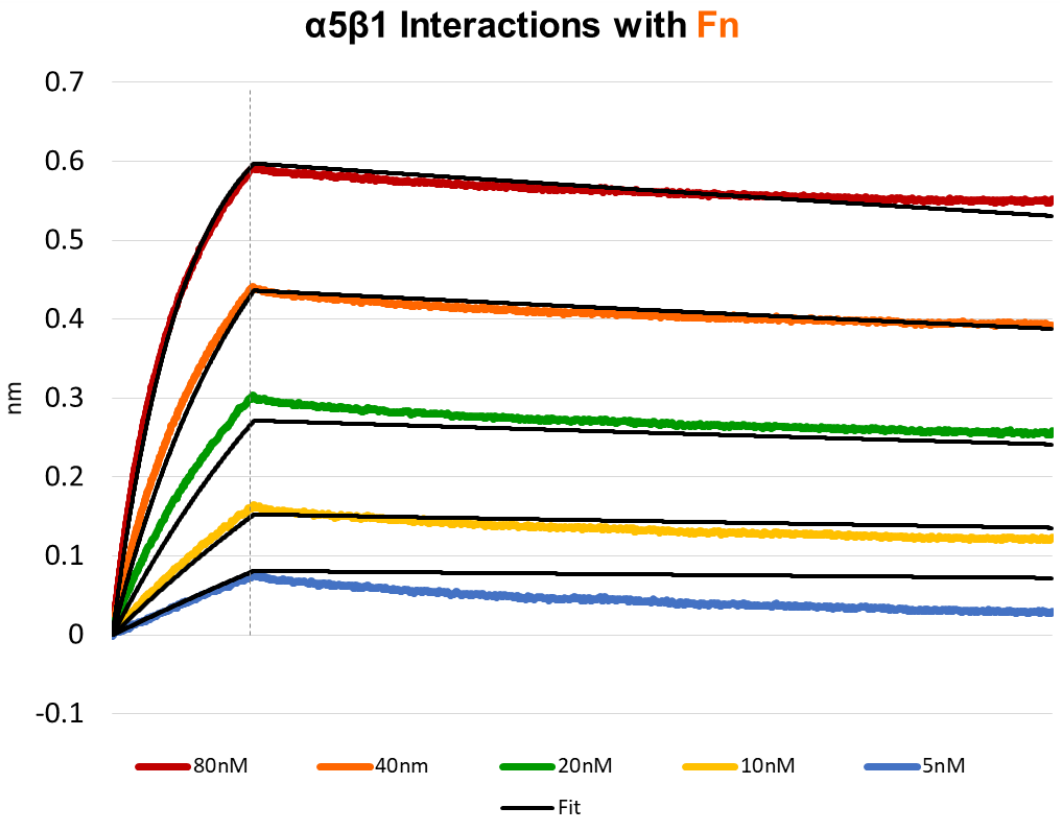

Figure 9: Alpha 5 Beta 1 Interferometry Curves with Fn:
Colored lines represent the processed data, and black lines represent the global 1:1 curve fits. The calculated K_{on} and K_D for this particular data set are 1.004 x 10^5 $M^{-1}S^{-1}$ and 1.197nM respectively.

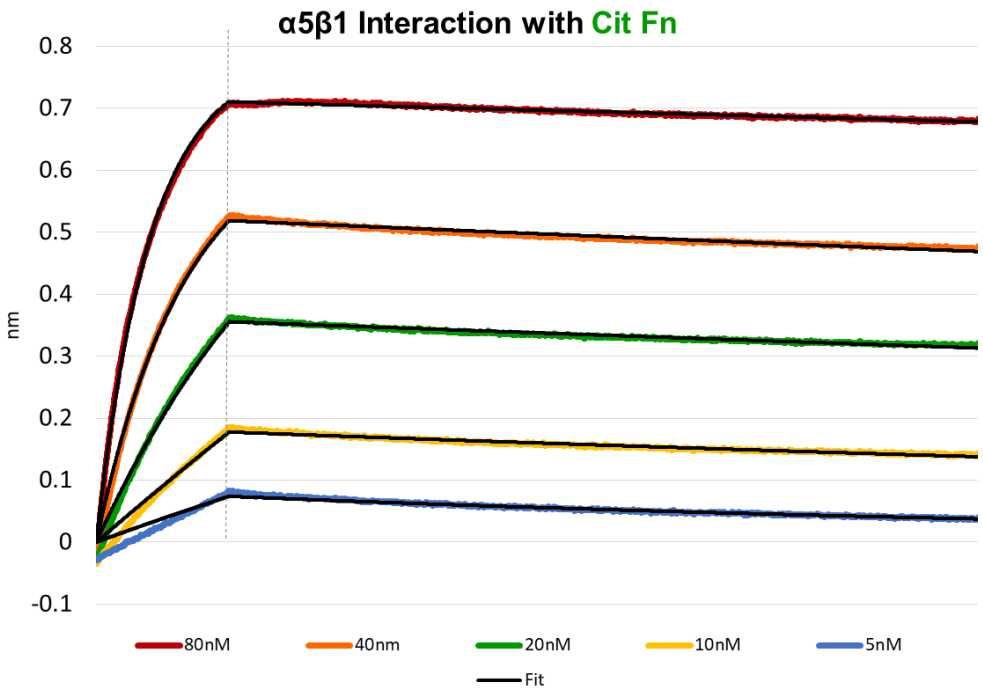

Figure 10: Alpha 5 Beta 1 Interferometry Curves with Cit Fn:
Colored and black lines represent processed data and global 1:1 curve fits, respectively. The calculated K_{on} and K_D for this data set are 1.774x 10^5 $M^{-1}S^{-1}$ and 0.363nM respectively.

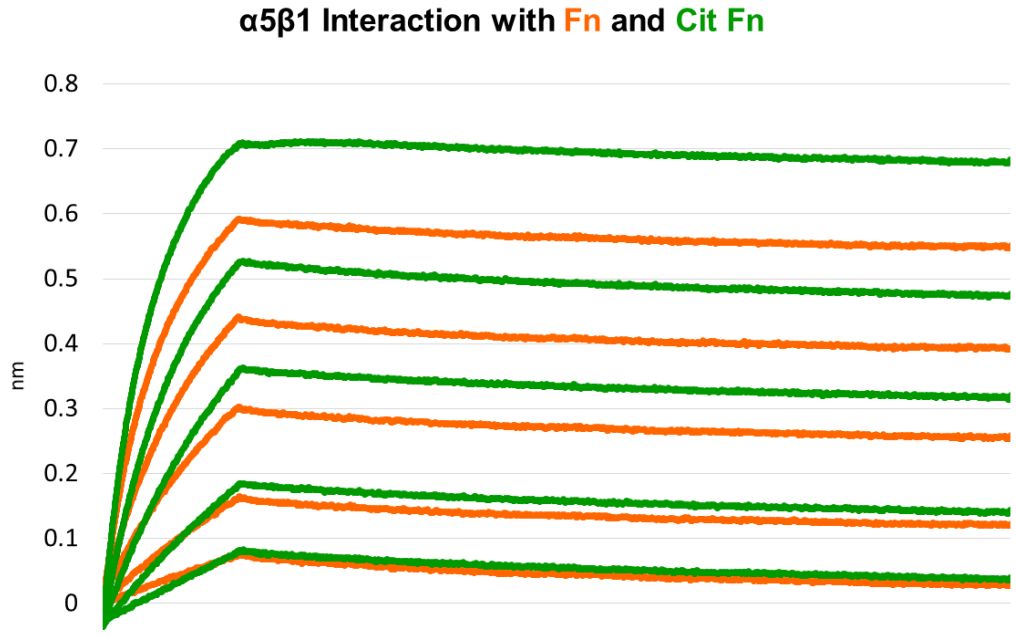

Figure 11: Overlay of Fn and Cit Fn Alpha 5 Beta 1 Interferometry Results
The physical overlay of Fn (orange) and Cit Fn (green) plots allows for direct comparisons of their interactions with α5β1 integrins, and in particular, the heighted signal achieved in the association phase of Cit Fn in comparison to Fn.

To investigate whether changes in integrin affinity as shown via interferometry resulted in functional differences in cell attachment to Cit Fn, adhesion assays using CHO cells specific for either αvβ3 or α5β1integrins were performed. Adhesion assays with CHO-αvβ3 cells resulted in a significant decrease in attachment to Cit Fn in comparison to Fn (Figure 12A), implying that αvβ3 attachment is detrimentally impacted by citrullination of Fn. CHO-αvβ3 attachment to fibrinogen, a negative control because its only integrin attachment site is through αvβ3 integrins showed a complete elimination of cell attachment, implying that citrullination's detrimental impacts may specifically involve the RGD site responsible for αvβ3 attachment. No significant differences were observed between CHO-α5β1 attachments on Fn vs Cit Fn (Figure 12B).

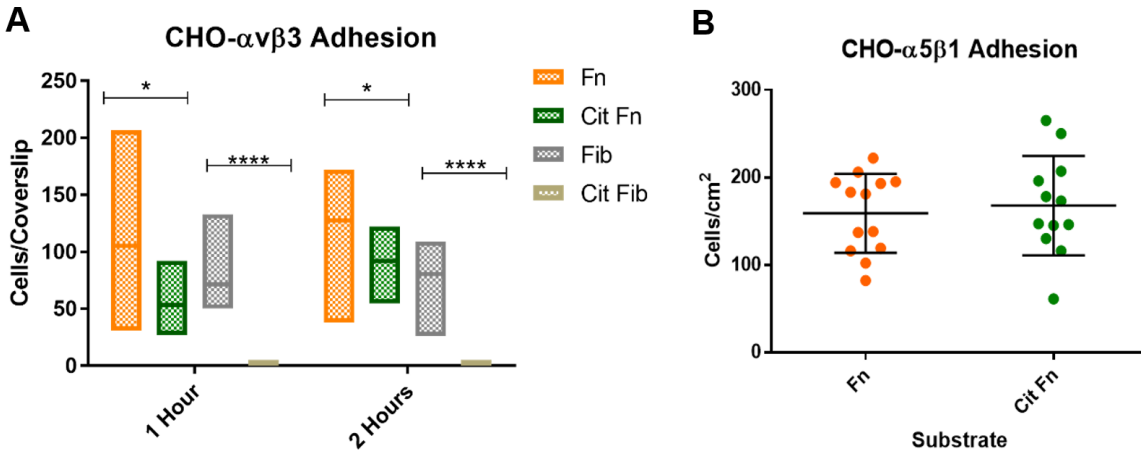

Figure 12: Adhesion Assays with Integrin-Specific Binding
CHO cells only expressing αvβ3 integrins (A) were challenged with adhesion to Fn/Cit Fn or Fibrin/Cit-Fibrin and CHO cells only expressing α5β1 integrins were challenged with adhesion on Fn/Cit Fn. The brown-colored bars representing CHO- αvβ3 are difficult to visualize as they are very near to zero. Results represent seven coverslips per condition.

3.4.4 Citrullination of Fn Results in a αvβ3 to α5β1 Integrin Switch

ICC staining for each of the integrin subunits αv, α5, β1, and αvβ3 revealed that the absolute quantity of both α5 and β1 integrin subunits within any given FA was enhanced within HFFs plated on Cit Fn compared to Fn (Figure 13A), with no such differences being observed with regards to either αv or αvβ3 integrins. When the ratio of total β1 signal to αvβ3 signal or α5 to αvβ3 signal per cell is measured, the result is significantly higher on Cit Fn for the former, and elevated but not statistically significant for the latter (Figure 13B). Analysis of co-localization via Pearson's correlation coefficient (r) for each pairwise combination of α5, β1, and αvβ3 shows that in all cases co-localization is significantly enhanced on Cit Fn in comparison to Fn indicating improved clustering on Cit Fn (Figure 13C). Magnetic bead force-inducible co-immunoprecipitation experiments show similar trends of integrin expression where there is no difference of baseline αv but an elevation of

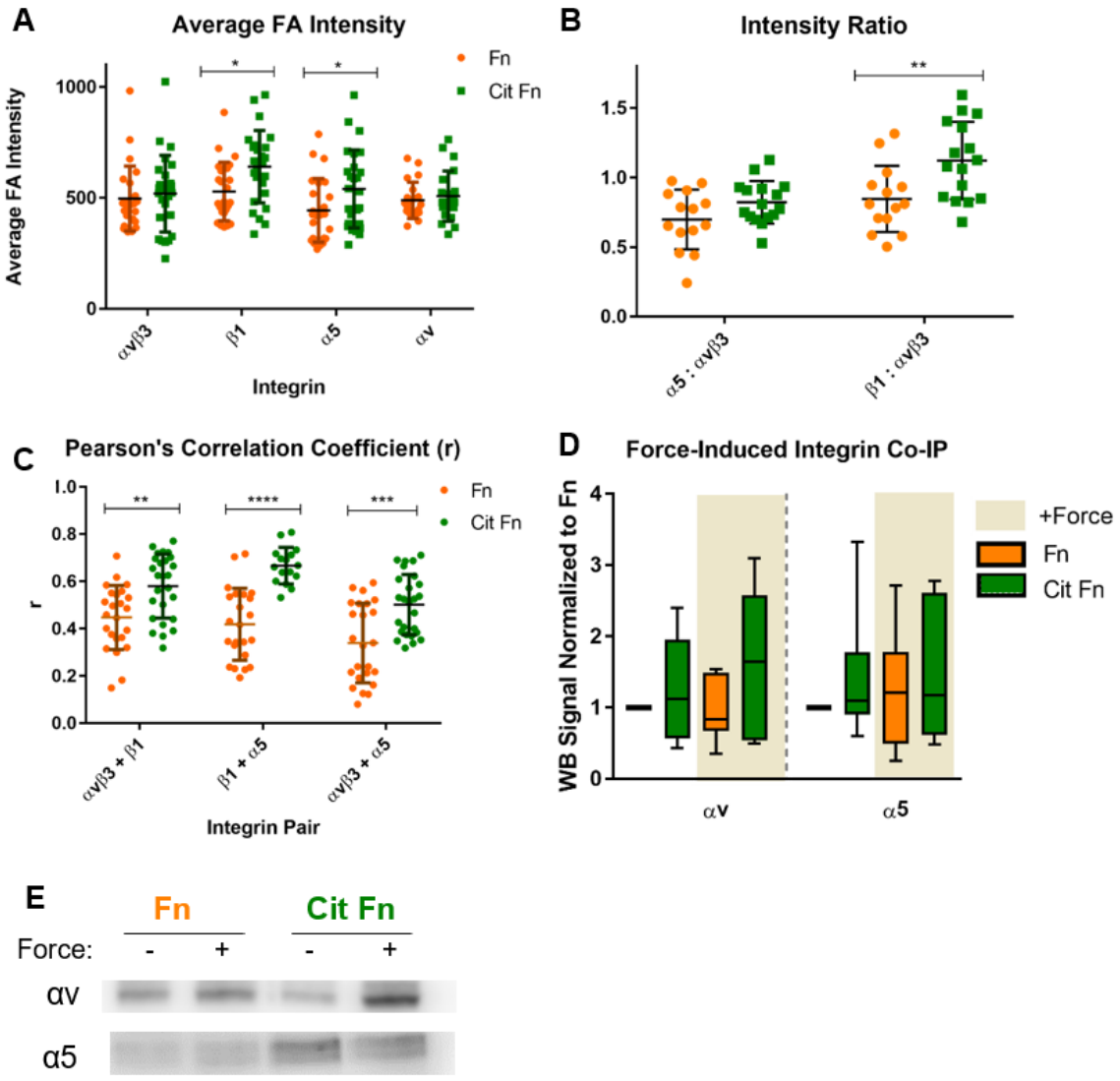

Figure 13: Integrin ICC Staining and Force-Inducible Co-Immunoprecipitation Assays Display a Preference for Alpha5 and Beta1 on Cit Fn
Quantification of integrin fluorescent signal in confocal ICC images is plotted to show (A) average signal per integrin subtype within FAs, (B) the ratio of total α5 or β1 signal per total αvβ3 cellular signal, and (C) the overall co-localization of integrin subtypes within the cellular area. Each data point represents the average for a single cell where n = 40 cells per condition. Western blot data from a total of seven different biological replicates (D) shows the relative quantities of integrin subunits pulled down with Fn or Cit Fn in the presence (brown shading) or absence of force. (E) Representative western blots for αv and α5 signal.

α5 on Cit Fn compared to Fn (Figure 13D, E). The main integrin-related revelation here is that αv integrins exhibit an increased force-inducible increase on Cit Fn compared to Fn.

Taken together these results point towards the existence of an overall greater quantity of both α5 and β1 integrins within FAs of HFFs on Cit Fn, and when compared to the amount of αvβ3 integrins, there appears to be a relatively greater quantity of α5 and especially β1 integrins on Cit Fn compared to Fn.

Identical ICC FA experiments on CCL210 human lung fibroblasts revealed a similar trend of both α5 and β1 upregulation on Cit Fn in comparison to Fn. Measurements of average integrin subunit staining within FAs show an increase of β1, a significant increase of α5, and no difference of αvβ3 signal on these cells plated on Cit Fn compared to Fn (Figure 14). Co-localization measurements again showed enhanced integrin clustering on Cit Fn with each pairwise comparison of integrin subunits, though to a somewhat lesser extent than with HFFs, since none of the differences were significant. P values were 0.0796, 0.1, and 0.2 for α5+αvβ3, β1+αvβ3, and α5+β1 co-localization, respectively.

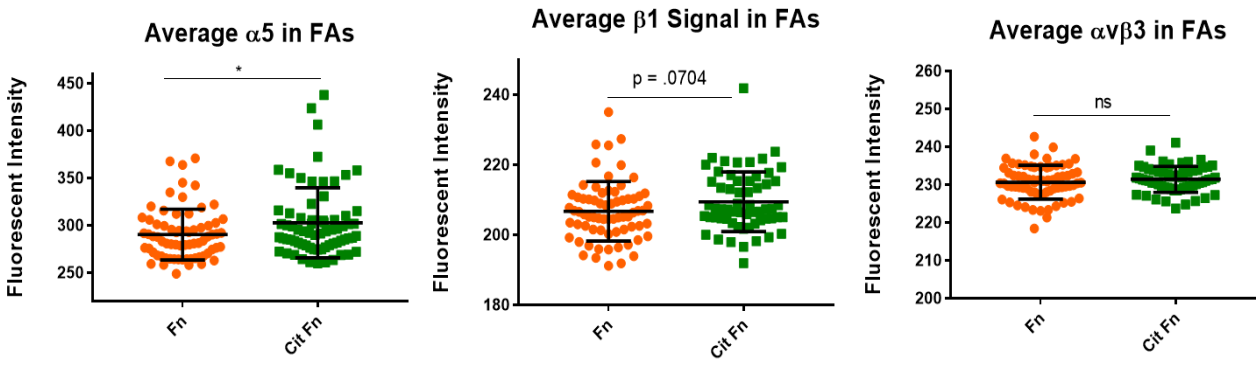

Figure 14: Integrin Expression in Human Lung Fibroblasts
The average fluorescent integrin signal for α5 and β1, but not for αvβ3, is enhanced within FAs of human lung fibroblast (CCL210) cells plated on Cit Fn in comparison to Fn. At least 70 cells per substrate were analysed across 4 coverslips.

It does appear that β1 integrins are at least in part responsible for the observation of enhanced integrin clustering, since within β1-KD HFFs, the average amount of both α5 and

αvβ3 integrin within FAs decreased on Cit Fn but not on Fn (Figure 15A, B). When β1 was knocked down from HFFs, there was a also reduction in average FA size in HFFs plated on both Fn and Cit Fn, but to a greater extent on Cit Fn (Figure 15C).

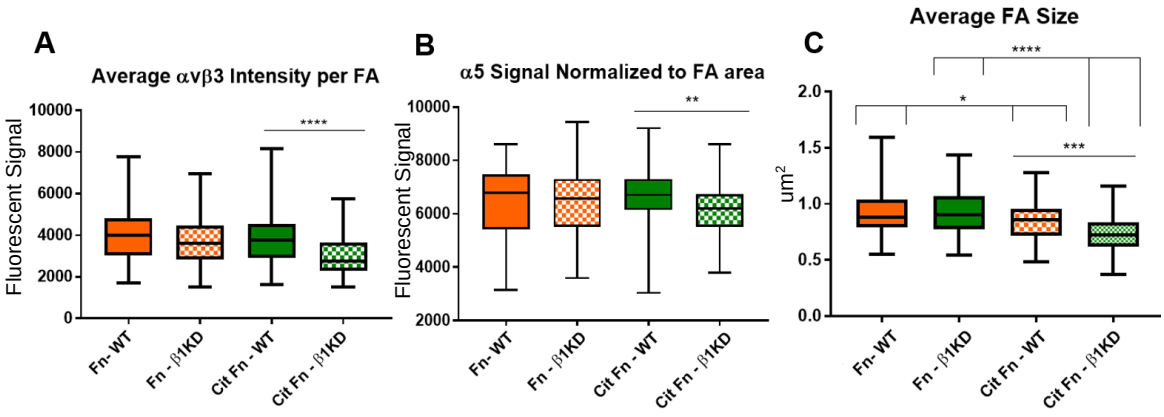

Figure 15: ICC Integrin Staining of Beta1-Knockdown Fibroblasts
Quantification of fluorescent signal for (A) αvβ3 integrins within FAs, (B) α5 integrins within FAs, and (C) average FA size based on paxillin represent a minimum of 75 cells each per substrate and condition.

3.4.5 Citrullination of Fn Causes Force-Sensitive Upregulation of FAK-SRC-ILK-GSK Signalling

Co-immunoprecipitation analysis of phosphorylated signaling proteins showed an enhancement in the baseline (no-force) levels of pFAK, pSRC, and pILK within cells plated on Cit Fn compared to Fn with this enhancement being most prominent on pILK (Figure 16A, B). Further, each of these proteins exhibited a greater amount of force-induced enhancement on Cit Fn in comparison to Fn, with the increase on pILK being particularly striking. For all phosphorylation western blot data, phosphorylated protein signal was normalized to total levels of the respective protein.

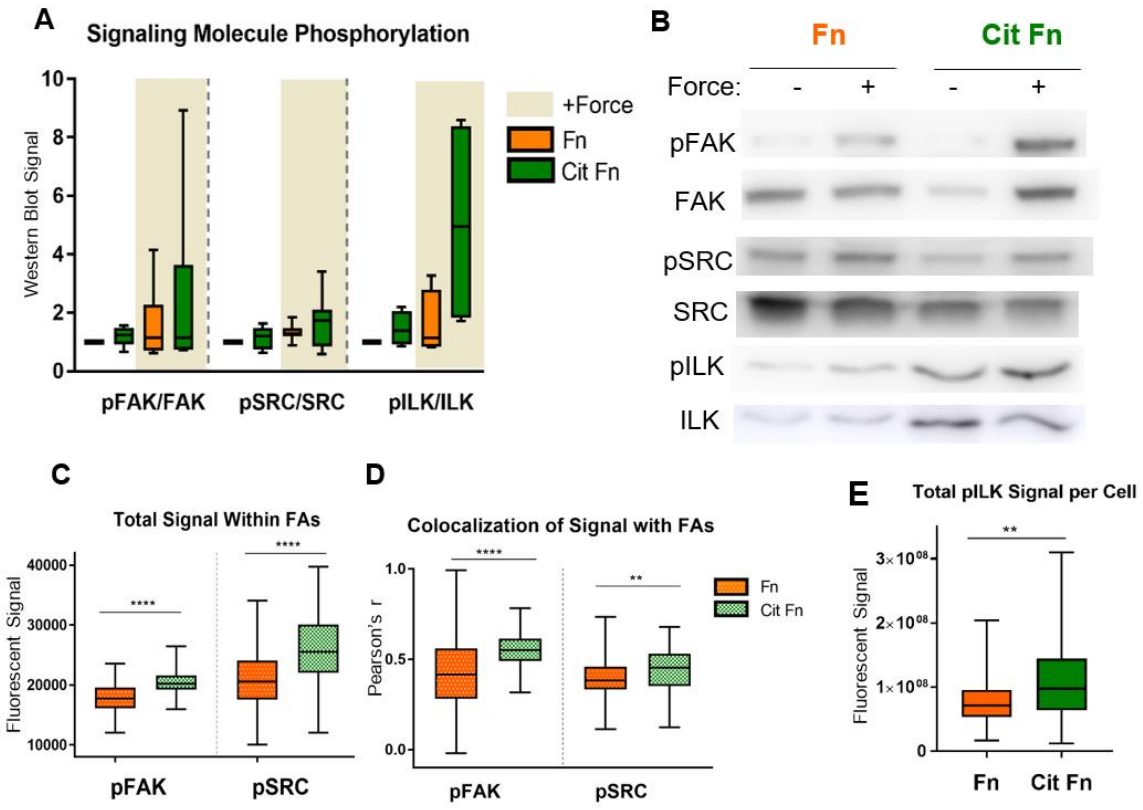

Figure 16: Downstream p-FAK, p-SRC, and p-ILK Signaling
Western blot data (A) represents average of at least six biological replicates each for pFAK and pSRC and four biological replications for pILK in force-inducible co-immuoprecipitation assays where Fn or Cit Fn were used to pull integrins and signaling complexes out with (brown background) or without force, with representative western blots shown in (B). Quantification of ICC of fibroblasts plated on Fn/Cit Fn-coated glass show the total pFAK or pSRC signal within FAs (C), the co-localization of pFAK and pSRC signal with FAs (D), and the total pILK signal per cell (E). For ICC data n = 75 cells per condition across 4 coverslips.

Force-induced co-immunoprecipitation assays represent FA adhesome formation in response to a localized external force, whereas fibroblasts plated on a stiff surface are capable of internally generating force via actin-myosin contraction; thus immunocytochemical (ICC) staining of cultured cells also reveals signaling as a function of strained cell state. ICC staining revealed an overall greater amount and co-localization of pFAK and pSRC within FAs of HFFs plated on Cit Fn in comparison to Fn (Figure 16C,

D). FA area was identified via paxillin stain. Likewise, total pILK (Figure 16E) and pGSK/GSK cellular signal was enhanced on Cit Fn-plated cells compared to on Fn (Figure 17A). In the case of pGSK, cells plated on Cit Fn also exhibited enhanced nuclear localization of pGSK (normalized to total cellular GSK signal) compared to on Fn (Figure 17B,C).

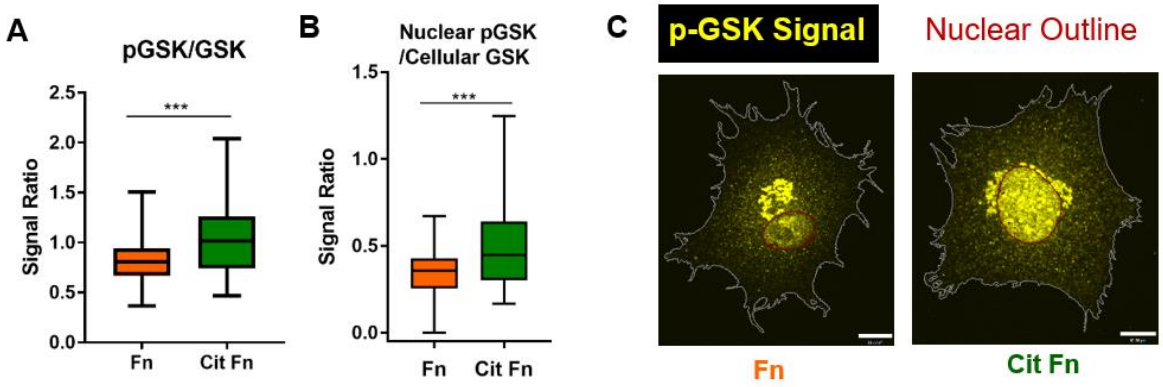

Figure 17: Glycogen Synthase Kinase (GSK) Analysis
Quantification of total cellular pGSK signal normalized to total cellular GSK signal is shown in (A), with nuclear pGSK signal normalized to cellular GSK signal shown in (B). Representative confocal maximum projection images of cells on Fn and Cit Fn (C) display p-GSK signal in yellow with the cell edge outlined in white and the cell nuclear region outlined in red. Results represent a minimum of 70 cells per condition across 4 coverslips.

3.4.6 Citrullination of Fn Results in Increases of Mechano-responsive proteins F-actin and Vinculin, but not Rac or Rho

Stress fiber or fibrillar actin (F-actin) assembly within cells is a force-sensitive event starting at around 2kpa and resulting in progressively increased fiber number and thickness on greater stiffnesses. F-actin content can therefore serve as a proxy for cell mechanotransduction. In a 3D confocal z-stack analysis of total F-actin content in cells plated on Fn/Cit-Fn coated polyacrylamide gels of varying stiffness, it was shown that total

F-actin content was significantly enhanced on Cit Fn compared to Fn on 25kpa gels and only modestly increased on 8kpa gels (Figure 18). No differences in F-actin content were

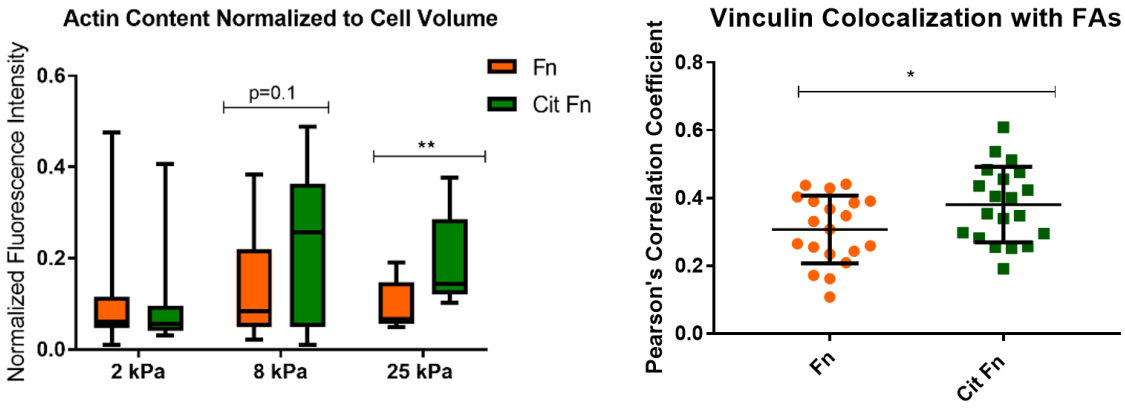

Figure 18: Mechano-sensitive Protein Products F-Actin and Vinculin are Upregulated on Cit Fn
The plots above depict quantification of phalloidin signal for F-actin detected within confocal z-stack images (left) of fibroblasts plated on protein-coated polyacrylamide gels of three different stiffnesses, and co-localization of vinculin signal (right) with paxillin, a proxy non-force sensitive marker of FA location. Results represent a minimum of 20 cells per condition.

observed between Cit Fn and Fn on 2kpa gels. ICC analysis of vinculin, a force-sensitive protein, demonstrated an increase in absolute quantity as well as co-localization with FAs (Figure 18). FA area was identified via paxillin stain. Finally, GLISA assays for Rac and Rho proteins, key mediators of several mechanotransduction pathways did not demonstrate any differences in the amounts of either of these proteins between HFFs plated on Fn vs Cit Fn (Figure 19).

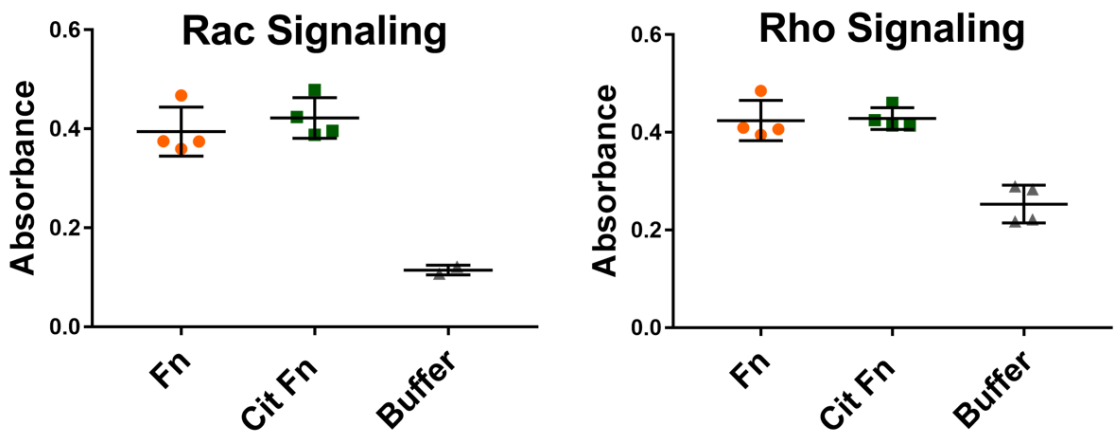

Figure 19: Rac and Rho Signaling
The above graphs depict quantification of GLISA assays for Rac1 and Rho protein activation after 30 minutes of fibroblast exposure to Fn or Cit Fn. No significant differences between experimental groups were observed. Results represent two biological replicates with n=2 per condition.

3.5 Discussion

3.5.1 Interpretation of Mass Spectrometry Results

Mass spectrometry of Cit Fn identified 24 unique citrullination sites modified as a result of PAD2 alone, PAD4 alone, or the combination of PAD2 and 4 together. These findings appear to be more comprehensive than the two previous MS analyses of Fn conducted by VanBeers et. al. [25] and Sipila et. al. [34] which identified just four or five citrullination sites, respectively. The VanBeers study which used Fn samples modified *in vivo* from human RA patients, was unfortunately limited by a low coverage of just 53 or 28 percent from two different patient samples, though two of the sites they identified, a double modification at residues R1035,1036, were also identified in the current study. Importantly these modification sites appear to possess potent immunogenicity, as 50% of established RA patients studied by VanBeers appeared to possess ACPA specific for this site.

None of the modification sites identified in the Sipila study matched the ones found here. Similar to our study, the Sipila group performed *in vitro* citrullination modifications, although it should be noted that they used a rabbit PAD2 enzyme, and PAD4 of unspecified species origin whereas our study utilized a mouse PAD2 enzyme and a human recombinant PAD4 enzyme. Inter-species sequence conservation for the various PAD isotypes ranges from 70-95%, so it's possible that the different sources of PAD enzymes may underlie the variation in findings. It's also of interest to note that three of the citrullination sites identified in the present study (R67, R1207, and R1802) were found to be modified both after *in vitro* PAD incubation, but also, in Fn samples that were not exposed to PAD enzymes. Since our Fn is purified in-house directly from patient plasma, it is possible that these samples were previously modified *in vivo* due to inflammatory processes in the patients through whom the plasma samples were sourced.

Seven identified sites of modifications reside within Fn regions of known biological function unrelated to cell-binding (R67, 107, 515, 1802, 1891, 1910, and 2223). As citrullination results in the loss of a positive charge it could be expected to influence Fn electrostatic interactions with fibrin and collagen to modify both the strength of attachment and also how these proteins pack together; changes in these protein-protein interactions may have larger implications for overall conformation and stiffness of *in vivo* cell-derived matrices. Elimination of positive charge would also be expected to negatively impact interactions with growth factors, most of which are negatively charged, as well as heparin, which is known to possess a very dense concentration of negative charges. A lesser ability to bind and therefore sequester growth factors could potentially make them more bio-available to local cells, thus providing an indirect mechanism for citrullination's modulation

of cell function. Somewhat counter-intuitively, however Cit Fn has previously been demonstrated to possess an enhanced affinity for VEGF [35], implying that citrullination's impacts may be mediated through means other than charge alone.

Table 2: Citrullination Sites and their locations within Fn Regions of Known Biologic Function

Position(s)	Description of functional region	Citrullinated sites identified by MS/MS	Total sites
52 – 272	Fibrin- and heparin-binding 1	67, 107	2
308 – 608	Collagen-binding	515	1
1267 – 1540	Cell-attachment	1274, 1284, 1410, 1434, 1452, 1476, 1479	7
1721 – 1991	Heparin-binding 2	1802, 1891, 1910	3
2206 – 2337	Fibrin-binding 2	2223	1
Other	Undefined	290, 751, 903, 911, 938, 953, 1035, 1036, 1207, 2356	10
		Total Citrullinated sites identified by MS/MS	**24**

Of prime interest, of course, are the five citrullination sites found within the cell binding domain, spanning across the 9th and 10th type III repeats, which were fully covered in MS analysis of Cit Fn (Figure 20). Similar to the studies of both Sipila and VanBeers, we were unable to detect a modification of the RGD site (R1524), which is surprising in part because one would expect this site, which exists as part of a loop extending 10 angstroms from the face of Fn, to be readily accessible to PAD enzymes. However, its lack of detectable modification does align with the biochemical prediction of PAD preferred binding originally described by Assohou et. al. [27]. Also, there exist three other verified citrullination sites within the 10th type repeat relatively nearby to the RGD at R1452, R1476,

and R1479, and further, molecular modeling shows that both R1476 and R1479 extend in the same direction as the RGD loop therefore making them likely to impact RGD interactions due to both proximity and protein conformation.

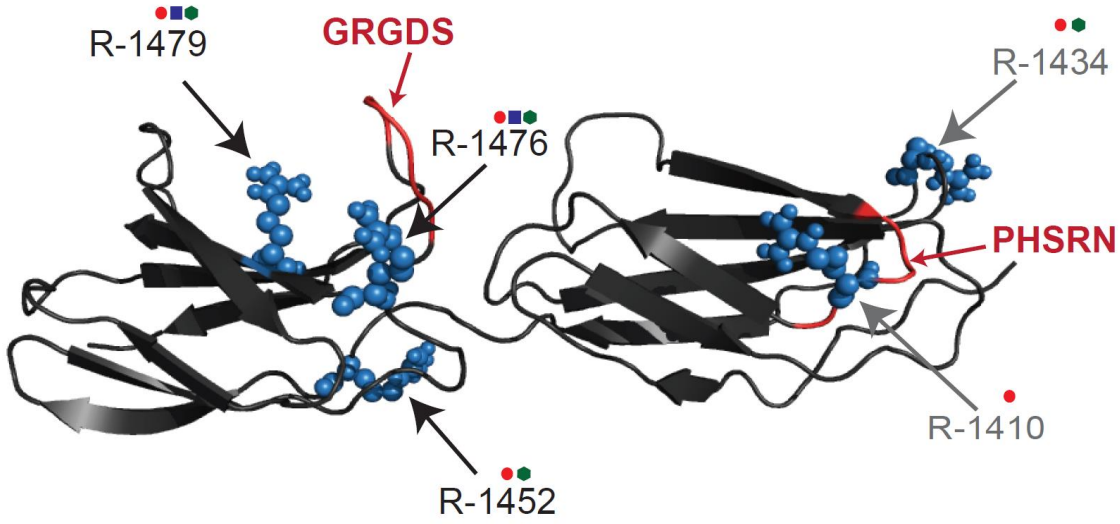

Figure 20: Molecular Model Citrullination Sites Within the FnIII 9-10 Cell Binding Domain
The molecular model of Fn cell binding domain depicts the relative three-dimensional positions the R1452, R1476, and R1479 citrullination sites within the Fn10th type III repeat with respect to the RGD site. Also shown is the citrullinated synergy site, PHSRN and the additional citrullination site at R1434 within the Fn 9th type III repeat.

Interestingly, we did find the PHSRN synergy sequence (R1410) to be citrullinated, which could have a direct impact on α5β1 integrin interactions, especially considering that previous mutagenesis studies have identified the R of PHSRN to be the most important residue in modulating α5β1 attachment [146]. A second citrullination site within the 9th type III repeat, R1434 may also impact α5β1integrin engagement due to both its proximity to as well as the fact that molecular modeling shows its placement with PHSRN on the same face of Fn. Of course, ability to detect citrullination at R1410 and R1434 does not guarantee that these locations are always citrullinated, and the stoichiometry of these modifications *in*

vivo may determine the ultimate impact of these modification sites on integrin and cell interactions.

There were also two citrullination sites at R1274 and R1284 within the 8th type III repeat that may also have the ability to influence α5β1 integrin binding. While the 8th type III repeat does not possess any cell binding functions on its own, its proper conformation along with the 9th and 10th type III has the capability of replacing the function of the PHSRN site. This fact was highlighted in a study by Altroff et al. where FnIII 8-10 fragments with mutated PHSRN sites were shown to possess the same affinity as unmodified FnIII 9-10 fragments for α5β1integrins, and both of these affinities were far greater than that of FnIII 10 fragments alone or FnIII 9-10 fragments with mutated synergy sites [142].

It's also important to note that the PHSRN synergy site, along with cell binding domain sites R1434 and R1452, was shown to only be modified by PAD2. This finding is potentially of vital significance due to the ongoing debate in the pharmaceutical industry and research labs worldwide as to whether citrullination inhibition efforts should be directed at just one PAD isotype, or all of them. To date, all PAD inhibitors of just a single isotype have been designed to target PAD4, possibly because it is the only isotype with a nuclear localization sequence, and thus it would be expected to have the greatest impact on gene regulation and NETosis via histone modifications [1, 24]. Alternately, BB-Cl-amidine is the most potent pan-PAD inhibitor currently in existence and has shown the ability to completely reverse disease or nearly so in mouse models of lupus [41] and collagen-induced arthritis (CIA) [68].

When it comes to efficacy of PAD inhibitors outside of BB-Cl-amidine, results are more mixed. BB-Cl-amidine's predecessor, Cl-amidine not only has lower bioavailability, but it possesses a PAD2 affinity a full ten times lower than that of BB-Cl-amidine, and it was shown to have no effect on the collagen antibody-induced arthritis (CAIA) model [26, 68]. These results, along with a PAD4-knockout study that did not prove efficacious in a KBxN model of arthritis [153], led Willis et. al. to argue that citrullination may not play a role in the effector phase of arthritis [152]. Of course, PAD4-specific inhibition has shown efficacy in two different CIA arthritis models [152, 154], a TNF-α model [155], and in a glucose-6-phosphate isomerase (GPI) arthritis model [156], although it should be noted that in the GPI, TNFα, and the Suzuki et. al. CIA models, only partial disease improvement was observed. The Suzuki study, in particular, documented an increased compensatory expression of PAD2 which may have contributed to their inhibitor's partial efficacy [154]. There certainly exists a significant amount of variation in pathology from one disease to another and also among the various animal models of individual diseases, so it would be impossible, at this point, to attribute the success, partial success, or failure of citrullination inhibition efforts to a particular PAD isotype. Nevertheless, these variations in results among studies strongly suggest that close attention should be paid to the extent of contribution of the various PAD isotypes.

A final observation of the MS results concerns the fact that there appears to be some inconsistency with regards to sites modified by a single PAD isotype compared to both. Theoretically, one would expect any site that can be modified by PAD2 or PAD4 alone to also be modified by the combination of PAD2 and PAD4 enzymes. Yet eight of our citrullination sites display a pattern of modification by PAD2 alone, PAD4 alone, or both

PADs 2 and 4 when they are individually applied, but not in the case where PADs 2 and 4 are administered together. It should be noted that our four groups of modified protein (PAD2 only, PAD4 only, PADs 2+4, or no PADs) were processed completely separately with regards to initial modification, protein degradation, and MS processing, and therefore the intrinsic variability of any one of these steps may account for this inconsistency. Indeed, these inconsistencies cannot be attributed to MS protein coverage, since all of these sites were covered in all four of the analyses. The sites R751, R953, R1410 and R2223, were definitely not citrullinated in the condition of PAD 2+4. The sites R67, R515 and R1910 were found to be citrullinated in the PAD 2+4 condition, but they were later eliminated from consideration due to low-quality MS2 spectra. Another hypothesis to explain these results is that the PAD2 and 4 enzymes are citrullinating themselves and/or one other leading to enhanced levels of inactivation at especially high levels of total PAD concentration. PAD4, in particular, has a documented ability for autodeimination [66] which leads to its inactivation, so it may not be surprising if it could also target PAD2 and visa versa.

3.5.2 Evidence for a αvβ3 to α5β1 Integrin Switch and its Potential Implications

Interferometry results indicate that the impact of citrullination of Fn with regards to α5β1 integrin affinity is a slight increase in affinity from 0.741nM to 0.3016nM. Nevertheless, even unmodified Fn's affinity of 0.741nM is in the range of monoclonal antibody affinity, and one would not expect this small difference to have a large biological impact. Indeed, CHO-α5β1adhesion results did not produce any significant changes in cell attachment on Cit Fn compared to Fn. The more interesting interferometry result is the decrease of αvβ3 K_{on} rate on Cit Fn in comparison to Fn from 27240 down to 25400 $M^{-1}s^{-1}$. CHO-αvβ3 binding assays hold up the biological impact of such a change in affinity, as

attachment to Cit-Fn was significantly reduced, and attachment to fibrin, which already possesses a relatively low level of cell adhesiveness mediated entirely through αvβ3 integrins, was completely eliminated. These results strongly suggest that citrullination of provisional ECM proteins is likely to have a functional cellular impact.

Even more interesting were the ICC results demonstrating an increase of both α5 and β1 integrin subunits within FAs on Cit Fn in comparison to Fn within both HFFs that express both αvβ3 and α5β1 integrins, along with several others that must all compete for the same binding sites. Since neither interferometry nor CHO-α5β1 adhesion data indicated a drastic change in α5β1 affinity for Fn due to citrullination, it would be difficult to argue that affinity underlies this increase of α5 and β1 presence. One explanation, based on the much more substantial reduction of αvβ3 adhesion on Fn due to citrullination, is that α5 and β1 subunits increase their attachment in compensation for loss of adhesion via αvβ3. Confounding this explanation, however, is the fact that there did not appear to be any difference in absolute quantities of αvβ3 integrins within FAs of HFFs on Fn or Cit Fn.

A more likely explanation for the increase of α5β1 integrins may therefore be a result of integrin binding kinetics. It is well established that αvβ3 integrins are able to both attach and detach from Fn more quickly than α5β1 integrins [120, 148], and thus at early attachment timepoints one would expect cells to use a relatively greater proportion of αvβ3 integrins in comparison to α5β1 on Fn substrates. Integrins possess an impressive clustering ability such that whichever subtype binds first and is able to link with talin can then recruit additional integrins of the same or different subtypes to existing adhesion sites [148, 157]. Thus on normal Fn, αvβ3 would tend to bind first and subsequently recruit additional αvβ3 as well as α5β1 integrins. Since it normally exhibits slower binding kinetics, the integrin

α5β1 only tends to dominate as a proportion of total integrin presence in the case where additional force is required for adhesion such as on stiff substrates or in the presence of externally applied forces, and this is a direct consequence of its noted ability to form strong catch-bond like adhesions that increase in strength as additional force is applied [119, 121, 158].

A logical explanation for the enhanced for altered integrin proportions on Cit Fn is that since αvβ3 affinity on Cit Fn is reduced, there is an abnormal increase of α5β1 integrin attachments at early timepoints, and these are subsequently able to recruit both additional α5β1 integrins as well as αvβ3 such that the final result is an overall integrin ratio that favors both α5 and β1 subunits compared to αvβ3 integrins, or an integrin switch from αvβ3 towards α5β1. Indeed, since each pairwise comparison of co-localized integrins (αvβ3+β1, αvβ3+ α5, and α5+β1) shows enhanced co-localization on Cit Fn compared to Fn, these results may further imply that α5β1 integrins are intrinsically better at clustering than are αvβ3 integrins.

The force-induced co-immunoprecipitation results certainly bear out the integrin switch theory. In the absence of force, again, there is no distinguishable difference in αvβ3 presence on Fn or Cit Fn, though baseline levels of α5 are greater on Cit Fn compared to Fn. The fact that α5 presence increases due to force on Fn but not on Cit Fn, where it stays constant, may be explained by α5 integrins having already maxed out their adhesion in the baseline state, so it was not possible for them to increase any further as force was applied. The increase of α5 on Fn due to force application can be explained by the necessity for the recruitment of stronger α5β1 integrins to resist the applied force. With regards to αv integrins, there does not appear to be a force-induced increase on Fn, which is as expected

since these integrins are not best suited to high-force regimes. The force-induced increase of αv on Cit Fn, however is a bit surprising, and could imply that the already enhanced α5β1 baseline presence was able to not only retain clustered αvβ3 integrins but recruit additional αvβ3 integrins due to the application of force.

With regards to downstream signal protein phosphorylation, co-immunoprecipitation assays showed an enhancement of both baseline and force-induced phosphorylation of FAK, SRC, and ILK on Cit Fn compared to Fn. Similar increases were also observed in ICC assays of HFFs plated on Cit Fn. FAK phosphorylation, specifically at Y397, which is what was stained for in this study, is known to be enhanced in tensioned cell adhesion states, specifically in association with β1 integrins [158], and since there is an increase of α5β1 on Cit Fn, it seems logical that there would therefore also be an increase of phospho-FAK Y397. Phosphorylation of FAK Y397 is also directly associated with activation of src and binding of the Grb2 adaptor protein [124], both of which, in complex with pFAK are capable of enacting a variety of further downstream signaling as depicted in Figure 2.

One of the more prominent mechanotransduction pathways activated by pFAK/pSRC signaling is that of Rac/Rho where differences between Fn and Cit Fn could not be observed via GLISA assay. This may very well be because Rac and Rho are not actually upregulated as a function of Cit Fn binding. However, the GLISA assays were only performed at the single timepoint of 30 minutes, since most signaling events occur relatively quickly, but it is also possible that these molecules were being observed through the wrong window of time and that differences do exist in a different window. It should also be acknowledged that the GLISA is a fairly low-throughput assay and the sample size of four per substrate

(two separate experiments using two separate groups of cells per substrate each) may have been too small for statistical significance.

Altogether, the enhancement of vinculin, pFAK, pSRC, and α5β1 integrins strongly indicate altered activation of meahanotransduction on Cit Fn compared to Fn; in this context, it's aberrant because it occurs in the absence of changes to substrate stiffness or external force application. To explore changes in stress fiber content, a proxy for perceived cell stiffness, HFFs were plated on Fn- or Cit Fn- coated polyacrylamide gels of 2kpa, 8kpa, or 25kpa stiffness. Differences stress fibers were observed only on 8kpa and 25kpa gels, and only significantly so on 25kpa gels, indicating that while citrullination of Fn may aberrantly enhance mechanotransduction signaling, it's not to such an extent that these events also play out in very soft environments where they would be supremely abnormal. It's also worth mentioning that both 8kpa and 25kpa represent relatively stiff surfaces in a biological context, well beyond what would be experienced in lung tissues, though well below that of cartilage and bone [159].

The lack of F-actin enhancement on 2kpa gels on Cit Fn compared to Fn by no means undermines the significance of aberrant mechanotransduction as a consequence of Cit Fn. A study by Friedland et. al. defined two different states of α5β1 binding: relaxed when it only binds to RGD, and tensioned with it binds to both RGD and PHSRN. Importantly, α5β1can be induced into a tensioned state either from application of external forces or those generated internally from the actin-myosin machinery, and indeed, the ratio of tensioned to relaxed α5β1 integrins increases on progressively stiff substrates. Since specific pathways of downstream signaling, and in particular phosphorylation of FAK Y397, become activated through tensioned versus relaxed α5β1binding, the authors propose that this divergent α5β1-

mediated signaling may constitute an intrinsic evolutionarily derived means of cellular mechanotransduction. Based on the results of the present study, it would appear that through enhancement of tensioned α5β1, citrullination of Fn effectively initiates this mechanotransduction mechanism. An important question that remains, however, is whether the mechanotransduction signaling is being activated on a purely artificial basis, or whether fibroblasts on Cit Fn also experience an enhancement of internally generated forces as a result of interactions with Cit Fn.

The final piece to the signaling puzzle is the striking elevation of phospho-ILK on Cit Fn compared to Fn. ILK can certainly be considered a mechanotransduction protein as it plays an integral role in cardiac stretch [160] and though it will bind to both β3 and β1 cytoplasmic tails, it possesses a strong preference for β1 [125, 130], the subunit most commonly associated with tensioned environments. Nevertheless, through ILK's many functions as both a scaffolding protein in conjunction with Pinch and Parvin, and as an independent kinase, it has the ability to precipitate several signaling pathways, including Akt, JNK, and MAPK/ERK, that are most commonly associated with cancer, and possess functions outside traditional mechanotransduction axes. In particular, Akt is associated with cell survival and growth [161], JNK is a regulator of apoptotic and cell death pathways, and MAP/ERK largely regulates the cell cycle and cell proliferation. At least in theory then, fibroblast interactions with Cit Fn have the potential to alter cell functions relating to survival, growth, and proliferation.

Phospho-ILK also has the ability to phosphorylate GSK3-β, leading to its inhibition, and indeed we also observed an enhancement of phospho- GSK3-β. Since active GSK3-β normally sequesters β-catenin, when it's inhibited, β-catenin is able to translocate into the

nucleus to carry out canonical Wnt pathway signaling, known to influence almost every cell phenotype in existence, including differentiation, apoptotic resistance, cell invasiveness, proliferation, growth factor secretion, ECM secretion, and more [134-136]. GSK3-β has been directly linked to cell migration through several disparate mechanisms including lamellipodial formation and decreased FA turnover through FAK phosphorylation at S722; therefore inhibitory GSK3-β phosphorylation would actually be expected to enhance FA turnover [162]. Pointedly, we noticed a clear preference of nuclear localization of phospho-GSK on Cit Fn compared to Fn, and while the literature is not clear what this means for phospho-GSK, nuclear localization of active GSK3-β is correlated with cell proliferation and NF-kB anti-apoptotic activity [163].

3.6 Conclusion

Fibronectin can be citrullinated at 24 unique sites through the enzymatic activity of PAD2 and PAD4 enzymes; five of these modifications occur within the cell-binding domain and have been shown to have a detrimental impact on αvβ3 integrin attachment. This diminished αvβ3 attachment results in an integrin switch whereby fibroblasts adopt a α5β1-dominant adhesion phenotype that we hypothesize is mediated through changes in early integrin binding kinetics. The α5β1-dominant adhesion aberrantly activates mechanotransduction signaling involving up-regulation of pFAK, pSRC, pILK, and vinculin that ultimately lead to increased GSK3-β phosphorylation and stress fiber formation. Upregulation of mechanotransduction signaling has several implications for cell phenotype including cell migration, proliferation, survivability, and contraction, all of which point towards citrullination being a contributing factor in the activation of fibroblasts. More generally, both αvβ3 and α5β1 integrins are present in a variety of cell

types, which therefore implies that Fn citrullination may have even more wide-reaching impacts.

CHAPTER 4. THE INFLUENCE OF CITRULLINATED PROVISIONAL EXTRACELLULAR MATRIX ON FIBROBLAST PHENOTYPE

4.1 Abstract

Activated fibroblasts have been identified as a premier exacerbating element of a variety of chronic inflammatory conditions including rheumatoid arthritis (RA), fibrotic diseases, and cancer. Characteristics underlying their damaging impacts specifically include invasiveness, hyperproliferation, apoptotic resistance, enhanced contraction, excessive matrix remodeling, and unwarranted cytokine secretion. To investigate whether citrullinated fibronectin (Cit Fn), a protein strongly correlated to a severe course of these diseases, is sufficient to elicit changes in fibroblast behavior several different assays were performed. These included adhesion, BrDU, MTT, gel contraction, and wound healing assays which were respectively implemented to analyze cell spreading, proliferation, metabolism, cell contraction, and directional migration. Additionally, atomic force microscopy (AFM) was employed to evaluate cell stiffness, and α-actinin staining along with confocal videography was applied to investigate focal adhesion (FA) turnover. Results indicate that in the absence of any other stimuli, Cit Fn is sufficient to influence healthy fibroblasts to reduce spread area, increase stiffness, and increase both random and directional migration; this latter phenomenon can largely be explained Cit Fn's ability to also produce enhanced FA turnover. No differences were observed in proliferation, metabolism, or apoptotic resistance, though for the latter citrullinated fibrin did produce a protective effect. Altogether, results indicate that Cit Fn does contribute to fibroblast activation and it may therefore constitute a promising therapeutic target.

4.2 Introduction

Fibroblasts are interstitial cells best known for secreting extracellular matrix (ECM) proteins and generally helping to maintain healthy tissue structure [69, 70]. While normally found in a senescent state, during instances of wound repair they are known for becoming activated and taking on several special functions that are temporarily beneficial to the wound healing process. These include hyperproliferation, migration into the wound area, enhanced secretion of ECM molecules to provide a scaffold for cell infiltration, cytokine secretion to recruit necessary immune and other cells to the wound, apoptotic resistance as protection from oxidative stress of the inflammatory environment, and enhanced contraction to help minimize the exposed wound area [71, 97]. At the conclusion of wound healing, these fibroblasts typically revert back to a senescent state or engage an apoptotic pathway so that their overall numbers return to normal. In some instances, however, fibroblasts maintain their activated state to the point that their presence and activities become pathological.

In the cases of fibrotic diseases and cancer both, the disease environment is widely considered to be one of perpetual and excessive wound healing [53, 98]. At a macroscale, this results in tissues that are burdened with copious amounts of ECM proteins and an overall elastic modulus much higher than would be seen in healthy tissue, such that normal tissue function becomes impaired [109]. Importantly, fibroblasts are capable of sensing and responding in kind to stiff surfaces, and they tend to initiate mechanotransduction pathways that exacerbate existing tissue abnormalities [103].

In the case of RA, ECM abnormalities exist in two distinct phases. The first involves excessive ECM protein secretion, which along with an enhanced migration phenotype, allows activated RA fibroblast-like synoviocytes (RA FLS) to invade into both cartilage and bone, compartments in which they would not normally be present [75, 79]. The second

involves excessive breakdown of ECM tissues; while this is a phenomenon that also occurs in fibrotic diseases and cancer, it's generally not to the extreme seen in RA. RA FLS secrete profuse quantities of matrix metalloproteinases (MMPs) and other proteases that drive the breakdown of cartilage and bone. Importantly, once activated, RA FLS are capable of executing these disease exacerbating activities in the absence of continued inflammation or immune activation [86].

While inflammation and immune stimulation are both certainly capable of aggravating activated fibroblast phenotypes, the question as to how fibroblasts initially become activated and maintain their activated states have stymied researchers for decades. There is certainly a genetic component, as fibrosis-associated fibroblasts (FAFs), cancer associated fibroblasts (CAFs) and RA FLS, are all known to acquire epigenetic and permanent genetic changers that accelerate aberrant behaviors [43, 73, 79]. Nevertheless it's difficult to ignore the fact that due to the chronic inflammation, excessive ECM deposition, and perpetual remodeling that is known to occur in all these diseases, the fibroblasts are constantly exposed to a very abnormal micro-environmental architecture that pointedly possesses a disproportionately high quantity of the provisional matrix proteins fibrin(ogen) and fibronectin [108, 164].

Importantly, a significant amount of the provisional ECM (pECM) in cancer, fibrosis, and RA is known to be citrullinated since antibodies can be detected that react to the citrullinated proteins and imunohistochemical staining has directly proven its existence within inflamed tissues of these diseases [22, 35, 80, 165]. Further, these matrices are known to become citrullinated at very early stages of disease progression [7], begging the question as to whether their intimate physical proximity to activated fibroblasts is more a correlative,

or causative factor in these diseases. In the current aim, the goal is to gain and understanding of how citrullinated fibronectin (Cit Fn), in the absence of any other stimuli influences fibroblast behavior so that we may better elucidate the contribution of citrullination in the pathophysiology of these diseases.

4.3 Materials and Methods

4.3.1 Adhesion and Cell Morphology Assays

To evaluate fibroblast adhesion and spreading, HFFs were plated in SFM for 15, 30, 45, or 60min on Cit Fn or Fn-coated coverslips, subsequently washed with PBS++ (supplemented with 2mM $CaCl_2$ and 1mM $MgCl_2$ for integrin activation), fixed with paraformaldeahyde, permeablized, and then stained with phalloidin and Hoescht. Large 10X magnification tile-scan images were taken of 0.5cm by 0.5cm regions of each coverslip using a Nikkon-Ti fluorescent scope and the absolute number of adherent cells was gauged by a count of distinct nuclei. Cell area, perimeter, and circularity ($C = 4*pi*area/perimeter^2$) were calculated from phalloidin stain using Nikkon elements software on a minimum of 100 unique cells imaged with a 20X objective. Only isolated cells (not touching any other cells) were included for analysis. For evaluation of cell adhesion on substrates of variable stiffness, HFFs were plated within wells of Matrigen SoftWell Easy Coat plate with defined gel stiffnesses of 2kpa, 8kpa or 25kpa for 45minutes, after which they were fixed, stained, and imaged as above.

*4.3.2 9*10 Cell Adhesion*

10mm diameter coverslips were coated overnight with 20ug/mL 9*10 fragments in PBS and subsequently blocked for 1 hour in 1% hd-BSA solution. HFFs were seeded at 4000cells/cm^2 for 45 minutes, after which they were washed 1X in PBS++, fixed with paraformaldehyde, and stained for phalloidin. Imaging and subsequent cell area analysis was conducted using a Nikon Eclipse Ti scope and associated Elements software.

4.3.3 AFM analysis of Cell Stiffness

HFFs were plated on CitFn/Fn-coated glass coverslips for 1 hour in SFM at which point beaded AFM tips were used to indent two unique locations per cell for a total of 50 cells per substrate over two dishes each. A subset of cells were subsequently fixed with paraformadahyde and re-assayed as a positive stiffness control. Cell plating was staggered such that all cells were assayed within two hours of initial plating. For evaluation of cell bulk modulus when plated on variable stiffness substrates, an identical procedures were followed using Matrigen EasyCoat gel-coated coverslips of defined 1kpa, 8kpa, or 25kpa stiffnesses. Gel stiffness was confirmed by directly indenting a 1mm region of the gel.

4.3.4 Apoptosis

Individual 35mm TC petri dishes were prepared for covalent linkage to thin fibrin clots by first being incubated with 2.5% glutaraldehyde solution in water for 1.5 hours at 37^{o}C, after which they were washed 2X with dH_2O. Clots were prepared to a final volume of 125uL with 1.5mg/mL fibrinogen, 0.5U/mL thrombin, and HEPES/5mM $CaCl_2$ solution. Upon thrombin addition, clots were spread using mini-cell scrapers to cover the entire surface area of petri dishes, after which they were allowed to dry at room temperature. Clots were washed once in 4X Citrullination buffer (400mM tris, 20mM $CaCl_2$) to quench

unreacted aldehyde groups. Citrullination buffer was subsequently replaced with 1X citrullination buffer with or without PAD2/4 enzymes for modified/un-modified substrates at concentrations of 10units PAD4/mg fibrinogen + 11.2 ug PAD2/mg fibrinogen. Citrullination reactions were allowed to proceed at room temperature with gentle shaking for 24 hours after which they were quenched with 20mM EDGA. Fibrin gels were washed 1X with PBS and then blocked with 1% hd-BSA. In the preparation of Fn/Cit Fn-coated dishes, the Fn/Cit Fn was passively absorbed overnight at 20ug/mL, with 1mL of total solution per 35mm dish.

Cells were plated at 12.2K cells/cm^2 (2 dishes per substrate per apoptotic treatment condition) for two hours in SFM before having media replaced with SFM containing 200, 100, 50, or 0uM (untreated controls) freshly opened and freshly mixed hydrogen peroxide. All hydrogen peroxide solutions were replaced with freshly prepared solutions after the first eight hours, after which cells were given an additional 6 hours of hydrogen peroxide exposure for a total of 14 hours, at which point cells were washed with PBS, trypsinized, and stained for caspase 3/7 and 7AAD (CellEvent kit, thermos) using standard protocols. A minimum of 10K cells per substrate per treatment condition was measured via Calibur flow cytometry with analysis in FCS express. Data represents an amalgamation of three replicate experiments. For single-stain live/dead controls, HFFs were plated in full-serum media for the duration of the experiment and then either stressed via heating at 65^oC for 5 minutes, followed by 3 minutes on ice, or left at room temperature.

4.3.5 Cell Proliferation Assays

HFFs were plated on Fib, Cit-Fib, Fn, Cit Fn, or hd-BSA-coated coverslips in SFM supplemented with 0.2% Fn-depleted serum for 2 hours after which they were fixed and analyzed using standard BrdU protocols for percent proliferating cells with a minimum of 10 coverslips per experimental substrate and 5 coverslips for negative controls.

4.3.6 Cell Metabolism Assays

HFFs were serum-starved in 0.2% Fn-depleted serum media for 48 hours before being plated in 0.2% Fn-depleted serum or SFM on top of either Fn, Cit-Fn, or BSA at cell densities of 20K, 10K, or 5K cells per well (96-well plate), with 6 wells prepared per substrate and cell density, for 2hours, after which MTT solution was allowed to incubate for an additional 4 hours. MTT metabolism and quantity was analyzed according to manufacturer's recommended protocols. For analysis on fibrin/cit-fibrin, 100uL clots of 0.1mg/mL fibrinogen and 1U/mL thrombin were polymerized in glutaraldehyde-treated wells and allowed to dry overnight. Clots were washed prior to plating of cells.

4.3.7 Strained Gel Contraction Assay

Gels were prepared in non-TC 24 well plates pre-blocked in 2% hd-BSA and washed with PBS, and air-dried. Fn-infused clots were 250uL and consisted of 2.5mg/mL fibrinogen, 200ug/mL fibronectin, and 1U/mL thrombin in HEPES/5mM CaCl2 solution. Clots were allowed to polymerize for 30minutes at 37ºC, after which 500uL 1X citrullination buffer (with/without 10U/mg protein PAD4 + 11.2ug/mg protein PAD) was added for a 24hr incubation culminated with quenching in 20mM EDTA. Clots were washed 2X with PBS before seeding HFFs at 30,000 cells/well in 1mL SFM supplemented with 0.2% Fn-depleted serum + 2uL stock aprotinin per well. Media was replaced after first

24 hours. At the 48-hour timepoint, clots were released from well bottoms using a 30G needle around the gel edge and allowed to contract for 15minutes at which point they were photographed. They were then fixed in 4% PFA for 15minutes, washed 3X in PBS, stained with Pierce 660nm Assay Reagent for 15minutes (for contrast), washed again in PBS, and finally imaged via flash photography. Image J was utilized to make measurements of final clot areas in photos both before and after fixation/staining. Twelve clots each were analyzed with or without citrullination. For no-contraction controls, un-citrullinated gels (n=5 each) were either exposed to media without cells or dosed with 12uM latrucuin B added 3 hours following initial cell seeding and replaced after the initial 24 hours.

4.3.8 Floating Gel Contraction Assay

Gels were prepared in non-TC 24 well plates pre-blocked in 2% hd-BSA, subsequently washed with PBS, and air-dried. Fn-infused clots of 250uL volume were prepared with 2.5mg/mL fibrinogen, 200ug/mL Fn, 1U/mL thrombin in HEPES/5mM $CaCl_2$ solution. Clots were allowed to polymerize for 30 minutes at 37^{o}C, after which 500uL 1X citrullination buffer (with/without 10U/mg protein PAD4 + 11.2ug/mg protein PAD) was added for a 24hr incubation culminated with quenching in 20mM EDTA. N=12 each Fn/Cit Fn gels.

HFFs were plated at 40,000 cells per well in 1mL SFM supplemented with 0.2% Fn-depleted serum and 2uL stock aprotinin. Cells in latrunculin wells were allowed to attach for 1 hour before the addition of 12uM latrunculin. All cells were allowed a total of 4 hours for gel attachment before gels were detached from well walls using 30 gauge needles. Wells were imaged at 24 hours post gel detachment from walls, both before and after fixation with

paraformaldehyde. Fixed gels were subsequently washed 3X in PBS, stained in Ponceau solution for 30 minutes (for enhanced contrast). They were subsequently washed with water.

4.3.9 α-actinin Analysis

HFFs were plated in SFM for 2 hours on coverslips pre-coated with Fn or Cit Fn. For negative controls of FA turnover, cells were plated on Fn in the presence of 10uM PF-28, a FAK-inhibitor for the full 2 hours, or 2uM of cytochalasin D for the last 30 minutes of cell plating. After 2 hours, cells were washed, fixed in paraformaldehyde, and stained with anti-α-actinin (ab18061, abcam) at 1:400, anti- rabbit paxillin (ab32084, abcam), and phalloidin. Only individual cells determined not to be in contact with any neighboring cells were imaged via PerkinElmer spinning disk confocal microscope using a 63X objective. A total of 75 over 4 coverslips were imaged per condition. Three biological replicates were performed, only one of which included sh-RNA β1 knockdown cells on Fn or Cit Fn as additional groups.

4.3.10 Real-time Paxillin Turnover Analysis

Low passage HFFs were transfected with RFP-paxillin (a kind gift from the Cassanova Lab at UVA), using 6ug per 200K cells along with 24uL of X-tremeGene Transfection Reagent (Sigma-Aldrich). Cells were allowed 14 hours for transfection, after which they were washed multiple times and provided fresh media. Cells were allowed to rest 24-hours in full-serum media before being plated on Fn/Cit-Fn coated coverslip-bottom petri dishes (FluoroDish) in serum-free media supplemented with 25mM HEPEEs. Cells were allowed to adhere for two hours, at which point they were washed, given fresh SFM+

25mM HEPES, and imaged via TIRF confocal microscopy within a temperature-controlled environmental chamber. FA turnover videos consisted of images taken once every 10 seconds for a total duration of 10 minutes per cell. Cell plating was staggered such that all cells were imaged within four hours of initial plating. A total of 14 cells were imaged per substrate across four separate dishes representing two biological replicates of unique RFP-paxillin transfection. Only isolated cells (those not touching any others) were imaged. FA turnover was quantified using Volocity quantitation software.

4.3.11 Random Migration Assays

Cell culture dishes were divided in half using thin PDMS inserts adhered to the bottom utilizing silicone glue and allowed to dry 24 hours. Dishes were sterilized via UV radiation prior to coating the two halves with 20ug/mL Fn or Cit Fn protein in PBS overnight at 4^{o}C, after which plates were blocked with 1% hd-BSA. HFFs were plated at 4000 cells/cm^2 and given two hours to adhere before exchanging media for fresh SFM supplemented with 1% BSA. The divided 35mm dishes were placed within the 37^{o}C, CO_2-supplemented cell culture chamber of a Nikon Biostation imaging apparatus, and cell migration was monitored for the next 20 hours with 10x phase contrast images captured once every 10 minutes of nine unique fields of view on each substrate. Cell movements were quantitated using the cell tracker plugin of Image J. Persistence distance is defined as the cumulative distance travelled by a single cell without a change of direction greater than or equal to 90 degrees. Only cells for which the entire nucleus was visible for a minimum of 20 frames were included in analysis for a total of at least 35 cells per condition.

4.3.12 Wound Healing Assays

Wound healing assays were conducted utilizing the CytoSelect 24-well Wound Healing Assay (Cell BioLabs, Inc.). Individual wells (n=4 per substrate) were coated with 50ug/mL Fib/Cit Fib or 20ug/mL Fn/Cit Fn overnight at 4^{o}C, and subsequently blocked with hd-BSA for 1 hour. HFFs were seeded at 200Kcells/cm^2 around 0.9mm plastic inserts for 4 hours in SFM supplemented with 0.2% Fn-depleted serum, after which inserts were removed, wells gently washed 2X with PBS, and fresh media was added. Following the (13 or 15) hour migration period (trials 2 and 1, respectively), cells were fixed in 4% PF, stained with cresyl violet solution, and imaged via brightfield microscopy. Thresholding, contrast enhancement, and subsequent calculations of percent wound coverage were performed in ImageJ and Matlab.

4.3.13 Statistical Analysis

All statistical analysis was performed using GraphPad Prism software with 2-tailed t-tests or one-way ANOVAs and Tukey post-hoc analysis, as appropriate for the experimental set-up. Alpha was set at 0.05 for all analyses. In the case of larger data-sets, such as with fluorescent signal analysis of cell components in microscopy images, outliers were removed using the ROUT method with a Q of 1% prior to further statistical analyses. The Shapiro-Wilk test was utilized to test for normality of data distribution, and in cases where null hypothesis was rejected, the Mann-Whitney test was applied to ascertain statistical significance.

4.4 Results

4.4.1 Fibroblast Adhesion and Spreading is Reduced on Cit Fn

While modest, citrullination of Fn results in a significant reduction in both the total number of adhered HFFs and also their total spread area (Figure 21A, B, E). Adhesion and spreading was significantly and much more obviously enhanced compared to that observed on the negative control of heat denatured BSA. These differences can be reproducibly observed as early as 30 minutes and extending through at least one hour with the greatest differences being observed at around 45 minutes (Figure 21D). HFF circularity, on a scale of 0 to 1 where 1 represents a perfect circle, was very low on both Fn (average = 0.2635) and Cit Fn (average = 0.2798) and although these measurements indicate that HFFs on Cit Fn are slightly more rounded this finding was not significant. Results from HFF adhesion on Cit 9*10 vs unmodified 9*10 show that a similar reduction in cell adhesion is observed on the citrullinated protein (Figure 21C). Since 9*10 contains only the portion of Fn representing the cell-binding domain, it is apparent that modifications within this region of Fn alone are capable of mediating changes in fibroblast adhesion.

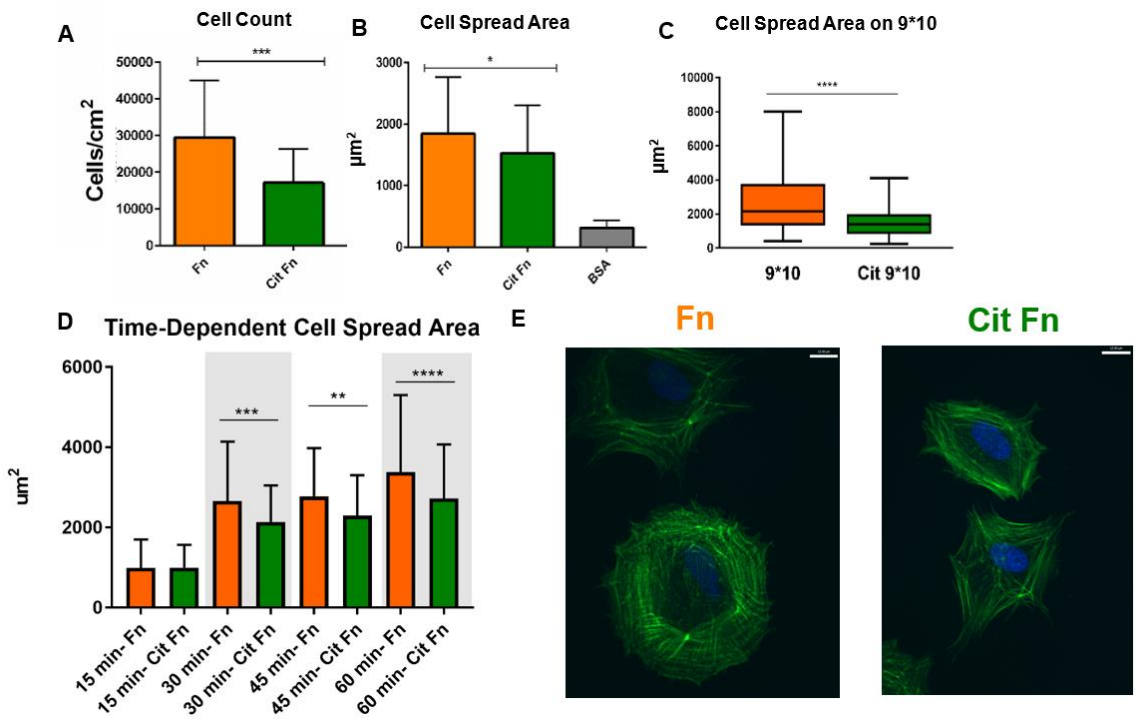

Figure 21: Fibroblast Adhesion and Spreading on Fn and Cit Fn
Graphs depict the relative numbers (A) and spread areas (B) of HFFs adhered to Fn or Cit Fn. Additionally, HFF spread area on citrullinated Fn cell binding domain fragments (Cit-9*10) or unmodified fragments (9*10) are shown in (C) along with a comparison of spread areas on Fn vs Cit Fn at timepoints ranging from 15 minutes through 1 hour (D). Representative images of phalloidin-stained cells are shown in (E) where white scale bar indicates 12um. Analyses across all experiments represent a minimum of 100 cells per substrate at each timepoint.

4.4.2 Fibroblast Proliferation, Metabolism, and Apoptotic Resistance are Not Impacted by Cit Fn

Results of HFF proliferation, metabolism, and apoptosis assays, as evaluated through BrDU, MTT, and caspase 3/7 plus 7AAD signal, respectively, failed to show any differences in fibroblast performance on Cit Fn compared to Fn surfaces (Figure 22A, B and Figure 23A). In all cases, negative control cells, plated on hd-BSA in the case of proliferation or metabolic assays, or not subjected to oxidative stress in the case of apoptotic assays, performed as expected, showing diminished levels of proliferation, metabolism, and cell death compared

to cells in experimental groups. It should also be noted that for each of these assays, identical versions were performed on citrullinated vs unmodified fibrin clots, and similar to Fn, no differences were observed in proliferation or metabolic assays. There did exist, however, elevated resistance to H_2O_2 in a dose-dependent manner within HFFs exposed to Cit-Fibrin compared to unmodified fibrin (Figure 23B). Statistical significance was only observed at the highest concentration of H_2O_2, but at every H_2O_2 dose, both caspase 3/7 and 7AAD was consistently observed at lower frequencies in cells on Cit Fibrin over all three trials of the experiment.

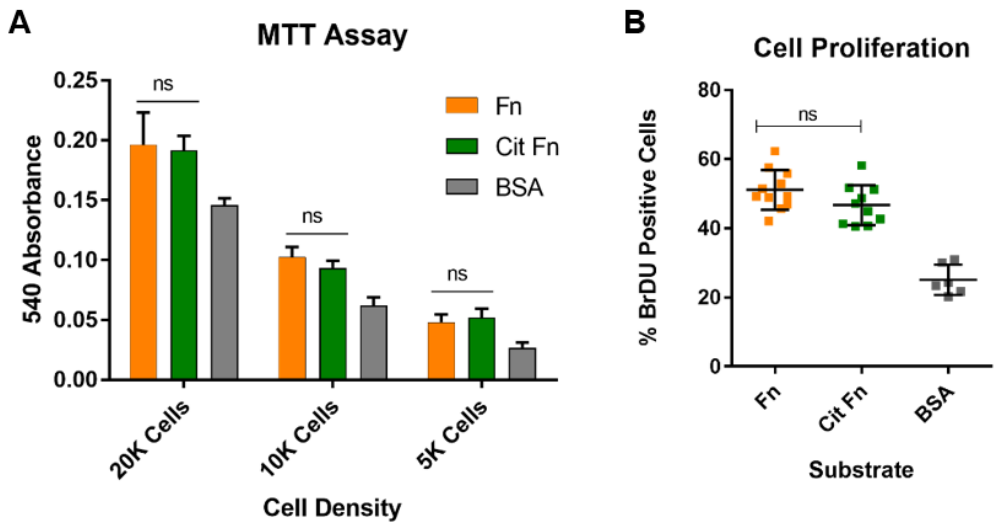

Figure 22: Fibroblast Metabolism and Proliferation
Quantification of MTT (A), and BrDU (B) signals are shown above. Conditions involving unmodified Fn are shown in orange, citrullinated Fn (Cit Fn) in green, and bovine serum albumin (BSA) in grey. Results represent n= 6 wells per substrate and cell density for MTT assay and n = 10 coverslips per experimental substrate and n = 5 coverslips for BSA.

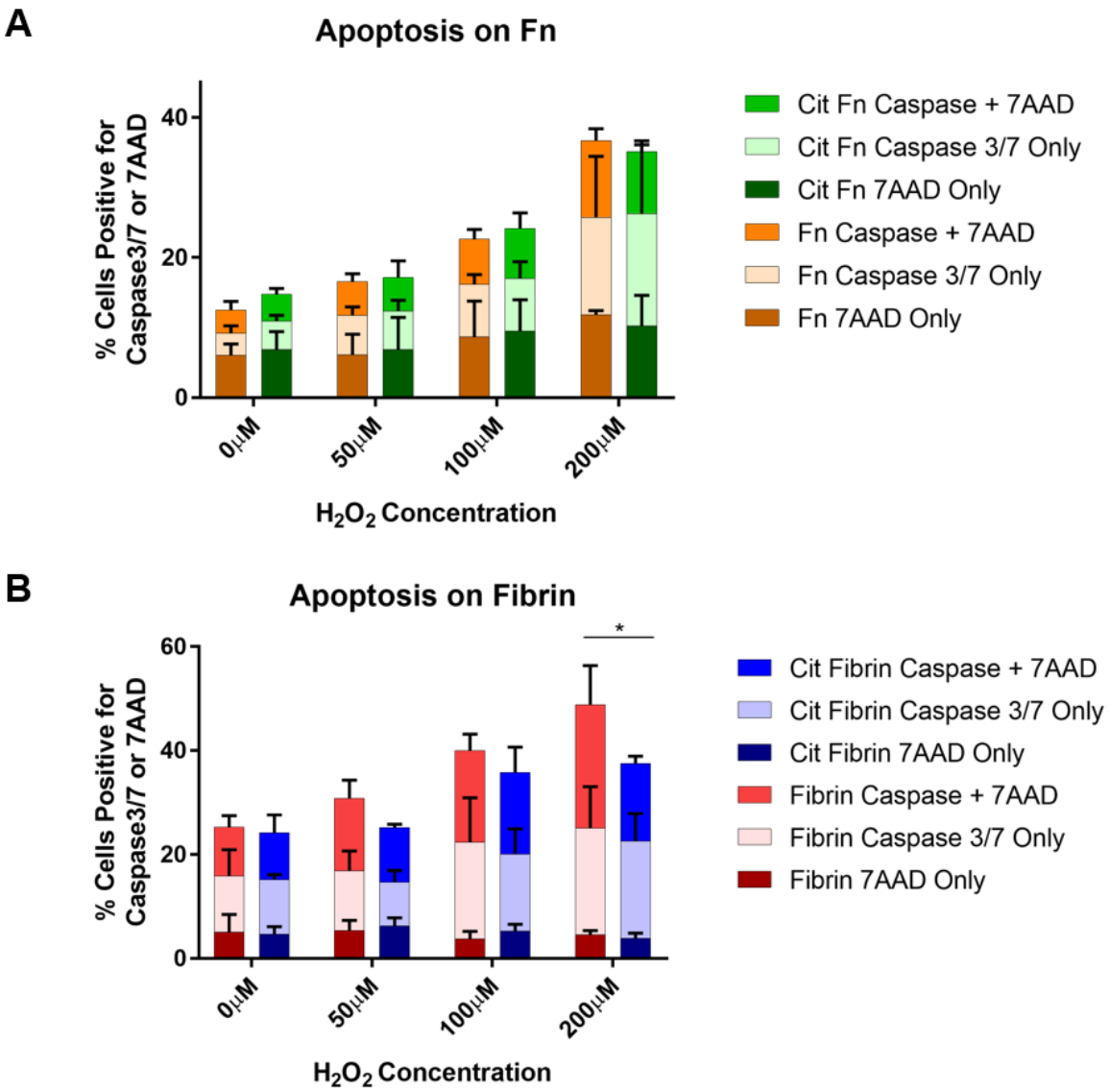

Figure 23: Apoptotic Resistance to Oxidative Stress
Combined results of three biological replicates in oxidative stress assays for apoptotic resistance on Cit Fn (A) or Cit Fibrin (B) compared to non-modified substrates are shown above. Each apoptotic trial measured a minimum of 10,000 cells per condition. Results are broken down according to detectable apoptotic/death markers including caspase 3/7 stain only (early apoptosis), 7AAD only (necrotic death), and caspase 3/7 + 7AAD (late apoptosis)

4.4.3 Fibroblast Stiffness is Enhanced on Cit Fn

AFM analysis of cell stiffness shows that HFFs plated on Cit Fn possess a median stiffness of 3.225 and a mean modulus of 5.773kPa compared to median and mean moduli

2.17 and 4.536, respectively on Fn (Figure 24). While modest, these results indicate that fibroblasts display a significant enhancement of overall stiffness on Cit Fn compared to Fn. When repeated on Fn or Cit-Fn coated polyacrylamide gels of 2kPa, 8kPa, or 25kPa stiffness, (results not shown) differences in stiffness were only observed on the stiffest of the gels tested mimicking the original results obtained on Fn or Cit Fn-coated glass.

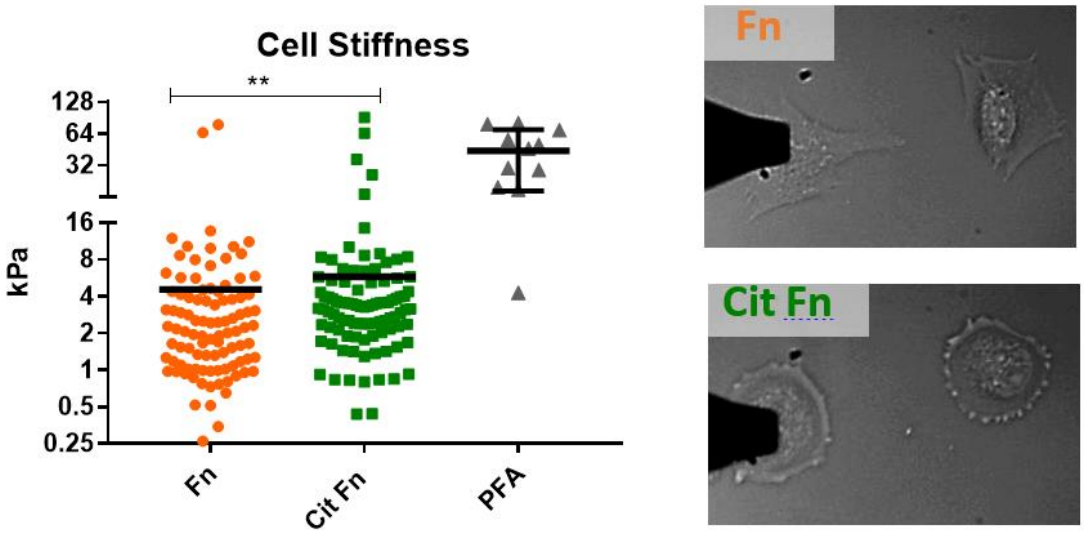

Figure 24: AFM to Probe Cell Stiffness:
AFM was used to probe at least 50 fibroblasts each plated on Fn or Cit Fn for 45 minutes at two different locations two cell, with the average force reading per cell being graphically depicted on the left. On the right are representative images of fibroblasts on Fn and Cit Fn with a top-down view of the beaded AFM tip as it's probing cell stiffness.

4.4.4 Fibroblasts Possess a Diminished Capacity to Contract Citrullinated Bulk Matrix

In both floating and strained versions of the gel contraction assay, HFFs possessed dramatically reduced capacity to contract the gels (Figure 25A, B). Minimal to no gel contraction was observed in gels without any cells seeded or where cells were treated with latrunculin B (lat B). In the floating version of this assay, a 48-hour timepoint was also separately observed (results not shown), but cells were overcrowd, and gels actually re-

expanded in comparison to their 24-hour areas. Nevertheless at both 24 and 48-hours the overall areas of un-modified gels were reduced compared to those that were citrullinated. In the case of strained assays, photos of the gels were taken pre-fixation, and pre-staining in case either of these treatments impacted gel area. While data for only the final stained gels is shown, gel areas were measured in all images. Fixation did appear to slightly reduce gel areas, although the same significant enhanced gel contraction on unmodified constructs compared to citrullinated was observed in each case.

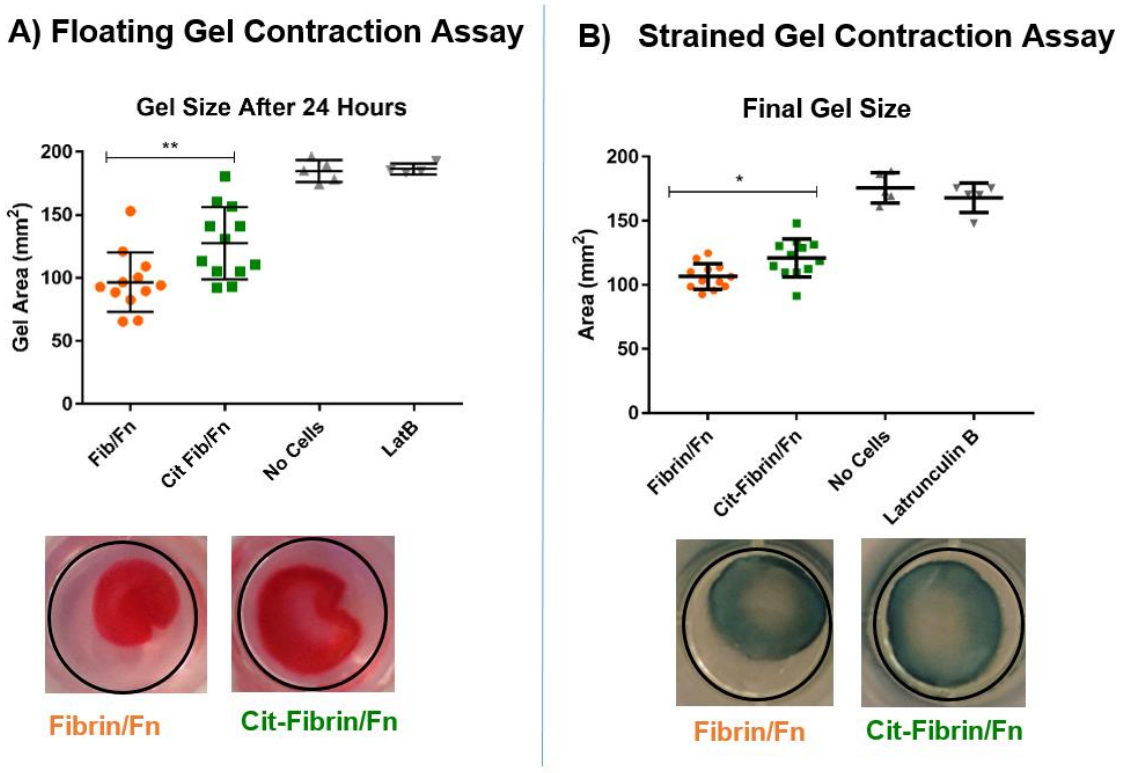

Figure 25: Gel Contraction Assays
Quantification of final Fibrin/Fn gel areas after 24 hours for those in the free-floating assay (A) and 15 minutes after release from well walls in the strained assay (B) is shown on top. Representative images of gels at their respective final timepoints are shown below well edges identified in black and gels stained with ponceau red for free-floating gels and 660 protein quantification reagent (dark blue) for strained gels. N = 12 gels each for Fibrin/Fn or Cit-Fibrin/Fn conditions and n=5 each for No Cells and Latrunculin B conditions.

4.4.5 Fibroblasts Display Increased Focal Adhesion Turnover on Cit Fn

Staining for α-actinin as a proxy for stable FAs showed that HFFs on Cit Fn possess a lower percentage of stable FAs compared to those plated on Fn. This was determined by quantification of the total amount of α-actinin fluorescent signal present within FAs, whose area was demarcated by paxillin stain, for each of 75 cells imaged per surface, whereby HFFs on Cit possessed lower absolute quantities of α-actinin signal within FAs (Figure 26A, B). The mander's coefficient, indicating the percentage of paxillin stain covered by α-actinin stain was also lower for HFFs plated on Cit Fn compared to Fn (Figure 26C). Positive control HFFs for stable FA complex that were treated with either the FAK-inhibiter PF-28 or the actin de-stabilizer cyotochalasin D displayed higher measurements for both α-actinin within FAs and mander's coefficient compared to either of the experimental groups. Knockdown of β1 integrin in HFFs resulted in an increase of FA stability by both aforementioned measurements on Cit Fn and a decrease of total α-actinin within FAs on Fn.

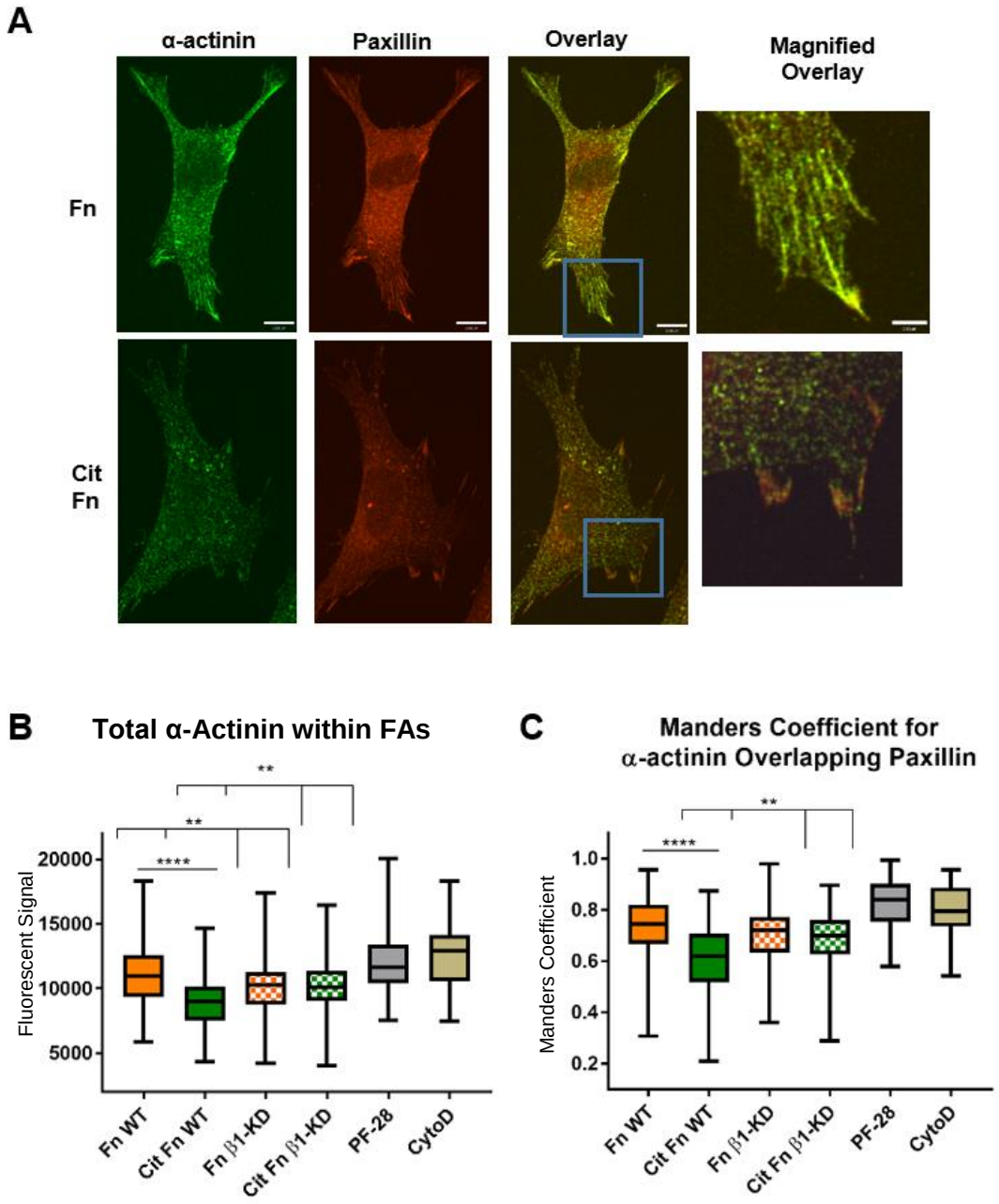

Figure 26: α-Actinin Staining of Stable Focal Adhesions
HFFs were stained with α-actinin as a proxy marker for stable FAs. Representative spinning disk confocal images (A) of HFFs plated on Fn (top row) or Cit Fn (bottom row) with staining for α-actinin in green, paxillin in red, and overlay highlight less co-localization of fluorescent signal within cells plated on Cit Fn (pearson's r = 0.523) compared to cells on Fn (pearson's r = 0.822). Scale bar = 12um. Blue box indicates region of magnified overlays on right, scale bar 1.5um. Quantitation of α-actinin signal within FAs is shown in (B) and quantitation of the manders coefficient for percent of FAs overlapped by α-actinin signal is shown in (C). Negative controls in B and C are HFFs exposed to PF-28 (grey), or cytochalasin D (CytoD), (brown). N = 75 cells per condition across 4 total coverslips.

TIRF videos of paxillin stain showed that the average lifetime of FAs, determined by the total number of frames in which a given FA possesses sufficient signal and size for detection, for any given cell was shorter for HFFs plated on Cit Fn compared to Fn with the average lifetime of FAs on Cit Fn being 196.5 seconds and 229.2 seconds out of a total possible 600 seconds (Figure 27A). At the same time, the average amount of FA displacement within any given cell, calculated from displacement divided by total lifetime, was greater within HFFs on Cit Fn compared to Fn with the average rate of displacement being 0.0187 um/sec on Cit Fn and 0.01247um/sec on Fn (Figure 27C). A histogram of FA duration plotted for all FAs across all cells shows that there is larger peak on the short duration side for Cit Fn and a larger peak on the long duration side for Fn indicating that a greater proportion of the FAs on Fn are long-lasting whereas a greater proportion of the FAs on Cit Fn are relatively short-lived (Figure 27B).

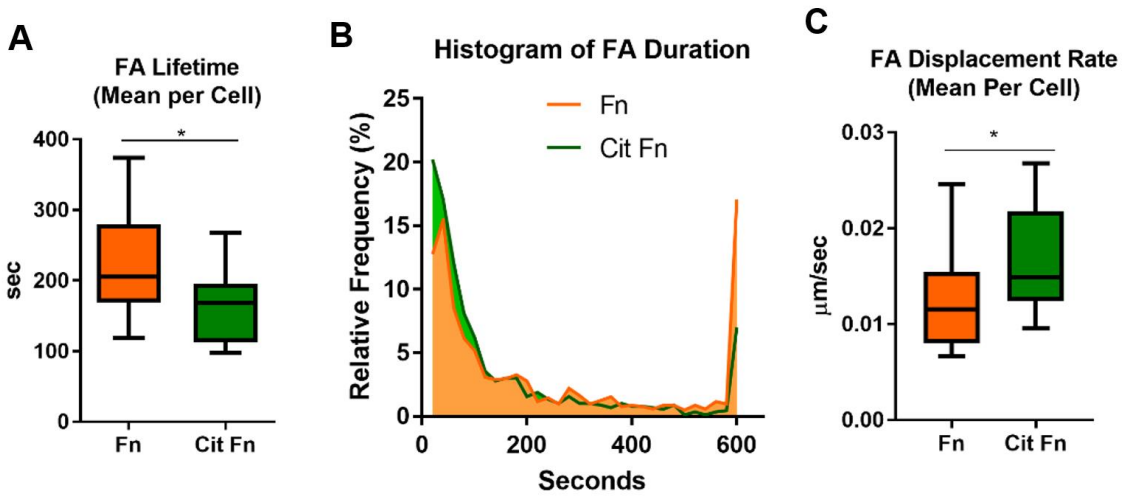

Figure 27: FA Turnover as Measured Via TIRF Confocal Videos
Tracking of FA presence over time via TIRF confocal microscopy of HFFs transfected with RFP paxillin reveals that HFFs on Cit Fn possess a greater number of short-lived FAs compared to those on Fn (A, B). The average rate of inward translocation (C) of FAs was simultaneously greater within HFFs plated on Cit Fn compared to Fn. Results represent 14 cells analyzed per substrate across two biological replicates.

4.4.6 Fibroblast Random and Directional Migration is Enhanced on Cit Fn

Random migration assays show that HFFs on Cit Fn compared to Fn possess a modestly enhanced migration capacity. This was determined by average migration rate per cell (Figure 28A), the maximal migration rate achieved by any given cell (Figure 28B), the average persistence distance (defined as cumulative distance travelled without a change in

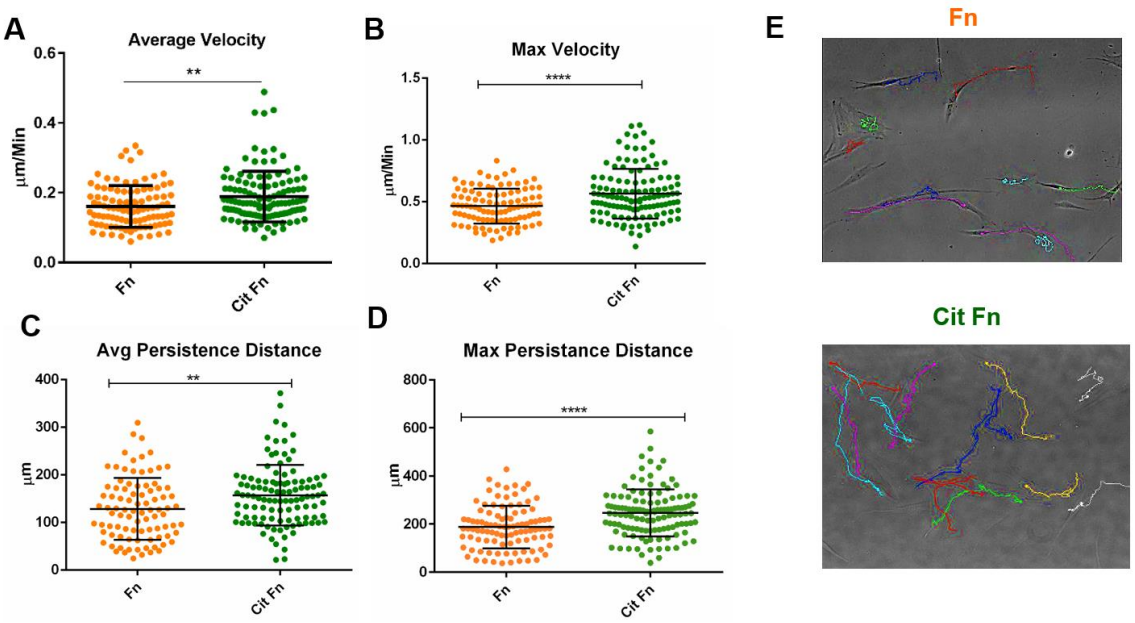

Figure 28: Random Fibroblast Migration
Quantification of average cell velocities (A) maximal velocities achieved per cell (B), average persistence distance (as defined by cumulated distance traveled without any changes of direction ≥ 90 degrees) (C) and maximal persistence distance achieved (D) are shown with cells on Fn shown in orange and Cit Fn shown in green. Representative images (E) of overall migration routes taken by individual cells show multiple overlaid colored lines, each representing the path taken by a unique cell on Fn (top) or Cit Fn (bottom). Results represent a minimum of 35 cells per substrate across nine unique fields of view.

direction > 90 degrees) (Figure 28C), and the maximal persistence distance achieved by any given cell (Figure 28D), all of which were greater on Cit Fn compared to Fn. Wound healing

assays, a proxy for directional migration, reveal that HFFs on Cit Fn compared to Fn were able to achieve a significantly greater amount of wound coverage (Figure 29A,B). The wound coverage of HFFs on both Fn and Cit Fn were substantially greater than that achieved on the negative control of adsorbed fibrinogen, which is a minimally adhesive surface for fibroblasts.

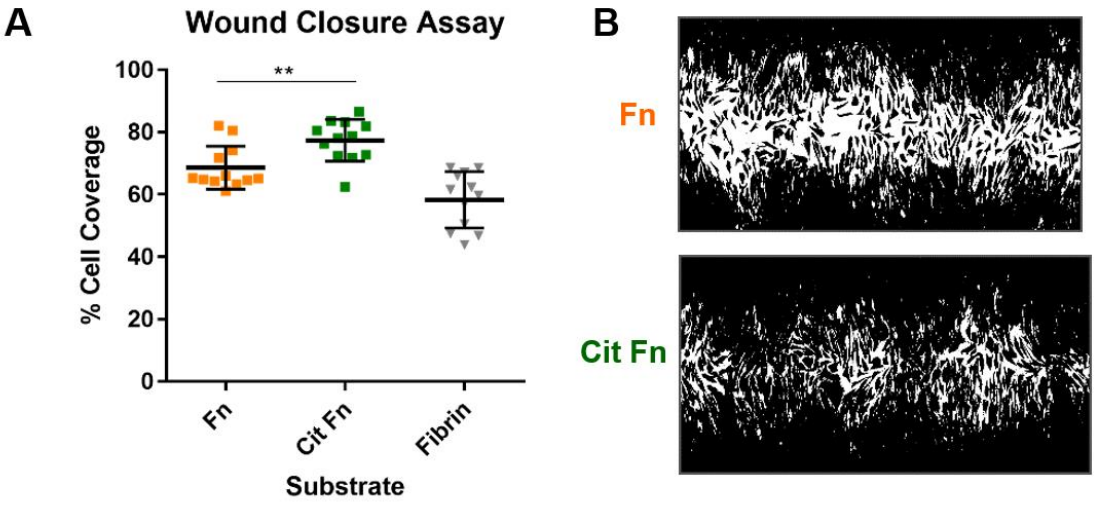

Figure 29: Wound Closure Directional Cell Migration
Representative contrast-enhanced and binarized images of wound defects (B) after HFFs were permitted 15 hours for inward migration show a white region representing the underlying wound defect and black regions representing that eventually covered by migrating HFFs. Quantification of binarized images in MatLab (A) reveals an overall greater amount of cell coverage on Cit Fn compared to Fn. Results represent four unique wells per substrate in which 3 separate fields of view were captured each.

4.5 Discussion

Fibroblasts possessed decreased adhesion ability on Cit Fn compared to Fn along with overall lower spread area. This is somewhat surprising based our previous results showing that fibroblasts on Cit Fn exhibit enhanced α5β1 integrin expression, and the fact that α5β1 integrins can bind with greater force than can αvβ3 integrins. Nevertheless, these results were previously confirmed using synovial fibroblasts on Cit Fn [4]. Further, we know fibroblasts on Cit Fn rely predominantly on α5β1 along with possessing reduced αvβ3 attachment strength, and it has been previously shown that β3-knockdown cells possess smaller areas whereas β1-knockdown cells possess larger areas than normal cells [149]; therefore it can be argued that cells on Cit Fn mimic the spreading of β3-kockdown cells, albeit to a much lesser extent.

One possible explanation for these differences in adhesion and spread area is that since fibroblasts on Cit Fn rely predominantly on α5β1 for adhesion, and α5β1 integrins bind with slower kinetics, at the timepoints examined, fibroblasts on Cit Fn may still have been weakly bound and were therefore washed away in greater numbers. Indeed, while α5β1integrins are capable of binding to Fn within 15 minutes of cell plating, the overall quantity of α5β1 attachments is less than 50% of that possible after a full hour of plating, and only a portion of these α5β1 integrin attachments would be expected to exist in a tensioned state (utilizing PHSRN + RGD)[158].

Further, citrullination of Fn significantly reduces the affinity of αvβ3-mediated integrin binding, and the most simplistic interpretation of this fact would be that elimination of a prominent binding residue should result in overall decreased adhesion. Indeed, though

the ratio of α5β1 to αvβ3 may be enhanced on Cit Fn, as well as the average amount of α5β1 within individual FAs, there may still be changes in the total surface coverage of FAs as well as the quality (active vs inactive) of α5β1 attachments. A similar reduction of spread area was observed on Cit-9*10 fragments, indicating that citrullination of the cell-binding domain alone is sufficient to elicit changes in cell adhesion; i.e. integrin interactions underlie the observed adhesion differences.

AFM analysis showed a modest but significant increase of bulk modulus on Cit Fn compared to Fn. Although this assay was performed on protein-coated glass, mean cell stiffness ranged between 4-6kpa, so we can conclude with reasonable confidence that measurements do not reflect the stiffness of the underlying substrate itself. Cells were plated for only 45 minutes prior to commencement of AFM probing, which is far less time than required for full cell spreading or attainment of complete "stiffness matching" [103]. Nevertheless, these results point towards early cellular efforts towards stiffness matching, a strong indication that the fibroblasts on Cit Fn are interpreting their environment as being artificially stiff, and reacting in kind. The enhanced F-actin content per cell volume on Cit Fn, as observed in Aim 1, may provide a direct physical explanation for the observed changes in bulk cell stiffness.

Apoptosis experiments did not elicit any changes in either apoptotic or necrotic cell death between Fn and Cit Fn. One possible explanation for these findings is that oxidative stress, a relatively broad intrinsic pathway was the only apoptotic stimulus tested, and results may have differed if an external pathway, such as Fas ligand or TNFα had been tested. Another explanation is that Cit Fn alone is insufficient to produce changes in apoptotic resistance. A study by Fan et al [3] demonstrated the protective benefits of Cit Fn in

comparison to Fn via both TUNEL and Annexin staining, but they used primary RA synovial fibroblasts which were already in an activated state, along with soluble Fn as their apoptotic stimulus. Therefore, it is possible that Cit Fn only produces an anti-apoptotic influence on fibroblasts that have already been epigenetically, genetically, and/or otherwise stimulated by the immune presence and chronic inflammation seen in RA. It's also possible that variation in the potential for activation exists among the different types and ages of fibroblasts being studied. Therefore, the differences seen in the Fan study may have been specific to synovial fibroblasts, or simply those that are older than the HFFs used in our experiments.

A final hypothesis for the lack of difference in apoptotic behavior is that conflicting signaling cascades may be engaged on Cit Fn as a result of enhanced α5β1 integrin presence. Specifically, NF-kB, ERK, Akt, and β-catenin pathways are all capable of being induced, and each of these contributes to cell survival. Concurrently, JNK signaling can also be induced by α5β1 binding, which is involved with activating apoptotic stimuli. If the wrong combination of these various pathways is enhanced or inhibited, it could ultimately have a net neutral result.

Exposure of fibroblasts to Cit-Fibrin did produce an apoptotic protective benefit, though the mechanism was not likely to have been mediated through integrin signaling. To start, without a PHSRN site, α5β1 integrins would not be expected to have enhanced attachment to Cit-fibrin, or at the very least to not exist in the tensioned state that would allow for typical β1-mediated mechanotransduction. A more likely explanation lies in the Toll-Like Receptor 4 (TLR4) which has previously demonstrated an enhanced ability to bind Cit-Fib in comparison to Fib, therefore stimulating the activation of macrophages and

enhancing their TNF-α production [33]. Fibroblasts are known to possess TLR4, and this can lead directly to enhancement of NF-kB pro-survival signaling. Based on these findings, within a provisional matrix consisting of both Fn and fibrin, citrullination may still be able produce apoptotic resistance in fibroblasts.

With regards to both cell metabolism and cell proliferation, no differences were observed between Cit Fn and Fn. The same held true for identical versions of these experiments performed on Cit Fibrin. While most phenotype experiments were performed in SFM, in the absence of serum-derived growth factors and other components, no proliferation could be observed on either Fn or Cit Fn. Therefore, both of these experiments were conducted using 0.2% Fn-depleted serum, which was sufficient to produce low levels of proliferation. Other than citrullination not actually impacting proliferation or metabolism, one explanation for these results is that fibroblasts require additional stimulus, in addition to Cit Fn before differences can be observed. Another is that the short timespan during which fibroblasts were exposed to Fn or Cit Fn was insufficient for both the necessary genetic changes and subsequent gene products that would have influenced proliferation or metabolism to be produced.

Finally, it should be noted that proliferation is not a universally accepted acquired phenotype across all different types of activated fibroblasts. There is a general consensus among the cancer literature that CAFs are hyperproliferative [73, 98], but among the RA literature, several studies have failed to demonstrate hyperproliferation of RA FLS [75]. Meanwhile, several RA studies have produced both evidence for the phenomenon of apoptotic resistance along with an explanation of mechanism in RA FLS [2, 75, 78, 79, 84]. Expectations of a proliferative phenotype in FAFs is more mixed with studies demonstrating

both enhanced growth, decreased growth, as well as no differences in proliferation [94, 101]. A majority of the fibrosis literature, however seems to suggest that FAFs do exhibit apoptotic resistance [71, 166, 167]. Therefore, in the case of both RA FLS and FAFs, the observed increases in total cell number may be more a consequence of increased apoptotic resistance rather than an increase in proliferation.

4.5.1 Interpretation of Enhanced Migration on Cit Fn

Possibly the most influential phenotypical changes observed were those related to enhanced migration, as this could directly to contribute to cell invasiveness. The most obvious explanation for these differences are β1 integrins, which play a larger role in Cit Fn adhesion and have also been implicated as the main fibroblast adhesive molecules responsible for migration. Case in point, β1-blocking was previously shown to result in an 85% decrease of fibroblast migration in a wound healing assay compared to αv-blocking which only reduced fibroblast migration by 15% [128]. Further, invasive tumor cells are also known to strongly express β1 [149], indicating that these integrins may have a causative role in tumor malignancy.

Somewhat less clear, however, is the fact that fibroblasts on Cit Fn also displayed enhanced persistence in random migration assays even though cells expressing only β1 integrins are associated with more random migration [147], and αv integrins are specifically associated with improved directional persistence [168, 169]. Nevertheless there is also evidence to suggest that α5β1forms such stable adhesions that they effectively reduce fibroblast migration rates as a direct result of slow trailing edge detachment [120, 169]; yet results from both our TIRF real-time analysis of FA turnover as well as α-actinin staining

for stable focal adhesions clearly demonstrate that FA turnover rates are actually enhanced on Cit Fn compared to Fn. This discrepancy may partially be explained by the fact that the Schiller study that showed a decrease in migration due to β1 studied fibroblasts that *only* expressed β1 whereas in the current system, αvβ3 integrins are also present and can still attach to Cit Fn, albeit more weakly, and thus the result is an intermediate phenotype. Our observation of enhanced migrational persistence may therefore also constitute an intermediate phenotype due to increased α5β1 presence intermixed with altered αvβ3 attachment.

The contribution of downstream integrin-mediated signaling also needs to be considered. In Aim 1 it was shown that fibroblasts on Cit Fn increase phosphorylation of FAK which is directly linked to both high FA turnover and enhanced fibroblast migration [124, 128]. These effects are mediated through phosphorylation of α-actinin, which decreases attachment to F-actin and allows for improved turnover [124]. Less likely, due to lack of evidence for change due to Cit Fn, is the FAK-rac-rho signaling axis which can impact migration via enhanced lamellipodial formation through p130cas and also increase actin-myosin contraction [120, 124]. ILK inhibition of GSK3-β, which we did find to be enhanced, also likely plays a role in migration persistence. Considering that active GSK3-β normally phosphorylates FAK at S722 leading to decreased FAK activity and cell migration, phospho-GSK3-β would be expected to produce the exact opposite result [162].

Finally, the contribution of citrullination towards alteration of fibroblast adhesion likely contributes to observed changes in migration. It is well established that there exists a biphasic relationship between cell adhesion and migration, and fibroblasts on Cit Fn possess decreased adhesion and spreading, which could potentiate the ease of rearwards FA release

in migrating cells. This theory is supported by our migration results on Cit-Fib in both types of migration assays, which similar to Cit Fn, demonstrated an enhancement of fibroblast migration over its unmodified protein counterpart. In the case of Cit Fib, however, this enhanced migration occurs despite the known lack of α5β1 binding, which suggests that a mechanism other than β1-mediated signaling may also contribute to enhanced migration on citrullinated proteins.

Possibly related to cell migration, both floating and strained fibrin/Fn gel contraction assays showed a significantly diminished ability of fibroblasts to contract citrullinated gels. Since adhesion assays showed overall weaker fibroblast attachment to Cit Fn compared to Fn, it is therefore plausible that fibroblasts on citrullinated gels simply possessed a reduced ability to generate sufficient forces for bulk gel contraction. However, successful gel contraction is known to be dependent on three main factors: strong cell adhesion, robust intracellular contractile machinery, and low mobility. Fast pseudopodial retraction during cell translocation is actually associated with release of tension from the matrix so much so that an inverse relationship has been observed between cell translocation and maintenance of substrate tension [170]. In support of this notion, traction forces in gel contraction assays have been documented as being the weakest when the most mobile and invasive cells are studied [171].

Since we have shown fibroblast motility to be enhanced on both Cit-Fib and Cit-Fn, this lack of gel contraction may therefore constitute additional evidence for enhanced fibroblast migration on provisional matrix rather than a deficit in ability to generate contractile forces. Indeed, while there is certainly abundant support for the existence of enhanced mechanotransduction signaling on Cit Fn mediated through an artificial elevation

of tensioned α5β1, it is still unclear whether this enhanced α5β1 presence simply mimics a tensioned state or if it is capable of creating increased cellular tensions. A more localized approach to measuring cell-generated forces, such as traction force microscopy (TFM) would likely be required to definitively resolve this query.

4.6 Conclusions

Phenotype analysis of fibroblasts interacting with Cit Fn reveals an overall decrease of cell attachment and spreading on Cit Fn in comparison to Fn. These findings were accompanied by an enhancement of cell stiffness on Cit Fn compared to Fn and no detectable differences in cell proliferation or metabolism on Cit Fn compared to Fn. There were also no measureable differences in apoptotic resistance to oxidative stress between Cit Fn and Fn, although Cit Fibrin was shown to provide protection from apoptosis; since fibroblasts are unable to engage PHSRN on Cit Fibrin, the mechanism underlying this protection likely lies outside the realm of integrin-mediated signaling. Fibroblasts on citrullinated Fibrin/Fn combination gels were less able to contract the bulk constructs in comparison to un-modified gels, though these results are likely indicative of a release of tension due to enhanced motility rather than a deficit of contraction, especially considering that both random and directional cell migration assays display increased cell motility on Cit Fn in comparison to Fn. Confocal TIRF videos and α-actinin staining for stable FAs confirm that a heightened level of FA turnover significantly contributes to enhanced cell migration. Altogether, these results indicate that citrullination of Fn as an independent stimulus is sufficient to elicit changes in cell migration, which is a key feature of all types of activated fibroblasts and contributes to their invasiveness. Therefore, inhibition of

citrullination may constitute a promising therapeutic strategy for combatting a variety of chronic inflammatory conditions.

CHAPTER 5. OVERALL CONCLUSIONS AND FUTURE DIRECTIONS

Citrullination of Cit Fn results in 24 unique sites of modification that ultimately influence integrin engagement in such a manner that they create an integrin switch where α5β1 integrins are preferred over αvβ3 integrins. The downstream mechanotransduction signaling resulting from this integrin switch leads to alterations in several fibroblast phenotypes, especially that of migration. The hypothesized inter-relationship of the complete findings of Aims 1 and 2 are summarized in Figure 30.

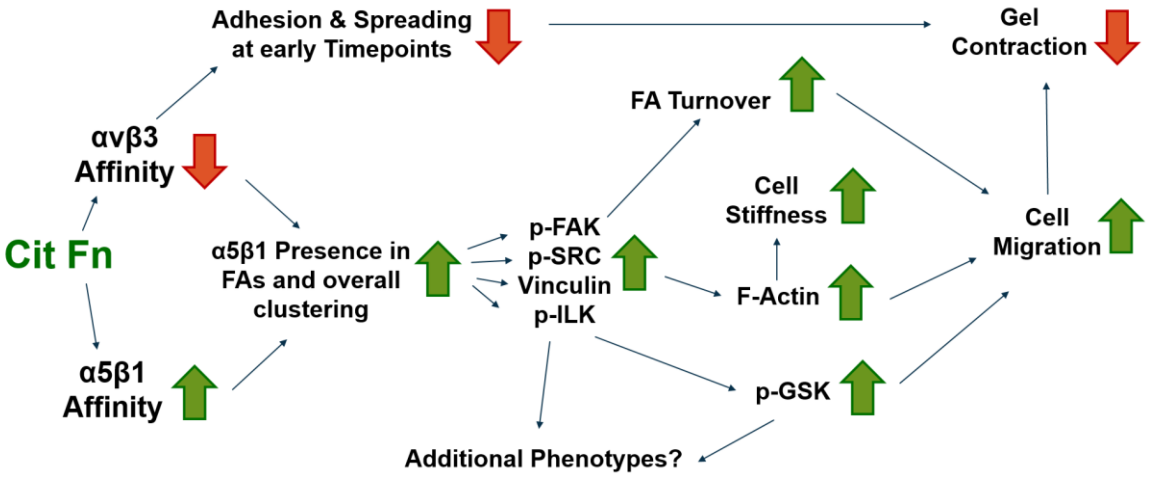

Figure 30: Overall Summary:
The citrullination of Cit Fn leads to an enhancement of α5β1 affinity and a decrease of αvβ3 affinity, the latter of which likely underlies decreased cell adhesion and spreading at early timepoints. The combined impact of altered integrin affinities leads to an integrin switch with an overall increase of α5β1 presence in focal adhesion (FA) along with increased integrin clustering. β1-dominated integrin signaling leads to enhancements of pFAK, pSRC, vinculin, and p-ILK, all of which are capable of contributing to enhanced F-actin formation , itself a likely contributor to increased cell stiffness. Phospho-FAK may directly lead to enhanced FA turnover, and p-ILK may directly lead to phosphorylation (and therefore inhibition) of GSK. The combination of enhanced FA turnover, increased, F-actin presence, and GSK inhibition likely all contribute to enhanced fibroblast migration. Enhanced cell migration along with low adhesion and cell spreading at early timepoints likely influences the low level of gel contraction. Finally additional phenotypes are possible as a result of enhanced pFAK/pSRC, vinculin, pILK, and pGSK.

Of course, to fully elucidate the impact of Cit-pECM, additional research will be required. Assuming the lack of detectable differences in Rho, Rac, and myosin II are real, this current work still identified at least three signaling pathways activated through interaction of fibroblasts with Cit Fn alone (Figure 31), including that of vinculin—FAK /SRC—α-actinin—F-actin, that of ILK—parvin—vinculin—F-actin, and that of ILK—p-GSK.

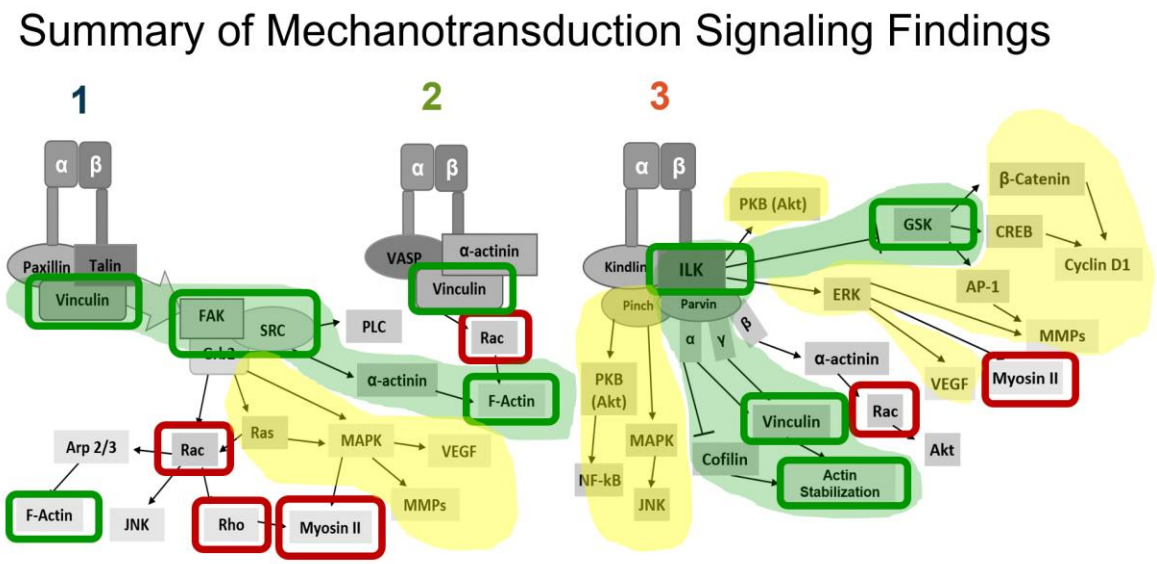

Figure 31: Summary of Mechanotransduction Signaling Findings and Future Avenues for Exploration
All three mechanotransduction signaling pathways have been combined into one diagram where entities found to exhibit no difference on Fn vs Cit Fn are outlined in red, and those that are up-regulated due to cell exposure to Cit fin are outlined in green. Overlaid green shading represents pathways that appear to be completely activated (from integrin engagement down to change in protein function) due to Cit Fn interaction. Overlaid yellow shading represents pathways that have yet to be explored but may potentially be influenced due to Cit Fn interaction.

Some of the key signaling nodes that are likely influenced by interaction with Cit Fn but have yet to be explicitly explored include that of MAPK/ERK signaling, Akt signaling, and β-catenin signaling.

A point of potential contradiction laid out in the current findings is that while several key signal transduction pathways appear to be activated as a result of Cit Fn interaction, cell phenotype differences were only observed in the area of cell migration. Granted, there are some phenotypes such as cytokine secretion and cell differentiation that were not tested and may actually be influenced by these interactions. A caveat however, is that in an effort to be well controlled, the current studies investigated the influence of Cit Fn as a stand-alone stimulus, and this is simply not a practical reality. Within an *in vivo* inflammatory environment, fibroblasts would also be exposed to copious amounts of cytokines, growth factors, as well as being directly stimulated by immune and other types of cells. Therefore, it is possible that in combination with additional stimuli, Cit Fn may be able to elicit changes in phenotypes beyond just that of cell migration. This idea is supported by the findings from previous studies using primary activated human RA synovial fibroblasts which did show enhancements of such characteristics as cytokine secretion and apoptotic resistance in the *in vitro* presence of Cit Fn [3, 4, 35].

The converse argument then is that the over-simplification of experiments conducted herein may have resulted in exaggerated outcomes. For instance, in any experimental setup where cells were exposed to Cit Fn, that protein was citrullinated to the maximal extent possible in solution, whereas this may not reflect the extent of citrullination possible *in vivo* due to both PAD enzyme concentrations and the fact that a portion of Fn would likely already have been incorporated into the matrix in an extended conformation. Further, our

cells were cultured in serum-free media to eliminate exposure to extraneous non-citrullinated Fn as well as growth factors and other bio-molecules, which in reality would be very likely to influence cell behavior. The combination of these additional stimuli with the possibility of a lower concentration of citrullinated Fn epitopes *in vivo* could potentially activate pathways that act counter to those demonstrated to be activated in the current research. Indeed, while consistent, the majority of Cit Fn impacts on cell phenotype in this research were fairly mild and required relatively high sample size to demonstrate an effect. Therefore, under more physiologically accurate conditions, it is possible that alterations to various fibroblast phenotypes due to exposure to Cit Fn would be muted or altogether cease to exist.

Another factor to point out is that almost every experiment in this research was conducted with Human Foreskin Fibroblasts, which are very young cells. While similar changes in integrin preference were also observed with CCL210 human lung fibroblasts, it is possible that the nature of integrin binding, molecular signaling, and cell phenotype may either be enhanced or diminished in other types of fibroblasts. Fibroblasts are intrinsically diverse cells, and from one fibroblast subtype to another, behaviors can vary significantly. Thus, before firm conclusions about the influence of Cit-pECM on fibroblast functions in specific diseases can be made, it is recommended to investigate the influence of Cit-pECM on the disease-relevant fibroblast subtype.

Yet another question that has yet to be fully answered is how the integrin switch from αvβ3 to α5β1 occurs at a molecular level. We demonstrated an enhancement of α5β1 attachment as well as a decrease of αvβ3 affinity, either or both of which may contribute to the integrin switch phenomenon to varying degrees. The citrullination sites specifically

responsible for these changes in affinity most likely include R1274 and R1284 within the 8th type III Fn repeat, R1410 within the PHSRN synergy site and/or R1434 within the 9th type III Fn repeat, and also R1452, R1476, and R1479 within the 10th type III Fn repeat. Site-specific mutagenesis would likely be required to elucidate the contribution of each of these modifications towards affinity changes with both αvβ3 and α5β1 integrins.

While determining the influence of specific citrullination sites may seem a needlessly onerous exercise, this discovery may have significant implications for the pharmaceutical development of citrullination inhibitors. In particular, the aforementioned R1410, R1434, and R1452 citrullination sites—all of which possess the highest likelihood of impacting α5β1 interaction due to proximity to PHSRN—were all demonstrated to be exclusively modified by PAD2 in the current study. Whether or not citrullination at these sites actually impacts α5β1 interaction and whether that in turn significantly influences the integrin switch from αvβ3 to α5β1 would dramatically influence the perceived importance of PAD2 enzyme inhibition for therapeutic intervention. There are currently exists a debate as to optimal mechanism and amount of PAD inhibition required for therapeutic efficacy. Many research efforts, especially those associated with cancer prevention, are focused on developing PAD4-specific inhibitors; therefore clarifying the contribution of PAD2 modifications toward both signaling and cell phenotype may have the capacity to shift the balance of this debate.

Certainly, the pharmaceutical debate as to whether PAD4 alone or more PADs should be inhibited in the pursuit of novel therapeutic interventions hinges largely on whether or not this inhibition would have any unwanted and/or off-target side-effects. No currently published PAD inhibition studies have indicated any sort of adverse side effects.

Yet in our attempts to use BB-Cl-amidine, the most potent pan-PAD inhibitor currently in existence in a preventative mouse model of lung fibrosis, we observed several unusual skin side effects. Briefly, freshly prepared BB-Cl-amidine from Cayman Chemical in DMSO+sterile saline was administered to mice subcutaneously at a dose of 5mg/kg/day for a total of 33 days. About 70% of mice receiving the BB-Cl-amidine treatment (compared to 0% of vehicle) developed one or more skin lesions over the course of the study. Furthermore, the skin of the treatment mice became noticeably less elastic over the course of the study to the point that it became more difficult to both scruff the mice as well as to insert a needle through the skin. These findings suggest first that owing to the role PAD enzymes play in maintenance of skin protein structure[1, 42] that subcutaneous administration of PAD inhibitors is inadvisable. Second, PADs type 1, 3, and 4 are known to function in the epidermis [2, 8, 15], and it is possible that their inhibition may be to blame for the side effects observed here. Either way, additional research as to the normal physiological role of PAD enzymes is recommended before choosing one or multiple PAD enzyme targets.

Yet another unanswered α5β1-specific question is how does citrullination of Fn influence the state—i.e. tensioned or relaxed—of its binding. As previously described, α5β1 integrins can bind through RGD only (relaxed state) or through RGD + PHSRN (tensioned state). While interferometry results showed a slight enhancement of Cit Fn affinity for α5β1 integrins, the experimental setup utilizing constant plate-shaking at 1000rpm may have artificially forced all or the majority of the α5β1 integrins into a tensioned state. ICC experiments performed on stiff glass coverslips would also likely have encouraged a tensioned state of α5β1integrins. It is therefore unclear whether the same enhancement of

α5β1 affinity and/or presence would be observed in a more physiologically accurate environment possessing both lower substrate stiffness and a lack intense shear force.

Further, interferometry provides an indirect measurement of the rate of interaction between two entities without necessarily specifying the strength of said interaction. Therefore, from interferometry results alone, it is not possible to conclude whether the α5β1 integrin binding events that occurred were in a tensioned or relaxed state, and further, whether or not citrullination of Fn influences the tendency of α5β1 integrins to exist in one state or another compared to with non-modified Fn. Certainly, our ICC staining for integrin subunits indicated an enhancement of both α5 and β1 subunits, but again, these results do not clarify the state of the integrin. Understanding the state of α5β1 integrins is important because the state can potentially influence downstream signaling. An experiment like traction force microscopy (TFM) could potentially clarify both the presence of α5β1 integrins in tensioned states as well as whether the apparent integrin switch allows the cells in turn to generate increased amounts of intracellular tension.

While the current research certainly raises several additional questions that warrant follow-up, in a broader context, our findings are already quite striking with regards to highlighting the importance of Cit Fn over other citrullinated matrix proteins. Of course, many citrullinated proteins possess an ability to stimulate an immune response, though the mechanisms are varied, and they include many outside the realm of integrin interactions. In the context of engagement with the matrix, including integrin activation of downstream signaling, Cit Fn truly does appear to be special. Though few previous studies of citrullinated ECM proteins (including collagen, fibrin, and fn) have been conducted, they have all tended to conclude that fibroblast attachment worsens as a consequence of

citrullination, and phenotypes typically associated with the respective ECM proteins consequently also become diminished. Ours is the first study to provide evidence of an activating consequence of any ECM protein both in the context of integrin engagement and downstream signaling. The fact that these effects were found on Cit Fn, which preferentially interacts with fibroblasts over other cell types may indicate that the effects of citrullination (outside of immune stimulation) may therefore possess a targeted effect on fibroblasts. This information may be essential both in understanding the process of fibroblast activation, but also the innate physiological role citrullination plays in the maintenance of normal fibroblast health and function.

In attempting to understand the evolutionary designed role of citrullination in human health, a piece of evidence from neurological citrullination patterns stands out. Namely, children under 2 years of age have almost all of their myelin basic protein (MBP) citrullinated, and this amount decreases over time to about 20% in adulthood; thus citrullination is thought to be important to brain plasticity in early development [19]. Our results indicate a role for citrullination in fibroblast activation similar to what may be seen in normal wound healing as well as the pathological "wound healing" that occurs in fibrotic conditions. The fields of regenerative medicine and wound healing often draw inspiration from tissue morphogenesis, as entities like Fn with alternate splice variants EDA and EDB exist in abundance and are thought to be important to mammalian tissue development and morphogenesis. EDA and EDB Fn variants decrease with age, though when they are present, they tend to be associated with wound healing and enhanced fibroblast migration. Citrullination may similarly play an as yet unspecified role in early mammalian tissue morphogenesis. Similar to both EDA/B variants and Cit-MBP, Cit Fn may have evolved to

decrease its presence and functionality with age, but in cases of disease and wound healing, it experiences localized spikes that can be helpful or harmful depending on the circumstances and duration of its presence.

Finally, regardless of the underlying cause for citrullination in humans, the fact is that it is known to occur in a broad range of conditions to varying extents, and it has the potential to impact a variety of cell types both in the context of immune stimulation and fibroblast activation. Citrullination therefore provides an important example of the idea of matrix memory—essentially that the influence of events, such as inflammation, on cell function and behavior can persist past the cessation of the instigating event. Especially in the case of citrullination, where modification of several protease cleavage sites renders them unrecognizable for degradation, citrullinated epitopes can become a much longer-lasting "memory".

This concept of matrix memory is important, because while the ECM is generally considered a dynamic entity that is constantly remodeled by its cellular denizens, it is dangerous to always rely on this dynamism. Specifically in the context of implantable tissue scaffolds and biomaterials, the potential for long-lasting impacts of PTMs creates a limit in the ability of scientists and engineers to control exact ECM properties and predict impacts on cell phenotypes. Considering that citrullination is inflammation mediated, it would very likely be present as a part of the foreign body response as a consequence of implantation of almost any natural or synthetic biomaterial; thus citrullination is a very real concern for the fields of regenerative medicine and biomaterials.

Indubitably, there is much more that needs to be understood about citrullination, its innate physiological function, and its biological consequences. This need is all the more

greater due to citrullination's potential implications in a variety of fields. Specifically, it constitutes a promising novel therapeutic target in a variety of chronic inflammatory diseases including RA, cancer, atherosclerosis, and more. Further, it is a widespread phenomenon with the ability to influence a host of basic biological functions that may constitute and an important consideration in regenerative scaffold and biomaterial design.

APPENDIX A.

A.1 Definitions and Abbreviations

Table 3: Cytokine Protein Abbreviations

Cytokine	Alternate ID	Full Name
CCL-5	MCP-1	Chemokine (c-c motif) ligand 5
SDF-1	CXCL-12	Stromal Cell-Derived Factor 1
CXCL-1		Chemokine (c-x-c motif) ligand1
CSF-1,2		Colony-Stimulating Factor
IFN-γ		Interferon Gamma
VEGF		Vascular Endothelial Growth Factor
IL 6,7,8,15,16,18,32,33		Interleukins
MCP-1	CCL-5	Monocyte Chemoattractant Protein
TGF-β		Transforming Growth Factor Beta
TNF-α		Tumor Necrosis Factor Alpha

Table 4: Growth Factor Abbreviations

Growth Factor Type	Full Name
bFGF	basic Fibroblast Growth Factor
EGF	Epidermal Growth Factor
GDF	Growth Differentiation Factor
IGF	Insulin-like Growth Factor
PDGF	Platelet-Derived Growth Factor
TGF-β	Transforming Growth Factor
VEGF	Vascular Endothelial Growth Factor

Table 5: Apoptosis Protein Abbreviations

Apoptosis Protein	Full Name
Bcl-xl	B-cell lymphoma-extra large
Mcl-1	Induced Myeloid Leukemia Cell Differentiation Protein
Bcl-2	B-cell lymphoma 2
RANKL	Receptor Activator of Nuclear Factor Kappa-B Ligand

5.1 Additional Interferometry Results

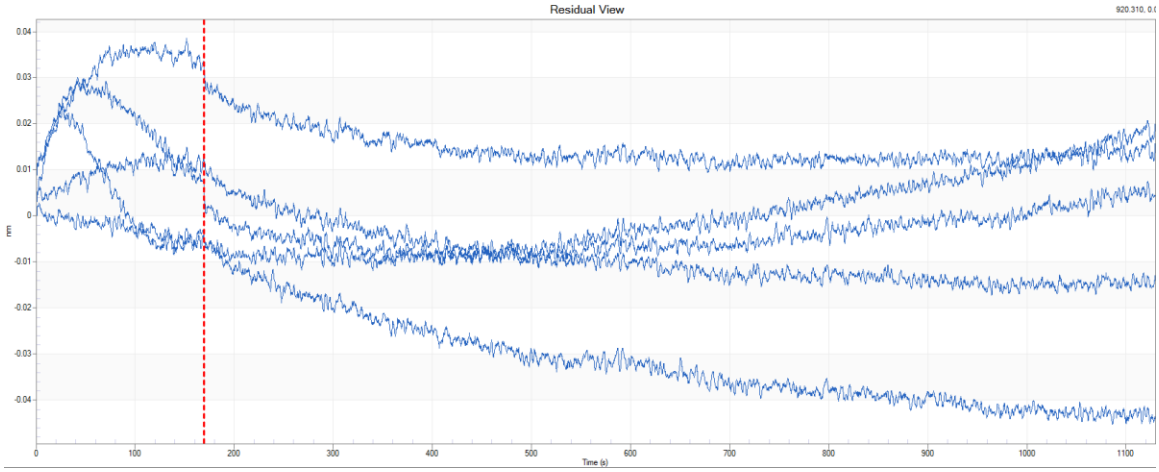

Figure 32: Residuals of alpha5 beta1 BLI interactions with Fn

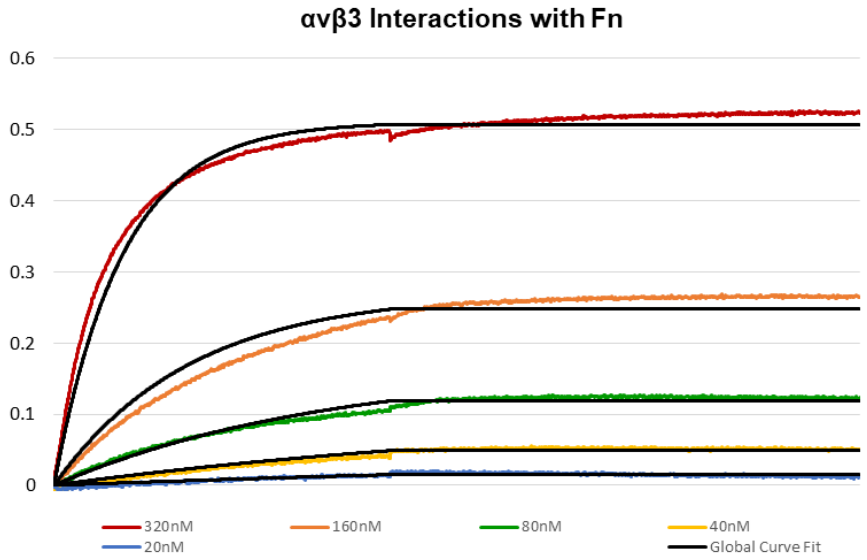

Figure 33: Sample BLI αvβ3 with Fn
Global 1:1 curve fits are overlaid in black

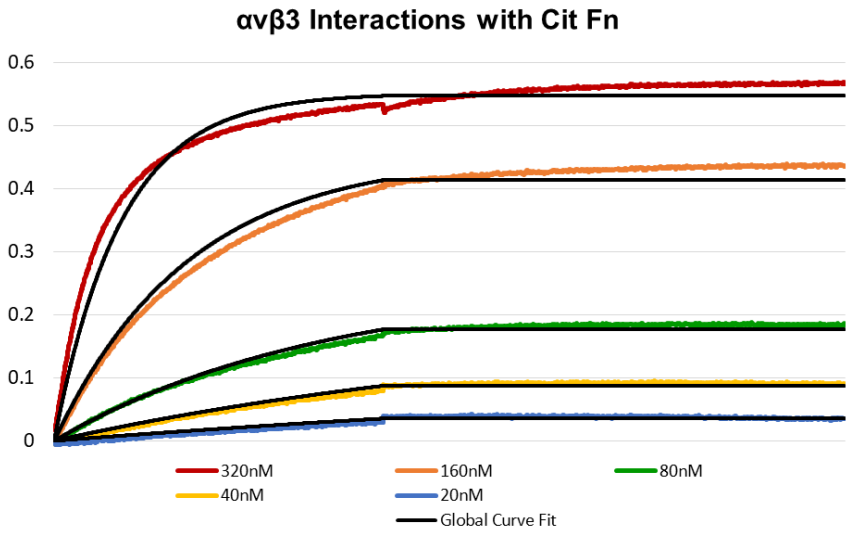

Figure 34: Sample BLI of αvβ3 with Cit Fn
Global 1:1 curve fits are overlaid in black

REFERENCES

[1] C. Zeltz and D. Gullberg, "Post-translational modifications of integrin ligands as pathogenic mechanisms in disease," *Matrix Biol,* vol. 40C, pp. 5-9, Nov 2014.

[2] G. Valesini, M. C. Gerardi, C. Iannuccelli, V. A. Pacucci, M. Pendolino, and Y. Shoenfeld, "Citrullination and autoimmunity," *Autoimmun Rev,* vol. 14, pp. 490-7, Jun 2015.

[3] L. Fan, Q. Wang, R. Liu, M. Zong, D. He, H. Zhang, *et al.*, "Citrullinated fibronectin inhibits apoptosis and promotes the secretion of pro-inflammatory cytokines in fibroblast-like synoviocytes in rheumatoid arthritis," *Arthritis Res Ther,* vol. 14, p. R266, 2012.

[4] M. A. Shelef, D. A. Bennin, D. F. Mosher, and A. Huttenlocher, "Citrullination of fibronectin modulates synovial fibroblast behavior," *Arthritis Res Ther,* vol. 14, p. R240, 2012.

[5] J. E. Jones, C. P. Causey, B. Knuckley, J. L. Slack-Noyes, and P. R. Thompson, "Protein arginine deiminase 4 (PAD4): Current understanding and future therapeutic potential," *Curr Opin Drug Discov Devel,* vol. 12, pp. 616-27, Sep 2009.

[6] K. Lundberg, S. Nijenhuis, E. R. Vossenaar, K. Palmblad, W. J. van Venrooij, L. Klareskog, *et al.*, "Citrullinated proteins have increased immunogenicity and arthritogenicity and their presence in arthritic joints correlates with disease severity," *Arthritis Res Ther,* vol. 7, pp. R458-67, 2005.

[7] D. A. Fox, "Citrullination: A Specific Target for the Autoimmune Response in Rheumatoid Arthritis," *J Immunol,* vol. 195, pp. 5-7, Jul 1 2015.

[8] E. A. V. Moelants, A. Mortier, J. Van Damme, P. Proost, and T. Loos, "Peptidylarginine deiminases: physiological function, interaction with chemokines and role in pathology," *Drug Discovery Today: Technologies,* vol. 9, pp. e261-e280, //Winter 2012.

[9] A. M. Quirke, B. A. Fisher, A. J. Kinloch, and P. J. Venables, "Citrullination of autoantigens: upstream of TNFalpha in the pathogenesis of rheumatoid arthritis," *FEBS Lett,* vol. 585, pp. 3681-8, Dec 1 2011.

[10] Z. Baka, P. Barta, G. Losonczy, T. Krenacs, J. Papay, E. Szarka, *et al.*, "Specific expression of PAD4 and citrullinated proteins in lung cancer is not associated with anti-CCP antibody production," *Int Immunol,* vol. 23, pp. 405-14, Jun 2011.

[11] H. Uysal, R. Bockermann, K. S. Nandakumar, B. Sehnert, E. Bajtner, Å. Engström, *et al.*, "Structure and pathogenicity of antibodies specific for citrullinated collagen

type II in experimental arthritis," *The Journal of Experimental Medicine,* vol. 206, pp. 449-462, 2009.

[12] E. B. Lugli, R. E. Correia, R. Fischer, K. Lundberg, K. R. Bracke, A. B. Montgomery, *et al.*, "Expression of citrulline and homocitrulline residues in the lungs of non-smokers and smokers: implications for autoimmunity in rheumatoid arthritis," *Arthritis Res Ther,* vol. 17, p. 9, 2015.

[13] A. I. Catrina, A. J. Ytterberg, G. Reynisdottir, V. Malmstrom, and L. Klareskog, "Lungs, joints and immunity against citrullinated proteins in rheumatoid arthritis," *Nat Rev Rheumatol,* vol. 10, pp. 645-653, 11//print 2014.

[14] W. J. van Venrooij and G. J. Pruijn, "How citrullination invaded rheumatoid arthritis research," *Arthritis Res Ther,* vol. 16, p. 103, 2014.

[15] E. R. Vossenaar, A. J. Zendman, W. J. van Venrooij, and G. J. Pruijn, "PAD, a growing family of citrullinating enzymes: genes, features and involvement in disease," *Bioessays,* vol. 25, pp. 1106-18, Nov 2003.

[16] M. Sebbag, S. Chapuy-Regaud, I. Auger, E. Petit-Texeira, C. Clavel, L. Nogueira, *et al.*, "Clinical and pathophysiological significance of the autoimmune response to citrullinated proteins in rheumatoid arthritis," *Joint Bone Spine,* vol. 71, pp. 493-502, Nov 2004.

[17] A. G. Pratt, J. D. Isaacs, and D. L. Mattey, "Current concepts in the pathogenesis of early rheumatoid arthritis," *Best Practice & Research. Clinical Rheumatology,* vol. 23, pp. 37-48, 2009.

[18] K. A. Kuhn, L. Kulik, B. Tomooka, K. J. Braschler, W. P. Arend, W. H. Robinson, *et al.*, "Antibodies against citrullinated proteins enhance tissue injury in experimental autoimmune arthritis," *Journal of Clinical Investigation,* vol. 116, pp. 961-973, 04/03, 04/21/received, 01/03/accepted 2006.

[19] M. Gogol, "Citrullination--small change with a great consequence," in *Folia Biologica et Oecologica* vol. 9, ed, 2013, p. 17.

[20] Y. Wang, P. Li, S. Wang, J. Hu, X. A. Chen, J. Wu, *et al.*, "Anticancer peptidylarginine deiminase (PAD) inhibitors regulate the autophagy flux and the mammalian target of rapamycin complex 1 activity," *J Biol Chem,* vol. 287, pp. 25941-53, Jul 27 2012.

[21] H. D. Lewis, J. Liddle, J. E. Coote, S. J. Atkinson, M. D. Barker, B. D. Bax, *et al.*, "Inhibition of PAD4 activity is sufficient to disrupt mouse and human NET formation," *Nat Chem Biol,* vol. 11, pp. 189-91, Mar 2015.

[22] S. Mohanan, B. D. Cherrington, S. Horibata, J. L. McElwee, P. R. Thompson, and S. A. Coonrod, "Potential role of peptidylarginine deiminase enzymes and protein citrullination in cancer pathogenesis," *Biochem Res Int,* vol. 2012, p. 895343, 2012.

[23] Z. Baka, B. Gyorgy, P. Geher, E. I. Buzas, A. Falus, and G. Nagy, "Citrullination under physiological and pathological conditions," *Joint Bone Spine,* vol. 79, pp. 431-6, Oct 2012.

[24] J. Fuhrmann and P. R. Thompson, "Protein Arginine Methylation and Citrullination in Epigenetic Regulation," *ACS Chemical Biology,* vol. 11, pp. 654-668, 2016/03/18 2016.

[25] J. J. van Beers, A. Willemze, J. Stammen-Vogelzangs, J. W. Drijfhout, R. E. Toes, and G. J. Pruijn, "Anti-citrullinated fibronectin antibodies in rheumatoid arthritis are associated with human leukocyte antigen-DRB1 shared epitope alleles," *Arthritis Res Ther,* vol. 14, p. R35, Feb 17 2012.

[26] V. C. Willis, A. M. Gizinski, N. K. Banda, C. P. Causey, B. Knuckley, K. N. Cordova, *et al.*, "N-α-Benzoyl-N5-(2-Chloro-1-Iminoethyl)-l-Ornithine Amide, a Protein Arginine Deiminase Inhibitor, Reduces the Severity of Murine Collagen-Induced Arthritis," *The Journal of Immunology,* vol. 186, pp. 4396-4404, April 1, 2011 2011.

[27] C. Assohou-Luty, R. Raijmakers, W. E. Benckhuijsen, J. Stammen-Vogelzangs, A. de Ru, P. A. van Veelen, *et al.*, "The human peptidylarginine deiminases type 2 and type 4 have distinct substrate specificities," *Biochim Biophys Acta,* vol. 1844, pp. 829-36, Apr 2014.

[28] G. L. Cuthbert, S. Daujat, A. W. Snowden, H. Erdjument-Bromage, T. Hagiwara, M. Yamada, *et al.*, "Histone deimination antagonizes arginine methylation," *Cell,* vol. 118, pp. 545-53, Sep 3 2004.

[29] K. N. Cordova, V. C. Willis, K. Haskins, and V. M. Holers, "A citrullinated fibrinogen-specific T cell line enhances autoimmune arthritis in a mouse model of rheumatoid arthritis," *J Immunol,* vol. 190, pp. 1457-65, Feb 15 2013.

[30] J. J. B. C. van Beers, R. Raijmakers, L.-E. Alexander, J. Stammen-Vogelzangs, A. M. C. Lokate, A. J. R. Heck, *et al.*, "Mapping of citrullinated fibrinogen B-cell epitopes in rheumatoid arthritis by imaging surface plasmon resonance," *Arthritis Research & Therapy,* vol. 12, pp. R219-R219, 12/23, 09/09/received, 11/22/revised, 12/23/accepted 2010.

[31] N. Okumura, A. Haneishi, and F. Terasawa, "Citrullinated fibrinogen shows defects in FPA and FPB release and fibrin polymerization catalyzed by thrombin," *Clin Chim Acta,* vol. 401, pp. 119-23, Mar 2009.

[32] S. Chapuy-Regaud, M. Sebbag, D. Baeten, C. Clavel, C. Foulquier, F. De Keyser, *et al.*, "Fibrin deimination in synovial tissue is not specific for rheumatoid arthritis but commonly occurs during synovitides," *J Immunol,* vol. 174, pp. 5057-64, Apr 15 2005.

[33] J. Sokolove, X. Zhao, P. E. Chandra, and W. H. Robinson, "Immune complexes containing citrullinated fibrinogen costimulate macrophages via Toll-like receptor 4 and Fcgamma receptor," *Arthritis Rheum,* vol. 63, pp. 53-62, Jan 2011.

[34] K. H. Sipilä, V. Ranga, P. Rappu, M. Mali, L. Pirilä, I. Heino, *et al.*, "Joint inflammation related citrullination of functional arginines in extracellular proteins," *Scientific Reports,* vol. 7, p. 8246, 2017/08/15 2017.

[35] X. Chang, R. Yamada, A. Suzuki, Y. Kochi, T. Sawada, and K. Yamamoto, "Citrullination of fibronectin in rheumatoid arthritis synovial tissue," *Rheumatology (Oxford),* vol. 44, pp. 1374-82, Nov 2005.

[36] F. Curnis, R. Longhi, L. Crippa, A. Cattaneo, E. Dondossola, A. Bachi, *et al.*, "Spontaneous formation of L-isoaspartate and gain of function in fibronectin," *J Biol Chem,* vol. 281, pp. 36466-76, Nov 24 2006.

[37] K. Sipila, S. Haag, K. Denessiouk, J. Kapyla, E. C. Peters, A. Denesyuk, *et al.*, "Citrullination of collagen II affects integrin-mediated cell adhesion in a receptor-specific manner," *FASEB J,* vol. 28, pp. 3758-68, Aug 2014.

[38] J. A. Hill, D. A. Bell, W. Brintnell, D. Yue, B. Wehrli, A. M. Jevnikar, *et al.*, "Arthritis induced by posttranslationally modified (citrullinated) fibrinogen in DR4-IE transgenic mice," *J Exp Med,* vol. 205, pp. 967-79, Apr 14 2008.

[39] D. D. Brand, K. A. Latham, and E. F. Rosloniec, "Collagen-induced arthritis," *Nat Protoc,* vol. 2, pp. 1269-75, 2007.

[40] S. Hida, N. N. Miura, Y. Adachi, and N. Ohno, "Influence of arginine deimination on antigenicity of fibrinogen," *J Autoimmun,* vol. 23, pp. 141-50, Sep 2004.

[41] J. S. Knight, V. Subramanian, A. A. O'Dell, S. Yalavarthi, W. Zhao, C. K. Smith, *et al.*, "Peptidylarginine deiminase inhibition disrupts NET formation and protects against kidney, skin and vascular disease in lupus-prone MRL/lpr mice," *Ann Rheum Dis,* vol. 74, pp. 2199-206, Dec 2015.

[42] J. Koziel, P. Mydel, and J. Potempa, "The link between periodontal disease and rheumatoid arthritis: an updated review," *Curr Rheumatol Rep,* vol. 16, p. 408, Mar 2014.

[43] I. B. McInnes and G. Schett, "The Pathogenesis of Rheumatoid Arthritis," *New England Journal of Medicine,* vol. 365, pp. 2205-2219, 2011.

[44] P. Mangat, N. Wegner, P. J. Venables, and J. Potempa, "Bacterial and human peptidylarginine deiminases: targets for inhibiting the autoimmune response in rheumatoid arthritis?," *Arthritis Res Ther,* vol. 12, p. 209, 2010.

[45] J. Giles, J. Fert-Bober, J. Park, C. Bingham, F. Andrade, K. Fox-Talbot, *et al.*, "Myocardial citrullination in rheumatoid arthritis: a correlative histopathologic study," *Arthritis Research & Therapy,* vol. 14, p. R39, 2012.

[46] M. Shaw, B. F. Collins, L. A. Ho, and G. Raghu, "Rheumatoid arthritis-associated lung disease," *European Respiratory Review,* vol. 24, p. 1, 2015.

[47] D. P. Ascherman, "Interstitial lung disease in rheumatoid arthritis," *Curr Rheumatol Rep,* vol. 12, pp. 363-9, Oct 2010.

[48] T. J. Doyle, A. S. Patel, H. Hatabu, M. Nishino, G. Wu, J. C. Osorio, *et al.*, "Detection of Rheumatoid Arthritis-Interstitial Lung Disease Is Enhanced by Serum Biomarkers," *Am J Respir Crit Care Med,* vol. 191, pp. 1403-12, Jun 15 2015.

[49] B. Marigliano, A. Soriano, D. Margiotta, M. Vadacca, and A. Afeltra, "Lung involvement in connective tissue diseases: a comprehensive review and a focus on rheumatoid arthritis," *Autoimmun Rev,* vol. 12, pp. 1076-84, Sep 2013.

[50] T. Bongartz, T. Cantaert, S. R. Atkins, P. Harle, J. L. Myers, C. Turesson, *et al.*, "Citrullination in extra-articular manifestations of rheumatoid arthritis," *Rheumatology,* vol. 46, pp. 70-75, 2007.

[51] K. Antoniou, K. Samara, I. Lasithiotaki, P. Pantelidis, N. Siafakas, and A. Wells, "Investigation of the citrullination pathway in the pathogenesis of fibrotic lung disorders," *European Respiratory Journal,* vol. 40, September 1, 2012 2012.

[52] K. M. Antoniou, K. D. Samara, I. Lasithiotaki, P. Pantelidis, N. Siafakas, and A. Wells, "Investigation Of The Citrullination Pathway In The Pathogenesis Of Fibrotic Lung Disorders: Preliminary Results," in *B64. PATHWAYS REGULATING FIBROBLAST GENE EXPRESSION*, ed: American Thoracic Society, 2011, pp. A3484-A3484.

[53] T. E. King, Jr., A. Pardo, and M. Selman, "Idiopathic pulmonary fibrosis," *Lancet,* vol. 378, pp. 1949-61, Dec 3 2011.

[54] A. J. Silman, J. Newman, and A. J. MacGregor, "Cigarette smoking increases the risk of rheumatoid arthritis. Results from a nationwide study of disease-discordant twins," *Arthritis Rheum,* vol. 39, pp. 732-5, May 1996.

[55] D. Makrygiannakis, M. Hermansson, A. K. Ulfgren, A. P. Nicholas, A. J. W. Zendman, A. Eklund, *et al.*, "Smoking increases peptidylarginine deiminase 2 enzyme expression in human lungs and increases citrullination in BAL cells," *Annals of the Rheumatic Diseases,* vol. 67, p. 1488, 2008.

[56] E. Perry, C. Stenton, C. Kelly, P. Eggleton, D. Hutchinson, and A. De Soyza, "RA autoantibodies as predictors of rheumatoid arthritis in non-cystic fibrosis bronchiectasis patients," *Eur Respir J,* vol. 44, pp. 1082-5, Oct 2014.

[57] V. Joshua, Reynisdottir, G, Ytterberg AJ, Engstrom, Eklund, Malstrom, Grunewald, Klareskog, Catrina, "CHARACTERIZATION OF LUNG INFLAMMATION AND IDENTIFICATION OF SHARED CITRULLINATED TARGETS IN THE LUNGS AND JOINTS OF EARLY RA," presented at the European League Against Rheumatism, 2014.

[58] X. Chang and J. Han, "Expression of peptidylarginine deiminase type 4 (PAD4) in various tumors," *Mol Carcinog,* vol. 45, pp. 183-96, Mar 2006.

[59] J. L. Slack, C. P. Causey, Y. Luo, and P. R. Thompson, "Development and use of clickable activity based protein profiling agents for protein arginine deiminase 4," *ACS Chem Biol,* vol. 6, pp. 466-76, May 20 2011.

[60] S. C. Stadler, C. T. Vincent, V. D. Fedorov, A. Patsialou, B. D. Cherrington, J. J. Wakshlag, *et al.*, "Dysregulation of PAD4-mediated citrullination of nuclear GSK3beta activates TGF-beta signaling and induces epithelial-to-mesenchymal transition in breast cancer cells," *Proc Natl Acad Sci U S A,* vol. 110, pp. 11851-6, Jul 16 2013.

[61] E. E. Witalison, X. Cui, C. P. Causey, P. R. Thompson, and L. J. Hofseth, "Molecular targeting of protein arginine deiminases to suppress colitis and prevent colon cancer," *Oncotarget,* vol. 6, pp. 36053-62, Nov 3 2015.

[62] H. Yao, P. Li, B. J. Venters, S. Zheng, P. R. Thompson, B. F. Pugh, *et al.*, "Histone Arg modifications and p53 regulate the expression of OKL38, a mediator of apoptosis," *J Biol Chem,* vol. 283, pp. 20060-8, Jul 18 2008.

[63] M. A. Callender and E. S. Antonarakis, "Rheumatoid arthritis masked by docetaxel chemotherapy in a patient with ovarian carcinoma," *J Clin Rheumatol,* vol. 14, p. 121, Apr 2008.

[64] Y. Zhao, Z. F. Chang, R. Li, Z. G. Li, X. X. Li, and L. Li, "Paclitaxel suppresses collagen-induced arthritis: a reevaluation," *Am J Transl Res,* vol. 8, pp. 5044-5051, 2016.

[65] K. Garber, "Bristol-Myers Squibb locks into novel autoimmune strategy," *Nat Biotech,* vol. 34, pp. 577-579, 06//print 2016.

[66] K. L. Bicker, L. Anguish, A. A. Chumanevich, M. D. Cameron, X. Cui, E. Witalison, *et al.*, "D-amino acid based protein arginine deiminase inhibitors: Synthesis, pharmacokinetics, and in cellulo efficacy," *ACS Med Chem Lett,* vol. 3, pp. 1081-1085, Oct 26 2012.

[67] J. S. Knight, W. Luo, A. A. O'Dell, S. Yalavarthi, W. Zhao, V. Subramanian, *et al.*, "Peptidylarginine deiminase inhibition reduces vascular damage and modulates innate immune responses in murine models of atherosclerosis," *Circ Res,* vol. 114, pp. 947-56, Mar 14 2014.

[68] J. Kawalkowska, A.-M. Quirke, F. Ghari, S. Davis, V. Subramanian, P. R. Thompson, *et al.*, "Abrogation of collagen-induced arthritis by a peptidyl arginine deiminase inhibitor is associated with modulation of T cell-mediated immune responses," *Scientific Reports,* vol. 6, p. 26430, 05/23/online 2016.

[69] R. T. Hannan, S. M. Peirce, and T. H. Barker, "Fibroblasts: Diverse Cells Critical to Biomaterials Integration," *ACS Biomaterials Science & Engineering,* 2017/06/13 2017.

[70] G. Sriram, P. L. Bigliardi, and M. Bigliardi-Qi, "Fibroblast heterogeneity and its implications for engineering organotypic skin models in vitro," *Eur J Cell Biol,* vol. 94, pp. 483-512, Nov 2015.

[71] P. J. Wolters, H. R. Collard, and K. D. Jones, "Pathogenesis of idiopathic pulmonary fibrosis," *Annu Rev Pathol,* vol. 9, pp. 157-79, 2014.

[72] N. C. Henderson, T. D. Arnold, Y. Katamura, M. M. Giacomini, J. D. Rodriguez, J. H. McCarty, *et al.*, "Targeting of alphav integrin identifies a core molecular pathway that regulates fibrosis in several organs," *Nat Med,* vol. 19, pp. 1617-24, Dec 2013.

[73] D. Öhlund, E. Elyada, and D. Tuveson, "Fibroblast heterogeneity in the cancer wound," *The Journal of Experimental Medicine,* vol. 211, pp. 1503-1523, 04/11/received, 06/18/accepted 2014.

[74] C. Ospelt, "Synovial fibroblasts in 2017," *RMD Open,* vol. 3, p. e000471, 10/15, 07/20/received, 09/14/revised, 09/28/accepted 2017.

[75] B. Bartok and G. S. Firestein, "Fibroblast-like synoviocytes: key effector cells in rheumatoid arthritis," *Immunological Reviews,* vol. 233, pp. 233-255, 2009.

[76] E. H. Noss and M. B. Brenner, "The role and therapeutic implications of fibroblast-like synoviocytes in inflammation and cartilage erosion in rheumatoid arthritis," *Immunol Rev,* vol. 223, pp. 252-70, Jun 2008.

[77] M. J. Flick, C. M. LaJeunesse, K. E. Talmage, D. P. Witte, J. S. Palumbo, M. D. Pinkerton, *et al.*, "Fibrin(ogen) exacerbates inflammatory joint disease through a mechanism linked to the integrin Î±(M)Î²(2) binding motif," *The Journal of Clinical Investigation,* vol. 117, pp. 3224-3235, 2007.

[78] D. Fu, Y. Yang, Y. Xiao, H. Lin, Y. Ye, Z. Zhan, *et al.*, "Role of p21-activated kinase 1 in regulating the migration and invasion of fibroblast-like synoviocytes from rheumatoid arthritis patients," *Rheumatology (Oxford),* vol. 51, pp. 1170-80, Jul 2012.

[79] C. Ospelt, "The role of synovial fibroblasts in rheumatoid arthritis," PhD, University of Amsterdam, 2012.

[80] G. Reynisdottir, R. Karimi, V. Joshua, H. Olsen, A. H. Hensvold, A. Harju, *et al.*, "Structural changes and antibody enrichment in the lungs are early features of anti-citrullinated protein antibody-positive rheumatoid arthritis," *Arthritis Rheumatol,* vol. 66, pp. 31-9, Jan 2014.

[81] D. S. Jones, A. P. Jenney, J. L. Swantek, J. M. Burke, D. A. Lauffenburger, and P. K. Sorger, "Profiling drugs for rheumatoid arthritis that inhibit synovial fibroblast activation," *Nat Chem Biol,* vol. 13, pp. 38-45, Jan 2017.

[82] S. L. Peng, "Fas (CD95)-related apoptosis and rheumatoid arthritis," *Rheumatology (Oxford),* vol. 45, pp. 26-30, Jan 2006.

[83] R. L. Wilder, "Integrin alpha V beta 3 as a target for treatment of rheumatoid arthritis and related rheumatic diseases," *Ann Rheum Dis,* vol. 61 Suppl 2, pp. ii96-9, Nov 2002.

[84] A. Baier, I. Meineckel, S. Gay, and T. Pap, "Apoptosis in rheumatoid arthritis," *Curr Opin Rheumatol,* vol. 15, pp. 274-9, May 2003.

[85] N. Rinaldi, M. Schwarz-Eywill, D. Weis, P. Leppelmann-Jansen, M. Lukoschek, U. Keilholz, *et al.*, "Increased expression of integrins on fibroblast-like synoviocytes from rheumatoid arthritis in vitro correlates with enhanced binding to extracellular matrix proteins," *Ann Rheum Dis,* vol. 56, pp. 45-51, Jan 1997.

[86] S. Lefevre, A. Knedla, C. Tennie, A. Kampmann, C. Wunrau, R. Dinser, *et al.*, "Synovial fibroblasts spread rheumatoid arthritis to unaffected joints," *Nat Med,* vol. 15, pp. 1414-20, Dec 2009.

[87] T. Lowin and R. H. Straub, "Integrins and their ligands in rheumatoid arthritis," *Arthritis Research & Therapy,* vol. 13, pp. 244-244, 10/28 2011.

[88] M. L. Barilla and S. E. Carsons, "Fibronectin fragments and their role in inflammatory arthritis," *Semin Arthritis Rheum,* vol. 29, pp. 252-65, Feb 2000.

[89] T. Vartio, A. Vaheri, R. V. Essen, H. IsomÄKi, and S. Stenman, "Fibronectin in synovial fluid and tissue in rheumatoid arthritis," *European Journal of Clinical Investigation,* vol. 11, pp. 207-212, 1981.

[90] E. Kimura, T. Kanzaki, K. Tahara, H. Hayashi, S. Hashimoto, A. Suzuki, *et al.*, "Identification of citrullinated cellular fibronectin in synovial fluid from patients with rheumatoid arthritis," *Mod Rheumatol,* vol. 24, pp. 766-9, Sep 2014.

[91] U. Muller-Ladner, J. Kriegsmann, B. N. Franklin, S. Matsumoto, T. Geiler, R. E. Gay, *et al.*, "Synovial fibroblasts of patients with rheumatoid arthritis attach to and invade normal human cartilage when engrafted into SCID mice," *The American Journal of Pathology,* vol. 149, pp. 1607-1615, 1996.

[92] N. G. Frangogiannis, "Fibroblast-Extracellular Matrix Interactions in Tissue Fibrosis," *Curr Pathobiol Rep,* vol. 4, pp. 11-18, Mar 2016.

[93] G. Epstein Shochet, E. Brook, L. Israeli-Shani, E. Edelstein, and D. Shitrit, "Fibroblast paracrine TNF-alpha signaling elevates integrin A5 expression in idiopathic pulmonary fibrosis (IPF)," *Respir Res,* vol. 18, p. 122, Jun 19 2017.

[94] C. Ramos, M. Montano, J. Garcia-Alvarez, V. Ruiz, B. D. Uhal, M. Selman, *et al.*, "Fibroblasts from idiopathic pulmonary fibrosis and normal lungs differ in growth rate, apoptosis, and tissue inhibitor of metalloproteinases expression," *Am J Respir Cell Mol Biol,* vol. 24, pp. 591-8, May 2001.

[95] H. Suganuma, A. Sato, R. Tamura, and K. Chida, "Enhanced migration of fibroblasts derived from lungs with fibrotic lesions," *Thorax,* vol. 50, pp. 984-9, Sep 1995.

[96] J. J. Tomasek, G. Gabbiani, B. Hinz, C. Chaponnier, and R. A. Brown, "Myofibroblasts and mechano-regulation of connective tissue remodelling," *Nat Rev Mol Cell Biol,* vol. 3, pp. 349-63, May 2002.

[97] E. S. White, M. H. Lazar, and V. J. Thannickal, "Pathogenetic mechanisms in usual interstitial pneumonia/idiopathic pulmonary fibrosis," *J Pathol,* vol. 201, pp. 343-54, Nov 2003.

[98] R. Kalluri, "The biology and function of fibroblasts in cancer," *Nat Rev Cancer,* vol. 16, pp. 582-98, Aug 23 2016.

[99] B. D. Bringardner, C. P. Baran, T. D. Eubank, and C. B. Marsh, "The role of inflammation in the pathogenesis of idiopathic pulmonary fibrosis," *Antioxid Redox Signal,* vol. 10, pp. 287-301, Feb 2008.

[100] A. C. Brown, V. F. Fiore, T. A. Sulchek, and T. H. Barker, "Physical and chemical microenvironmental cues orthogonally control the degree and duration of fibrosis-associated epithelial-to-mesenchymal transitions," *J Pathol,* vol. 229, pp. 25-35, Jan 2013.

[101] T. Mio, S. Nagai, M. Kitaichi, A. Kawatani, and T. Izumi, "Proliferative characteristics of fibroblast lines derived from open lung biopsy specimens of patients with IPF (UIP)," *Chest,* vol. 102, pp. 832-7, Sep 1992.

[102] V. F. Fiore, P. W. Strane, A. V. Bryksin, E. S. White, J. S. Hagood, and T. H. Barker, "Conformational coupling of integrin and Thy-1 regulates Fyn priming and fibroblast mechanotransduction," *J Cell Biol,* vol. 211, pp. 173-90, Oct 12 2015.

[103] J. Solon, I. Levental, K. Sengupta, P. C. Georges, and P. A. Janmey, "Fibroblast Adaptation and Stiffness Matching to Soft Elastic Substrates," *Biophysical Journal,* vol. 93, pp. 4453-4461, 11/20/received, 06/21/accepted 2007.

[104] J. Baum and H. S. Duffy, "Fibroblasts and Myofibroblasts: What are we talking about?," *Journal of cardiovascular pharmacology,* vol. 57, pp. 376-379, 2011.

[105] H. Miki, T. Mio, S. Nagai, Y. Hoshino, T. Nagao, M. Kitaichi, *et al.*, "Fibroblast contractility: usual interstitial pneumonia and nonspecific interstitial pneumonia," *Am J Respir Crit Care Med,* vol. 162, pp. 2259-64, Dec 2000.

[106] C. Kuhn and J. A. McDonald, "The roles of the myofibroblast in idiopathic pulmonary fibrosis. Ultrastructural and immunohistochemical features of sites of active extracellular matrix synthesis," *Am J Pathol,* vol. 138, pp. 1257-65, May 1991.

[107] F. Klingberg, B. Hinz, and E. S. White, "The myofibroblast matrix: implications for tissue repair and fibrosis," *J Pathol,* vol. 229, pp. 298-309, Jan 2013.

[108] J. A. McDonald, "The Yin and Yang of Fibrin in the Airways," *New England Journal of Medicine,* vol. 322, pp. 929-931, 1990.

[109] K. Rasanen and A. Vaheri, "Activation of fibroblasts in cancer stroma," *Exp Cell Res,* vol. 316, pp. 2713-22, Oct 15 2010.

[110] P. Gascard and T. D. Tlsty, "Carcinoma-associated fibroblasts: orchestrating the composition of malignancy," *Genes & Development,* vol. 30, pp. 1002-1019, May 1, 2016 2016.

[111] K. Shiga, M. Hara, T. Nagasaki, T. Sato, H. Takahashi, and H. Takeyama, "Cancer-Associated Fibroblasts: Their Characteristics and Their Roles in Tumor Growth," *Cancers,* vol. 7, pp. 2443-2458, 12/11, 09/23/received, 12/07/accepted 2015.

[112] P. Cirri and P. Chiarugi, "Cancer associated fibroblasts: the dark side of the coin," *American Journal of Cancer Research,* vol. 1, pp. 482-497, 03/12, 02/15/received, 03/08/accepted 2011.

[113] J. S. Desgrosellier and D. A. Cheresh, "Integrins in cancer: biological implications and therapeutic opportunities," *Nat Rev Cancer,* vol. 10, pp. 9-22, Jan 2010.

[114] J. Roman, J. D. Ritzenthaler, S. Roser-Page, X. Sun, and S. Han, "α5β1-Integrin Expression Is Essential for Tumor Progression in Experimental Lung Cancer," *American Journal of Respiratory Cell and Molecular Biology,* vol. 43, pp. 684-691, 10/12/received, 01/11/accepted 2010.

[115] F. Schaffner, A. M. Ray, and M. Dontenwill, "Integrin alpha5beta1, the Fibronectin Receptor, as a Pertinent Therapeutic Target in Solid Tumors," *Cancers (Basel),* vol. 5, pp. 27-47, Jan 15 2013.

[116] I. Cornil, D. Theodorescu, S. Man, M. Herlyn, J. Jambrosic, and R. S. Kerbel, "Fibroblast cell interactions with human melanoma cells affect tumor cell growth as

a function of tumor progression," *Proceedings of the National Academy of Sciences of the United States of America,* vol. 88, pp. 6028-6032, 1991.

[117] A. Orimo, P. B. Gupta, D. C. Sgroi, F. Arenzana-Seisdedos, T. Delaunay, R. Naeem, *et al.*, "Stromal fibroblasts present in invasive human breast carcinomas promote tumor growth and angiogenesis through elevated SDF-1/CXCL12 secretion," *Cell,* vol. 121, pp. 335-48, May 6 2005.

[118] E. R. Horton, P. Astudillo, M. J. Humphries, and J. D. Humphries, "Mechanosensitivity of integrin adhesion complexes: role of the consensus adhesome," *Exp Cell Res,* vol. 343, pp. 7-13, Apr 10 2016.

[119] M. J. Paszek, N. Zahir, K. R. Johnson, J. N. Lakins, G. I. Rozenberg, A. Gefen, *et al.*, "Tensional homeostasis and the malignant phenotype," *Cancer Cell,* vol. 8, pp. 241-54, Sep 2005.

[120] S. Seetharaman and S. Etienne-Manneville, "Integrin diversity brings specificity in mechanotransduction," *Biol Cell,* vol. 110, pp. 49-64, Mar 2018.

[121] T. Yeung, P. C. Georges, L. A. Flanagan, B. Marg, M. Ortiz, M. Funaki, *et al.*, "Effects of substrate stiffness on cell morphology, cytoskeletal structure, and adhesion," *Cell Motility and the Cytoskeleton,* vol. 60, pp. 24-34, 2005.

[122] P. Roca-Cusachs, N. C. Gauthier, A. Del Rio, and M. P. Sheetz, "Clustering of alpha(5)beta(1) integrins determines adhesion strength whereas alpha(v)beta(3) and talin enable mechanotransduction," *Proc Natl Acad Sci U S A,* vol. 106, pp. 16245-50, Sep 22 2009.

[123] D. S. Harburger and D. A. Calderwood, "Integrin signalling at a glance," *Journal of Cell Science,* vol. 122, p. 159, 2009.

[124] S. K. Mitra, D. A. Hanson, and D. D. Schlaepfer, "Focal adhesion kinase: in command and control of cell motility," *Nat Rev Mol Cell Biol,* vol. 6, pp. 56-68, Jan 2005.

[125] M. Widmaier, E. Rognoni, K. Radovanac, S. B. Azimifar, and R. Fässler, "Integrin-linked kinase at a glance," *Journal of Cell Science,* vol. 125, p. 1839, 2012.

[126] C. Wu and S. Dedhar, "Integrin-linked kinase (ILK) and its interactors: a new paradigm for the coupling of extracellular matrix to actin cytoskeleton and signaling complexes," *J Cell Biol,* vol. 155, pp. 505-10, Nov 12 2001.

[127] D. Riveline, E. Zamir, N. Q. Balaban, U. S. Schwarz, T. Ishizaki, S. Narumiya, *et al.*, "Focal contacts as mechanosensors: externally applied local mechanical force induces growth of focal contacts by an mDia1-dependent and ROCK-independent mechanism," *J Cell Biol,* vol. 153, pp. 1175-86, Jun 11 2001.

[128] X.-K. Zhao, Y. Cheng, M. Liang Cheng, L. Yu, M. Mu, H. Li, *et al.*, "Focal Adhesion Kinase Regulates Fibroblast Migration via Integrin beta-1 and Plays a Central Role in Fibrosis," *Scientific Reports*, vol. 6, p. 19276, 01/14/online 2016.

[129] V. J. Fincham, M. James, M. C. Frame, and S. J. Winder, "Active ERK/MAP kinase is targeted to newly forming cell–matrix adhesions by integrin engagement and v-Src," *The EMBO Journal*, vol. 19, pp. 2911-2923, 10/22/received, 04/25/revised, 04/25/accepted 2000.

[130] G. E. Hannigan, C. Leung-Hagesteijn, L. Fitz-Gibbon, M. G. Coppolino, G. Radeva, J. Filmus, *et al.*, "Regulation of cell adhesion and anchorage-dependent growth by a new β1-integrin-linked protein kinase," *Nature*, vol. 379, p. 91, 01/04/online 1996.

[131] K. Fukuda, S. Gupta, K. Chen, C. Wu, and J. Qin, "The pseudo-active site of ILK is essential for its binding to α-parvin and localization to focal adhesions," *Molecular cell*, vol. 36, pp. 819-830, 2009.

[132] C. Beyer, A. Schramm, A. Akhmetshina, C. Dees, T. Kireva, K. Gelse, *et al.*, "beta-catenin is a central mediator of pro-fibrotic Wnt signaling in systemic sclerosis," *Ann Rheum Dis*, vol. 71, pp. 761-7, May 2012.

[133] P. J. Morin, "beta-catenin signaling and cancer," *Bioessays*, vol. 21, pp. 1021-30, Dec 1999.

[134] S. G. Pai, B. A. Carneiro, J. M. Mota, R. Costa, C. A. Leite, R. Barroso-Sousa, *et al.*, "Wnt/beta-catenin pathway: modulating anticancer immune response," *Journal of Hematology & Oncology*, vol. 10, p. 101, 05/05, 03/23/received, 04/25/accepted 2017.

[135] H. A. Baarsma, A. I. R. Spanjer, G. Haitsma, L. H. J. M. Engelbertink, H. Meurs, M. R. Jonker, *et al.*, "Activation of WNT / β-Catenin Signaling in Pulmonary Fibroblasts by TGF-β1 Is Increased in Chronic Obstructive Pulmonary Disease," *PLOS ONE*, vol. 6, p. e25450, 2011.

[136] C.-m. Yang, S. Ji, Y. Li, L.-y. Fu, T. Jiang, and F.-d. Meng, "β-Catenin promotes cell proliferation, migration, and invasion but induces apoptosis in renal cell carcinoma," *OncoTargets and therapy*, vol. 10, pp. 711-724, 02/20 2017.

[137] C. Bergmann, A. Akhmetshina, C. Dees, K. Palumbo, P. Zerr, C. Beyer, *et al.*, "Inhibition of glycogen synthase kinase 3beta induces dermal fibrosis by activation of the canonical Wnt pathway," *Ann Rheum Dis*, vol. 70, pp. 2191-8, Dec 2011.

[138] R. Pankov and K. M. Yamada, "Fibronectin at a glance," *Journal of Cell Science*, vol. 115, p. 3861, 2002.

[139] J. W. Weisel, "Fibrinogen and fibrin," *Adv Protein Chem*, vol. 70, pp. 247-99, 2005.

[140] H. Bachman, J. Nicosia, M. Dysart, and T. H. Barker, "Utilizing Fibronectin Integrin-Binding Specificity to Control Cellular Responses," *Adv Wound Care (New Rochelle),* vol. 4, pp. 501-511, Aug 1 2015.

[141] L. Cao, J. Nicosia, J. Larouche, Y. Zhang, H. Bachman, A. C. Brown, *et al.*, "Detection of an Integrin-Binding Mechanoswitch within Fibronectin during Tissue Formation and Fibrosis," *ACS Nano,* vol. 11, pp. 7110-7117, Jul 25 2017.

[142] H. Altroff, C. F. van der Walle, J. Asselin, R. Fairless, I. D. Campbell, and H. J. Mardon, "The eighth FIII domain of human fibronectin promotes integrin alpha5beta1 binding via stabilization of the ninth FIII domain," *J Biol Chem,* vol. 276, pp. 38885-92, Oct 19 2001.

[143] J. Schnittert, R. Bansal, G. Storm, and J. Prakash, "Integrins in wound healing, fibrosis and tumor stroma: High potential targets for therapeutics and drug delivery," *Advanced Drug Delivery Reviews,* 2018/02/04/ 2018.

[144] S. E. Ochsenhirt, E. Kokkoli, J. B. McCarthy, and M. Tirrell, "Effect of RGD secondary structure and the synergy site PHSRN on cell adhesion, spreading and specific integrin engagement," *Biomaterials,* vol. 27, pp. 3863-74, Jul 2006.

[145] S. Johansson, G. Svineng, K. Wennerberg, A. Armulik, and L. Lohikangas, "Fibronectin-integrin interactions," *Front Biosci,* vol. 2, pp. d126-46, Mar 1 1997.

[146] S. D. Redick, D. L. Settles, G. Briscoe, and H. P. Erickson, "Defining Fibronectin's Cell Adhesion Synergy Site by Site-Directed Mutagenesis," *The Journal of Cell Biology,* vol. 149, pp. 521-527, 11/22/received, 02/23/rev-request, 03/09/accepted 2000.

[147] H. E. Balcioglu, H. van Hoorn, D. M. Donato, T. Schmidt, and E. H. Danen, "The integrin expression profile modulates orientation and dynamics of force transmission at cell-matrix adhesions," *J Cell Sci,* vol. 128, pp. 1316-26, Apr 1 2015.

[148] M. Bharadwaj, N. Strohmeyer, G. P. Colo, J. Helenius, N. Beerenwinkel, H. B. Schiller, *et al.*, "αV-class integrins exert dual roles on α5β1 integrins to strengthen adhesion to fibronectin," *Nature Communications,* vol. 8, p. 14348, 01/27/online 2017.

[149] P. Costa, T. M. E. Scales, J. Ivaska, and M. Parsons, "Integrin-Specific Control of Focal Adhesion Kinase and RhoA Regulates Membrane Protrusion and Invasion," *PLOS ONE,* vol. 8, p. e74659, 2013.

[150] M. Knipp and M. Vasak, "A colorimetric 96-well microtiter plate assay for the determination of enzymatically formed citrulline," *Anal Biochem,* vol. 286, pp. 257-64, Nov 15 2000.

[151] A. Shevchenko, H. Tomas, J. Havlis, J. V. Olsen, and M. Mann, "In-gel digestion for mass spectrometric characterization of proteins and proteomes," *Nat Protoc,* vol. 1, pp. 2856-60, 2006.

[152] V. C. Willis, N. K. Banda, K. N. Cordova, P. E. Chandra, W. H. Robinson, D. C. Cooper, *et al.*, "Protein arginine deiminase 4 inhibition is sufficient for the amelioration of collagen-induced arthritis," *Clin Exp Immunol,* vol. 188, pp. 263-274, May 2017.

[153] A. S. Rohrbach, S. Hemmers, S. Arandjelovic, M. Corr, and K. A. Mowen, "PAD4 is not essential for disease in the K/BxN murine autoantibody-mediated model of arthritis," *Arthritis Research & Therapy,* vol. 14, pp. R104-R104, 05/02, 01/11/received, 04/10/revised, 05/02/accepted 2012.

[154] A. Suzuki, Y. Kochi, H. Shoda, Y. Seri, K. Fujio, T. Sawada, *et al.*, "Decreased severity of experimental autoimmune arthritis in peptidylarginine deiminase type 4 knockout mice," *BMC Musculoskelet Disord,* vol. 17, p. 205, May 5 2016.

[155] M. A. Shelef, D. A. Bennin, N. Yasmin, T. F. Warner, T. Ludwig, H. E. Beggs, *et al.*, "Focal adhesion kinase is required for synovial fibroblast invasion, but not murine inflammatory arthritis," *Arthritis Res Ther,* vol. 16, p. 464, 2014.

[156] Y. Seri, H. Shoda, A. Suzuki, I. Matsumoto, T. Sumida, K. Fujio, *et al.*, "Peptidylarginine deiminase type 4 deficiency reduced arthritis severity in a glucose-6-phosphate isomerase-induced arthritis model," *Sci Rep,* vol. 5, p. 13041, Aug 21 2015.

[157] J. Franco-Barraza, R. Francescone, T. Luong, N. Shah, R. Madhani, G. Cukierman, *et al.*, "Matrix-regulated integrin α(v)β(5) maintains α(5)β(1)-dependent desmoplastic traits prognostic of neoplastic recurrence," *eLife,* vol. 6, p. e20600, 01/31, 08/14/received, 01/05/accepted 2017.

[158] J. C. Friedland, M. H. Lee, and D. Boettiger, "Mechanically activated integrin switch controls alpha5beta1 function," *Science,* vol. 323, pp. 642-4, Jan 30 2009.

[159] T. R. Cox and J. T. Erler, "Remodeling and homeostasis of the extracellular matrix: implications for fibrotic diseases and cancer," *Dis Model Mech,* vol. 4, pp. 165-78, Mar 2011.

[160] G. Bendig, M. Grimmler, I. G. Huttner, G. Wessels, T. Dahme, S. Just, *et al.*, "Integrin-linked kinase, a novel component of the cardiac mechanical stretch sensor, controls contractility in the zebrafish heart," *Genes & Development,* vol. 20, pp. 2361-2372, 05/09/received, 07/07/accepted 2006.

[161] G. Song, G. Ouyang, and S. Bao, "The activation of Akt/PKB signaling pathway and cell survival," *J Cell Mol Med,* vol. 9, pp. 59-71, Jan-Mar 2005.

[162] T. Sun, M. Rodriguez, and L. Kim, "Glycogen synthase kinase 3 in the world of cell migration," *Dev Growth Differ*, vol. 51, pp. 735-42, Dec 2009.

[163] G. P. Meares and R. S. Jope, "Resolution of the nuclear localization mechanism of glycogen synthase kinase-3: functional effects in apoptosis," *J Biol Chem*, vol. 282, pp. 16989-7001, Jun 8 2007.

[164] O. Sanchez-Pernaute, R. Largo, E. Calvo, M. A. Alvarez-Soria, J. Egido, and G. Herrero-Beaumont, "A fibrin based model for rheumatoid synovitis," *Ann Rheum Dis*, vol. 62, pp. 1135-8, Dec 2003.

[165] C. Foulquier, M. Sebbag, C. Clavel, S. Chapuy-Regaud, R. Al Badine, M. C. Mechin, *et al.*, "Peptidyl arginine deiminase type 2 (PAD-2) and PAD-4 but not PAD-1, PAD-3, and PAD-6 are expressed in rheumatoid arthritis synovium in close association with tissue inflammation," *Arthritis Rheum*, vol. 56, pp. 3541-53, Nov 2007.

[166] T. M. Maher, I. C. Evans, S. E. Bottoms, P. F. Mercer, A. J. Thorley, A. G. Nicholson, *et al.*, "Diminished prostaglandin E2 contributes to the apoptosis paradox in idiopathic pulmonary fibrosis," *Am J Respir Crit Care Med*, vol. 182, pp. 73-82, Jul 1 2010.

[167] Y. P. Moodley, P. Caterina, A. K. Scaffidi, N. L. Misso, J. M. Papadimitriou, R. J. McAnulty, *et al.*, "Comparison of the morphological and biochemical changes in normal human lung fibroblasts and fibroblasts derived from lungs of patients with idiopathic pulmonary fibrosis during FasL-induced apoptosis," *J Pathol*, vol. 202, pp. 486-95, Apr 2004.

[168] G. L. Lin, D. M. Cohen, R. A. Desai, M. T. Breckenridge, L. Gao, M. J. Humphries, *et al.*, "Activation of beta 1 but not beta 3 integrin increases cell traction forces," *FEBS Letters*, vol. 587, pp. 763-769, 2013.

[169] H. B. Schiller, M. R. Hermann, J. Polleux, T. Vignaud, S. Zanivan, C. C. Friedel, *et al.*, "beta1- and alphav-class integrins cooperate to regulate myosin II during rigidity sensing of fibronectin-based microenvironments," *Nat Cell Biol*, vol. 15, pp. 625-36, Jun 2013.

[170] P. Roy, W. M. Petroll, C. J. Chuong, H. D. Cavanagh, and J. V. Jester, "Effect of Cell Migration on the Maintenance of Tension on a Collagen Matrix," *Annals of Biomedical Engineering*, vol. 27, pp. 721-730, 1999/11/01 1999.

[171] A. K. Harris, D. Stopak, and P. Wild, "Fibroblast traction as a mechanism for collagen morphogenesis," *Nature*, vol. 290, p. 249, 03/19/online 1981.